ACTIVITY IN THE CRAB NEBULA

Thesis by

Jeffrey D. Scargle

In Partial Fulfillment of the Requirements

For the Degree of

Doctor of Philosophy

California Institute of Technology

Pasadena, California

1968

(Submitted February 8, 1968)

Frontispiece

Composite made from 200-inch plates taken 9 years apart, showing the general field of motions in the Crab Nebula; yellow polaroid plates (PH 1300, 1955.7; PH 4642, 1964.8) with the magnetic vector of the transmitted light in the E-W direction; north is at the top, west to the right.

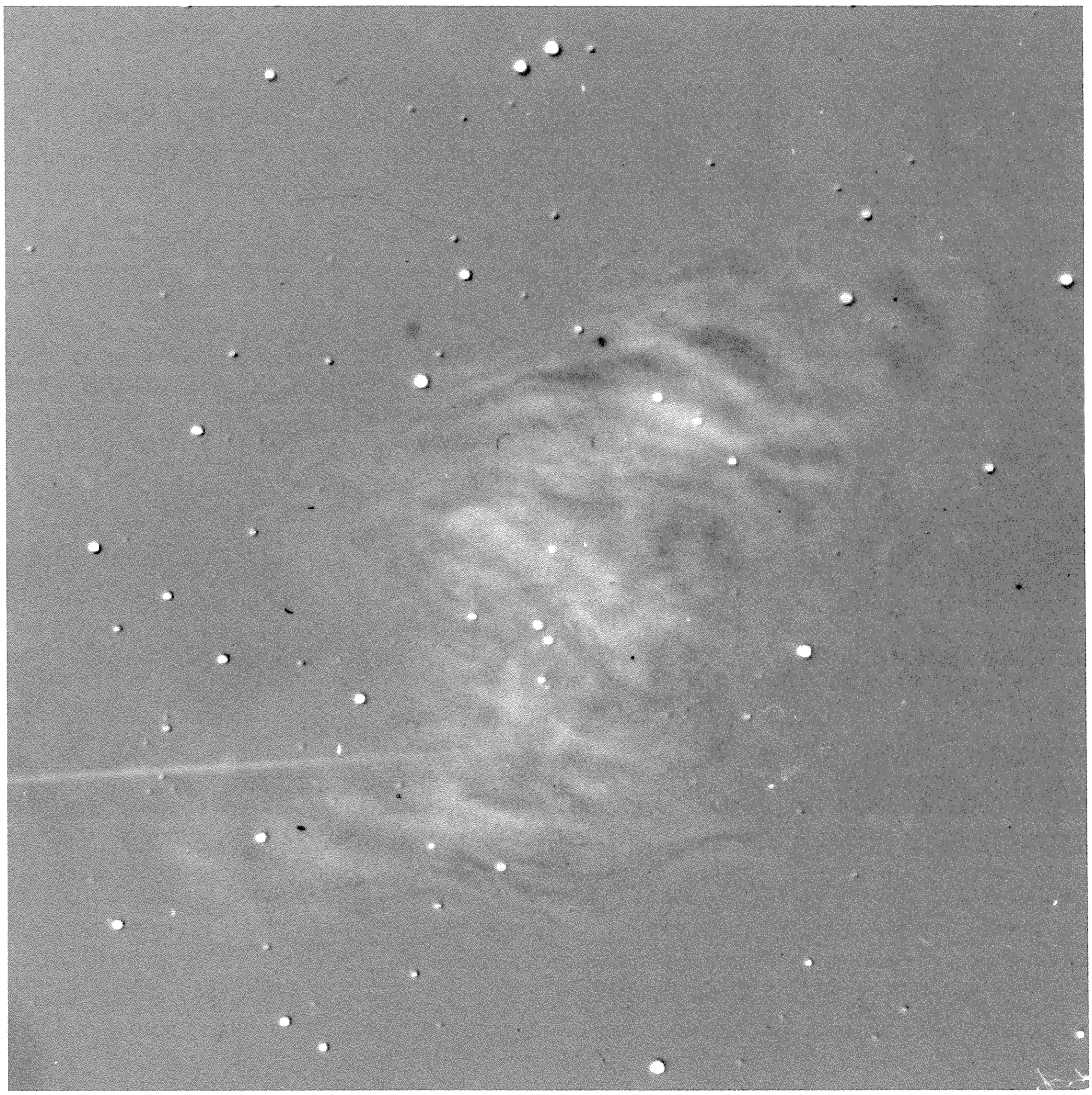

PREFACE

One day Guido Münch, aware that I had been working on the theory of synchrotron radiation, showed me one of the 200-inch plates and pointed out the wisp. This curious object has always been the focus of the project, even though it led to other aspects of the Crab Nebula. I am grateful to Dr. Münch for suggesting and advising this thesis — more especially because it was not a clearly defined or routine problem, and was therefore challenging and interesting.

Several individuals have helped in general ways that do not appear explicitly in the thesis, but nevertheless made it possible. My wife, Karin, has shown much patience, understanding, and encouragement. George Field introduced me to theoretical astronomy and collaborated on the specific project which indirectly led to this topic. Jesse Greenstein, both in his official capacities and otherwise, has helped me in many ways. Nearly everyone in astronomy at Caltech and elsewhere that I have associated with--including astronomers, staff, and students--has been helpful in many ways.

Turning to specifics, I am especially grateful to those who have read all or part of the manuscript and offered numerous valuable suggestions, many of which have been directly incorporated: Fritz Bartlett, Jim Gunn, Dick McCray, Guido Münch, and Michael Simon. I thank Chip Arp for taking several 200-inch plates, and

assisting with two very long and cold 48-inch exposures. Fritz Zwicky kindly lent me several plates from his file. It is impossible to remember and acknowledge all the discussions which have contributed to this thesis. Guido Münch guided much of the work in very major ways. Bev Oke provided much wisdom concerning the photoelectric observations, and gave me access to his unpublished data. Leverett Davis, Jim Gunn, Ian Lerche, and Eugene Parker substantially aided my understanding of the basic theory of relativistic hydrodynamics. Virginia Trimble communicated helpful insight and data concerning the filaments. Other discussions of much use were had with: Chris Anderson, Becklin, G. Burbidge, Castor, Field, Ginzburg, Goldreich, Jokippii, Kabakow, Keeley, Leighton, Melrose, William Miller, Minkowski, Morrison, O'Connell, Shklovskii, and Woltjer. Tom Gehrels, Oke, and Visvanathan kindly offered to make polarization measures in connection with the ultraviolet excess, but various circumstances intervened. I am grateful to Barry Lasker and Fritz Bartlett for the loan of their interference and Gaussian filters, respectively. Several nights on the 100-inch were shared with Bruce Peterson, who aided some aspects of the observations. Grant Snellen and Ed Dobies were extremely helpful with various aspects of the interpretation and measurements of the plates. Maggie Hayden's expert typing under difficult circumstances does not deserve to be mentioned last.

ABSTRACT

Changes in the structure shown by the continuous emission from the Crab Nebula are investigated observationally and theoretically. A beautiful series of 200-inch plates from 1955 to the present provides the data on the morphology of the activity. Near the center of the nebula is a striking series of strongly polarized, elongated features called "wisps". The wisps in this series appear to move at velocities a significant fraction of the speed of light. The first and most prominent wisp is probably a permanent feature which moves about a characteristic position. Nearby is a fainter but similar region which sometimes shows one or more wisps. Centrally placed with respect to these two regions is a very thin wisp which shows more restricted motions. Since the two active regions are symmetrically placed about it, this thin wisp is in a sense the center of the activity. The nearby star is probably not associated with the nebula. Motion can be detected as well at the edges of the nebula. At the northwest edge in particular are rapidly moving objects which may be wisps which have propagated outward from the central region. The area of the nebula intermediate between the central wisps and these features near the edge is studied with a special technique, and there are indications of motions here too. In a general way all of the motions can be understood as disturbances in the plasma composed of relativistic gas, thermal gas, and magnetic field.

The main wisp may act as a piston, exciting the other wisps in the form of propagating compressional waves. The velocity of propagation is set by the density of the thermal gas, which must be on the order of 10^{-1} cm^{-3} to produce the observed velocities. Damping of these waves by resonance phenomena may be a source of energy for the relativistic particles sufficient to restore the synchrotron losses. Photoelectric observations show that the intrinsic spectrum is probably a power law with a slight excess of ultraviolet radiation. The power law, which decreases with increasing frequency, becomes steeper away from the center of the activity. This may be caused by the evolution of the electron energy distribution or by the injection of energy where the activity is strongest.

TABLE OF CONTENTS

I. INTRODUCTION

In the heart of the relativistic plasma in the Crab Nebula lies an elongated object. It would be remarkable by its very appearance - - the high surface brightness, strong polarization, and sharply defined boundaries make it stand out from the rest of the continuous synchrotron emission. But in addition, it moves at velocities approaching one-quarter of the speed of light. The present thesis is an attempt to understand this and other features of the nebula which exhibit rapid motions and changes. This activity is important not only because it exists and is unexplained, but also because of its probable association with three other aspects of the nebula.

The most remarkable of these is the point source visible at low radio frequencies (Andrew, Branson and Wills, 1964; Hewish and Okoye, 1965; Branson, 1965; Bell and Hewish, 1967). It is definitely known to be rather small ($0\overset{''}{.}2 \pm 0\overset{''}{.}1$ according to Bell and Hewish) and to have a very steep spectrum. Its location has been ludicrously discrepant as reported by at least three observers using three completely different techniques. The original occultation placed the source far to the southeast of the center of the nebula (Andrew *et al*, 1964). But Moffet (unpublished public remarks) has pointed out that

refraction in the atmosphere of the earth might substantially affect the position determined in this way, because of the low frequencies involved. Interferometry carried out at Jodrell Bank (Kronberg, 1966) gave a position far to the northwest of the center, but Bell and Hewish (1967) express the opinion that the source was misidentified in this observation. A clever differential method (Gower, 1967), making use of the scintillation of the point source, and not affected by refraction, places it very near the centroid of the radio emission. The error box is centered about 10" west of the central double star, and is 20" wide in right ascension and 2' long in declination. It is interesting that the occultation brightness distribution obtained by Davies, Gardner, Hazard, and Mackey (1966) shows a peak at precisely the position given by Gower, of approximately the intensity expected at the observed frequency of 404 MHz. They did not notice it because they were expecting the source to lie off to the southeast. Although the position cannot be regarded as firmly determined, it seems most likely that it is near the center of the nebula, close to the region showing the violent activity. It is tempting to make the admittedly circumstantial identification of the point source with the seat of the activity. This idea is strengthened by

the indications that the mechanism producing the radiation is synchrotron maser action (Zheleznyakov, 1966; McCray, 1966) or coherent plasma emission (Ginzburg and Ozernoy, 1966). Both mechanisms require high but not unreasonable densities (10^5 to 10^8 particles per cm^3), and the maser action also requires an energy distribution which <u>increases</u> with increasing energy over an appropriate energy range. The latter circumstance could obtain if high-energy particles were injected, either with a low-energy cutoff or merely preferentially at high energies. All of these conditions could exist in or near a condensed remnant, acting as a source of energetic particles or adding energy to the particles already present.

This brings us to the second aspect of the Crab which might be associated with the activity, namely the remains of the star which exploded. It is an open question whether or not there is a condensed object resembling a star left over from the supernova. Despite three unpublished attempts at the difficult spectroscopy (by Kraft, Minkowsky, and Zwicky), proper motion measurements (see the summary and references in Brosche, 1966; Orlova, 1966; Trimble, 1968), and somewhat crude photometry (Baade, 1942), neither of the two 15^m stars near the center is positively indicated as the remnant. The study of the

rapid motions presented in this thesis might have suggested one of the visible stars as the center or source of the activity, but did not (see Chapter II). Some of the numerical models of supernova explosions leave stellar remnants (Colgate and White, 1966; see also the references listed by Melrose and Cameron, 1967), generally in the form of collapsed or neutron stars. But it is by no means established that such calculations represent reality, and in particular the unusual explosion which produced the Crab Nebula. There is no fundamental reason why the debris could not be rather widely dispersed, perhaps leaving a remnant which is very dense compared to the rest of the nebula, but not visible as a star.

We have already hinted at the third point, the possible association of the activity with a supply of energy for the relativistic particles, and in particular for the electrons. The necessity for there being such an energy supply can be seen by evaluating the synchrotron losses during the earlier history of the nebula (Scheuer, 1966). The losses were much greater when the magnetic field was stronger, and Scheuer estimated that the total energy half-life of the nebula was a few years at $t = +100$ years. The quantitative results depend on how the magnetic field is assumed to vary (which is not obvious)

and the effects of self-absorption, but it is not possible to construct an evolutionary model which arrives at the present-day state without postulating improbably high initial energies or a continuing source of energy. As soon as it was discovered, the activity in the nebula was taken to be a manifestation of the process by which energy is supplied. The idea that the moving features are some form of hydromagnetic wave seems to have occurred to many people independently, perhaps the first being J. H. Piddington (apparently unpublished remarks, mentioned by Mayall, 1962; also, Piddington, 1955), but credit for the most detailed theoretical discussion probably is due Shklovskii (1957); the clearest insight to the observational evidence was probably that of Woltjer (as quoted by Mayall, 1962).

The X-ray source is not considered as a possible candidate for identification with the small objects discussed above, because it is now known to be quite large (Oda et al, 1967), possibly as large as the entire nebula as seen in optical continuum radiation. This fact and the X-ray spectrum are, at the very least, not inconsistent with the X-rays being produced by the synchrotron process. If so, the argument for a continuing source of energy is even stronger. We shall discuss the X-ray source in this and one other connection later.

The picture which rather naturally arises from the observational data is that the remnant of the star which exploded is now producing low-frequency radio emission from a region about 0".2 in diameter near the center of the nebula, and is generating the activity which appears in the form of features moving at relativistic velocities and which somehow transfers energy to the relativistic particles. We shall present observational data on the nature of the activity (Chapters II, III, and IV), and then investigate the theory which describes how such activity should behave in a relativistic gas.

II. THE CHANGING WISPS

The discovery of changes in the Crab Nebula was made by Lampland (1921) during a survey for variability in nebulae with the 40-inch Lowell reflector. He described three specific features: (1) the "wisp" mentioned in the Introduction, in a location and orientation which are still characteristic of it today, (2) an elongated mass about halfway to the edge of the nebula in the northwest quadrant, and (3) a "partially cleared space" near the row of three stars (S4, S5, and S6 in Figure II.1) at the northwest edge. All three showed definite changes, and all three will be discussed below. Lampland's work did not become widely known, and it is not clear just when Baade became aware of it. What matters is that Baade discovered <u>rapid</u> changes in the Crab, which occur too fast to have been seen on Lampland's rather widely spaced plates. Baade's description of some of the motions from 100-inch plates taken in 1944-45 was subsequently published (Oort and Walraven, 1956). Since then, the primary new observational material is a remarkable series of 200-inch plates begun in 1955 by Baade and continued to the present by Münch. Some of the earliest of these plates have been published (Baade, 1956) and a few other remarks about them have appeared in the literature (Woltjer, as quoted

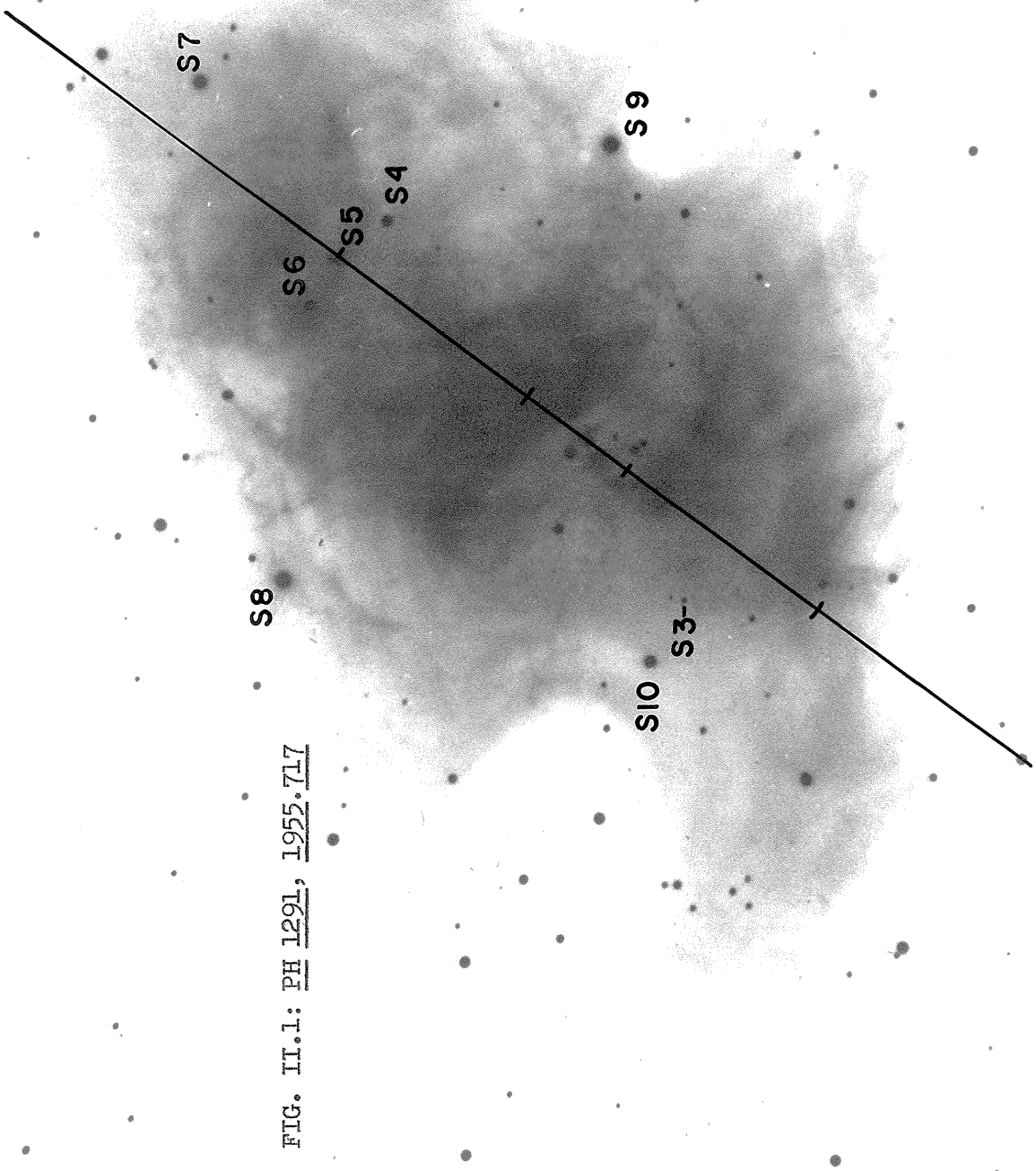

FIG. II.1: PH 1291, 1955.717

by Mayall, 1962; Shklovskii, 1957). In addition, there have been several motion measurements which will be discussed later in this chapter. Numerous interpretative discussions have appeared, some of which will be considered below. Unfortunately, the lack of a definitive and detailed publication of the observational material has led to some confusions, and we will attempt to clarify these points.

At the risk of repeating well-known facts, we shall begin with a brief general description of the nebula. The purposes of this discussion will be the elimination of any possible confusion about the basic facts, and the establishment of a definite terminology. In the first place, the Crab Nebula (M1, GC 1157, NGC 1952, Taurus A, 3C 144, 4C 21.19, Parkes 0531+22, Taurus XR-1) appears to be composed of two entities, commonly called the <u>filaments</u> and the "<u>amorphous region</u>". The physical and spatial connection between them is not clear, and it will not even be assumed that they represent different regions of space (Trimble, 1968). They can be completely distinguished by the characteristics of their optical radiation, the former emitting practically solely lines and the latter continuum only. There is also a conventional distinction that the filaments are sharply defined, sometimes pointlike, whereas the continuum emission is

"amorphous." While there is an obvious morphological basis for a distinction of this sort, the implication that there is no fine structure in the continuum emission is totally false. In good seeing, the continuum region is largely resolved into myriad filamentary features.[1] Herschel (1912) indicated with some hesitancy that the Crab was resolvable into stars! On the best polarization plates the nebula reminds one of a fibrous ball of cotton which has been stretched and drawn out in a direction which rotates with the polaroid filter. The correspondence is such that the magnetic field lines run through the fibers parallel to the direction of their elongation, on the assumption that the polarized radiation is produced by the synchrotron process. The same is true of the wisps to be discussed below. A possible physical mechanism for the existence and alignment of the fibers is to be found in the thermo-synchrotron instability developed by Simon and Axford (1967), who suggest that the mechanism may explain the filaments in the Crab and the fine structure of strong radio sources. In any case, diffusion of the electrons along the field lines would naturally tend to produce the alignment. Considering the smoothing due

---

1. The wisps are sometimes confused with the filaments, and to call <u>these</u> features filaments would add to the confusion - even though the term is probably more appropriate here. Hence we shall use the term "fibers" for these filamentary structures.

to seeing and line-of-sight integration, it is quite likely that the continuum emission originates entirely from such fibers. Typical widths are 2" and typical separations between the fibers are 5". As remarked by Shklovskii (1957), it is interesting that the fibers do not very often screen each other. Of course the topology of the field lines prevents them from actually intersecting. In addition, the strong selection by polarization direction enables one to see fibers from a limited sample of the radial dimension on any one plate, and this would reduce the screening of the fibers in projection.

The general appearance of the nebula (see Figure II.1) is well-known. Special attention is called to the hole near the center, which is actually part of a roughly S-shaped region of reduced intensity. It is not possible to know what the true three-dimensional shape of this cavity is. Since even in projection on the sky we see rather sharp edges, it probably has sharp interfaces with the brighter regions. The smaller intensity must be the result of a generally smaller magnetic field or of fewer particles with the right energies to radiate in the optical region, or both. Whatever the nature of the hole, the main wisp - at least in projection - seems to traverse it and cross

its boundaries.

The rest of this chapter is a description of the activity depicted on the above-mentioned series of direct plates. At the outset we shall discuss some important ambiguities which must arise in any such description. Consider two plates, 1 and 2, taken some time apart. Suppose on plate 1 we observe a conspicuous feature at point A, and on plate 2 we see no such feature at A but a similar feature at point B. One is tempted to call this circumstance "motion from A to B". If the two features are distinctive and reasonably similar given the seeing and other differences between the two plates, then the inference that they are related is probably justified. Obviously, however, it is not possible to say with certainty what occurred during the intermediate period. It could be that the feature at A disappeared and then a feature appeared at B and was similar because of a similar environment. Then there would be no real motion.[1] The apparent velocity could, for example, exceed the speed of light. This

---

1. This ambiguity could be resolved by taking plates at shorter time intervals (e.g., $\lesssim$ light travel time across the object). Even then it would not be established that there was a real motion. The experiment in which the intersection of two lines can move arbitrarily fast suggests the kind of situation imagined. A related question is whether or not mass motion is involved, as opposed to the propagation of a wave in which the particles remain on the average stationary.

ambiguity is important because it shows up as an uncertainty as to whether the wisps are forming, moving away from the center, and disappearing, or whether they are permanent features. The former has been the usual interpretation of the few remarks about the wisps in the literature (Oort and Walraven, 1956), but the ambiguity just discussed makes it impossible to decide this question with certainty. As we shall see, the general impression given by the plates now available is that at least the main wisp is more likely a permanent feature undergoing violent inward and outward motions. The question could be settled by a series of plates closely spaced (say 2 per month) over one or several observing seasons.

Let us begin the description of the activity with a schematic picture of the central region as it appeared on the early 200-inch plates of Baade, Figure II.2. The most prominent feature to casual inspection is labeled WISP 1, and has been called "the wisp", "the lens", "a light ripple", etc. We shall always use the term WISP for this and other similar elongated features. Quite generally there is a series of wisps, more or less parallel and on the same side of the star S1. In most cases the first wisp in the series has the greatest surface brightness, but this is not always so. In February of 1962 (see Figure A.1(d)) the first two wisps

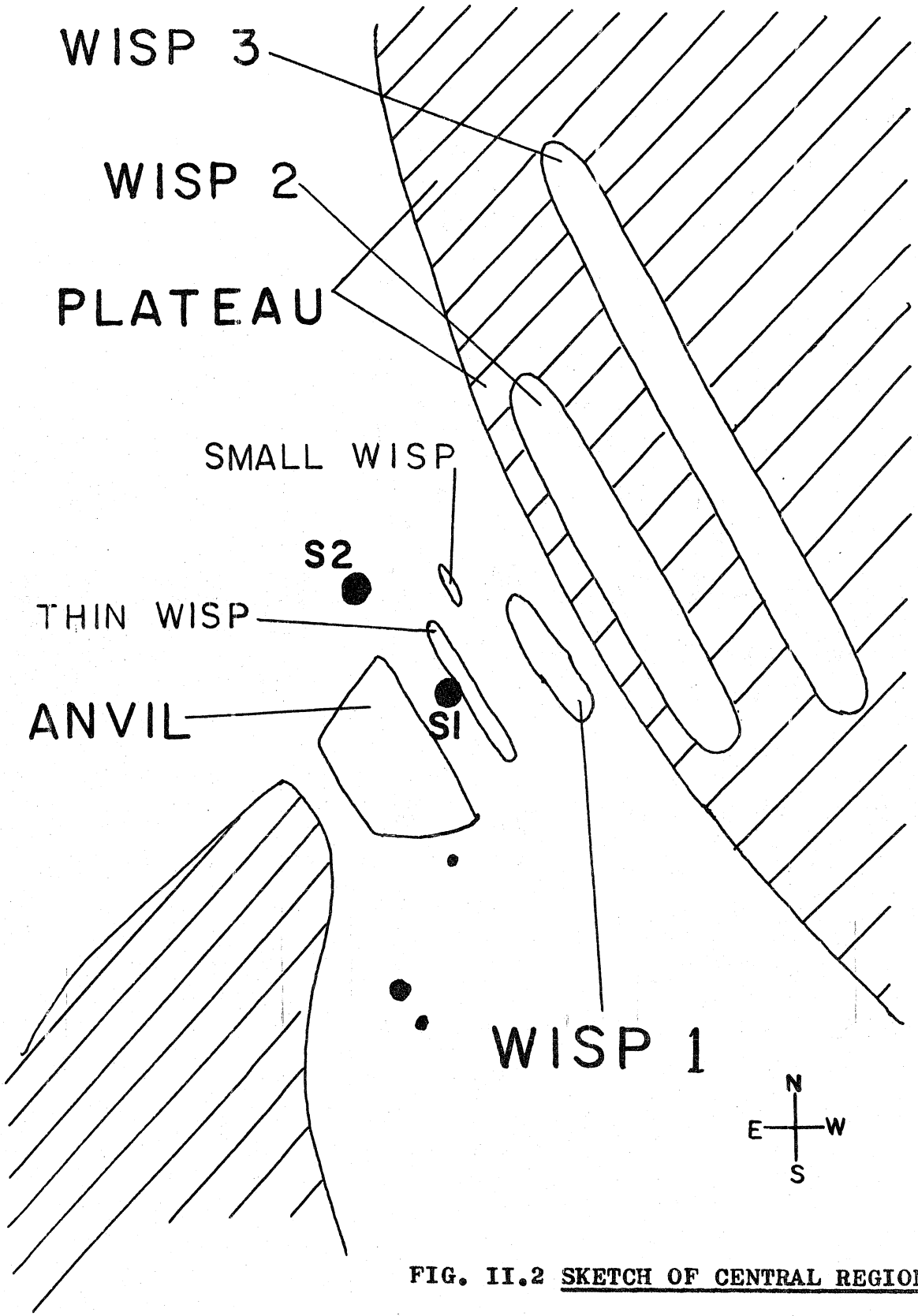

FIG. II.2 SKETCH OF CENTRAL REGION

were approximately equally prominent. There is a clear trend for the wisps which are further from S1 to be longer and, somewhat less clearly, thicker. Sometimes, however, the outer wisps appear as fragments which are comparable to or smaller than the main wisp. The relative inconspicuousness of the outer wisps is largely due to the fact that they are superimposed on the bright background region labeled the PLATEAU in Figure II.2. In fact, on some of the plates (notable PH 1624) the outer wisps are so bright as to be very conspicuous even above the PLATEAU. The "elongated mass" in this region reported by Lampland (1921) is probably an example of a very prominent wisp far from S1. But in addition to this background effect, there may also be a real decrease in the surface brightness of the wisps with increasing distance from the center. Besides the series of wisps, there is almost always an extraordinary wisp not far ($\sim$ 1") from the star S1 and roughly parallel to the other wisps. This has been dubbed the THIN WISP because it is frequently very thin and sharply defined. On the other side of S1 from these wisps is a region that also shows activity, but much less obviously. On the early plates this region showed little structure and was roughly trapezoidal; hence we shall call it the ANVIL. Finally, there is sometimes a small, faint wisp between the THIN WISP and WISP 1, called

the SMALL WISP. It disappears if the seeing is not good, but may be absent even in good seeing. It should be stressed that all the wisps are strongly polarized. The direction of polarization is such that the wisps are elongated along the field lines. Notes on the morphology and polarization of the features listed here are contained in Appendix A. We shall now consider each feature in turn and summarize these notes, emphasizing changes and motions.

The Wisp Series

WISP 1 is the most active object in the nebula, and WISP 2 is closely associated with it, as we shall see. Measures were made on the Grant engine of the displacement of the first two wisps in the series projected on the direction defined by S1 and S3 (see Figure II.1). This direction is essentially perpendicular to the characteristic elongation of the wisps and parallel to their motions. The measurement refers to that portion of the wisps between two parallel lines 6".6 apart centered on S1. As the wisps tilt and move perpendicular to this direction to some extent, the physical meaning of this distance is not straightforward. But in some sense we are measuring the component of the motion along the given direction. The results are plotted in Figure II.3. Attention should be first concentrated on the filled symbols, which refer to WISP 1. The squares are from sets of polaroid plates and

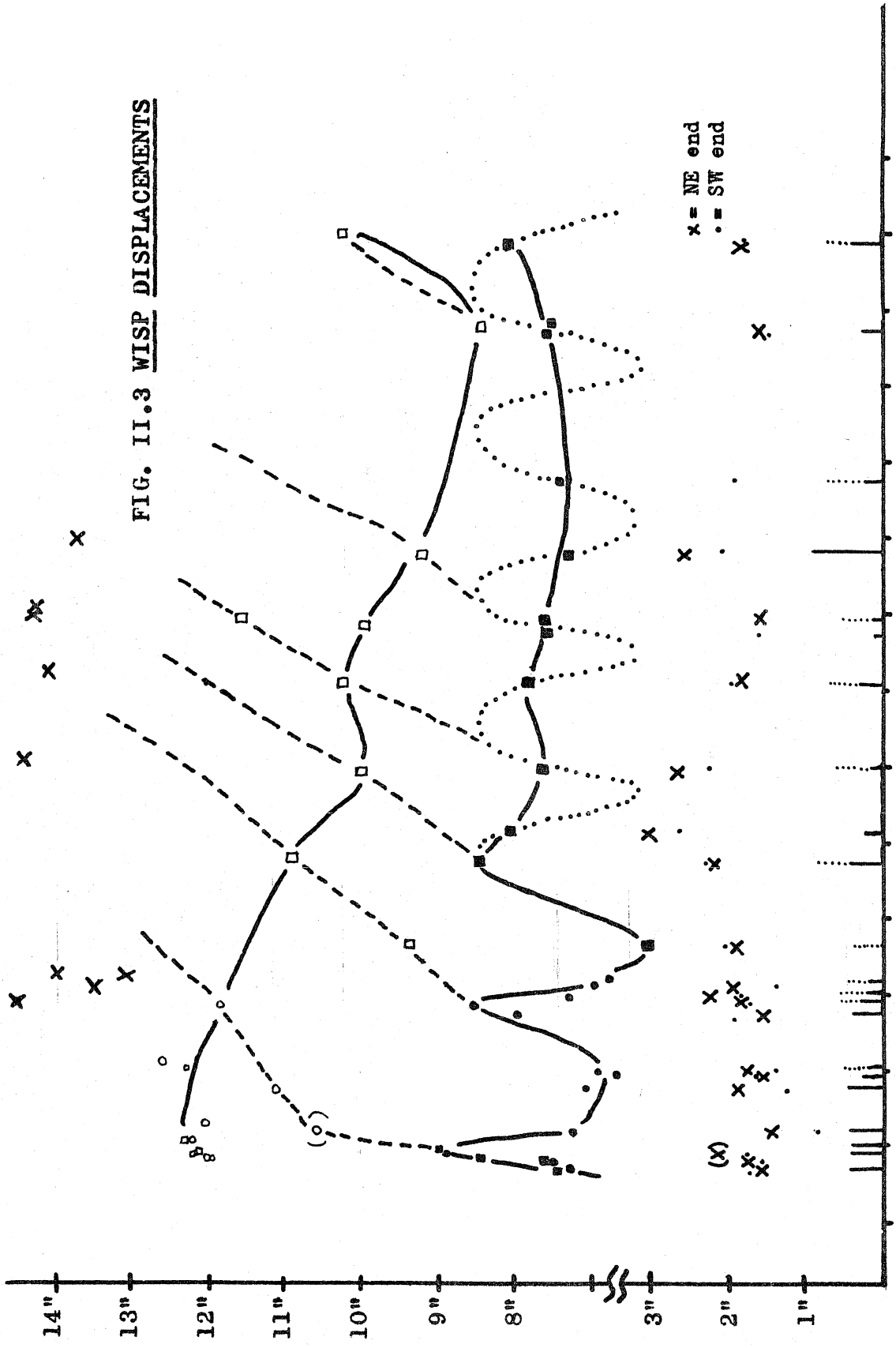

FIG. II.3 WISP DISPLACEMENTS

are the averages of the values for the different orientations (all four were not always suitable for measurement); the circles are non-polaroid plates, and usually represent one measurement. The range of the values at a given epoch was always less than 0".6, and usually on the order of 0".3. Some of this scatter is due to the polarization of the wisps and the background, and will tend to cancel in the averages. It is felt that an expected error of ±0".1 is a rather generous estimate. The actual errors of measurement are nil. The major source of error is simply uncertainty as to what part of the contour to measure, an effect greatest when the profile of the wisp is not symmetrical (which is true on a significant fraction of the plates). An attempt was made to measure the centroid of the contour rather than the peak, which would be more sensitive to gradients in the background. The solid line is a smooth fit to the filled symbols. If we take WISP 1 to be a single object, and suppose that this line represents a real motion, we see that high velocities are involved ($\underline{v}$ projected on the plane of the sky is $\sim$ 0.2c for d = 1500 pc., a distance which will be used in all such calculations unless stated otherwise; for the distance of 2000 pc. suggested by Trimble (1968), and if the real motion is at 45° to the plane of the sky, v $\sim$ 0.4c). There is no indication that the motion is always outward

as opposed to inward, except that by chance the series of plates most closely spaced in time (18 plates between 1955.715 and 1955.943) covered a period of rapid outward motion. Unfortunately the more recent plates are more widely spaced; this makes the true motion much more ambiguous and may be responsible for the apparent damping suggested by the solid line. Otherwise it is a coincidence that the motion became smoother when the plates became less frequent. For illustration only we have drawn the dotted line, compatible with the assumption that the violent surges seen at first are continuing. A rough two-year periodicity is suggested by the early motion, but this should be regarded as tentative. To try to test this picture, we looked for other properties which might be correlated with the motion. The length of WISP 1 is an obvious choice. As noted in Appendix A, this wisp is sometimes very nearly a point, and it would be strange if this extraordinary phenomenon were not connected with the origin and dynamics of the wisp. The lengths of the vertical lines at the bottom of Figure II.3 are proportional to the length of WISP 1 as measured with a reticle and hand viewer (the vertical scale is multiplied by a factor of ten). When the wisp has a definite core surrounded by fainter extensions on one end or both, the core is denoted by the solid line and the extensions by

the dotted line. There appears to be a very rough correlation such that the wisp has a small core when it is nearest the center. This relation would be expected if the outward motion of the wisp were initiated by the injection of electrons at a point, and subsequently diffusion lengthened the point to a wisp. If this process were repeated when the wisp returned, one would expect a core embedded in the residue of the earlier wisp.

Does the motion of WISP 1 affect the other wisps? Plate PH 5002 (Figure A.2(d)) provides a clear affirmative answer, because there is a distinct bending of WISP 2 around the contour of WISP 1. In addition, measurements of the positions of the wisps also indicate a relation. Often there was a definite feature that could be called the second wisp, and this was measured in exactly the same manner as WISP 1. Less frequently a third feature could be identified as WISP 3, and it was measured also. But it is important to keep in mind that not all three wisps could be measured at all epochs, and that even when they were, there was some margin for confusion. In particular, it is not likely that the feature called WISP 2 is really the same object from plate to plate. The measurements of WISP 2 are shown by open symbols, and their connection by the solid line

seems the most reasonable. If this is the actual motion, the first two wisps moved roughly parallel after 1960. The relation between 1955 and 1960 is not so clear. An alternative interpretation of the motion is drawn as dashed lines, and is based on considering the motion of WISP 2 as a continuation of that of WISP 1. The physical picture suggested is WISP 1 playing the role of a piston moving back and forth, generating compressional waves which propagate outward. Neither of these interpretations is conclusively supported by the data, but it is clear that there is some kind of relation between the neighboring wisps in the series. Again, an extended series of plates with small time intervals is needed to delineate these motions clearly.

The THIN WISP

The THIN WISP is a very remarkable feature. It shows great variety of length, thickness, tilt, and brightness. It is so close to the star S1 that it was hoped that study of its motion would reveal a definite relation to the star, thus identifying it as the stellar remnant of the supernova. It seems fairly clear that there is no relation. During its motions the THIN WISP stubbornly refuses to pay any attention to S1. The proximity of the wisp to the star is the only evidence for a connection. The distance varies between 1" and 3",

and this is not too unreasonable for a chance coincidence given the number of strange features near the center of the Crab. The opposite view has been argued by Shklovskii (1964). On several occasions (November 1955, Figure A.1. (a); December 1957; February 1958; February 1962, Figure A.1.(d)) the THIN WISP was curved away from S1, but it has never been seen concave toward S1. Also, the length of the wisp and its location in the N-S direction varies considerably, but shows no symmetry about S1. Because of this and any lack of direct evidence for peculiarity in the star, there is no reason to consider S1 as the supernova remnant.

The displacements of both ends of the THIN WISP were measured as already described, and are plotted near the bottom of Figure II.3. The north end was measured midway between S1 and S2, the other end about 3" south of S1, both displacements being referred to S1 in the same way as for the wisp series. Again the true errors are hard to estimate, but they are probably somewhat larger than for WISP 1. Comparison of the measures for close epochs indicates scatter on the order of $\pm$0".3, unless there are very rapid and erratic motions. Motion larger than the errors is clearly shown in Figure II.3. The amplitude is about 2", but the motion is not well determined and does not show any particular regularity. That there is motion

and more especially tilting of this wisp is evident from direct inspection of the plates (see Appendix A and accompanying plates). It should be remarked that the THIN WISP is sometimes totally absent. None of the changes in this wisp is clearly correlated with the motion of WISP 1 in any way.

The ANVIL

As described in Appendix A the ANVIL, seemingly amorphous on the early plates, often contains one or more wisp-like structures which are similar in every way to the wisps in the series so prominent on the other side of S1, except that they are substantially fainter. The ANVIL contained a particularly striking wisp in the plate by Ritchey (1910), and several are visible in Figure A.1 and A.2. The brightest example is that of October 1963 (Figure A.2(c)), when there was a very sharp wisp in the ANVIL, 6".35 from S1. A by-product of the photometry described in Part IV is a determination of the relative intensities of the ANVIL and the series of wisps. For this date the wisp series contained three times the intensity in a swath 5" wide than did the ANVIL in a similar swath. It may be noted from Figure II.1 that the path of the microphotometer scan cut across the wisp series more centrally than it did the ANVIL, so that the true intensity ratio is somewhat smaller. An average factor

of from 2 to 3 is reasonable. In Chapter VI we shall show how it is possible for the wisp series on both sides to be intrinsically of the same brightness, so they may be similar structures placed symmetrically about the source of the activity. Another suggestive similarity is the occurrence of point structures in the ANVIL similar to the appearance of WISP 1 at its shortest. If we take the ANVIL features to be symmetrically related to the wisp series, an approximate center is defined. In particular, the midpoint of WISP 1 and the prominent wisp in the ANVIL of October of 1963 is well defined at 1".4 from S1 toward WISP 1. This is close to the mean position of the THIN WISP, and also within the error box recently reported by Gower (1967) for the location of the low-frequency point source. On the other hand, on some of the plates the THIN WISP and WISP 1 are curved toward one another by approximately the same amount, so possibly the center of symmetry is midway between at 4".8 from S1. Thus we cannot definitely locate the center of activity, but it probably lies a few " from S1. It is a curious fact, which needs explanation, that the location of the seat of the activity is not better determined by these very obvious motions. If there is no center, it is hard to understand how the motions are excited.

The SMALL WISP

This feature is quite faint even at its brightest, but is very definitely present on a number of occasions. In particular we mention the epoch of October 21, 1963, shown in Figure A.2.(c), when there was a small feature near the usual location of the SMALL WISP, visible on all five plates taken at that epoch, but visible on no plate before or since. It was small but definitely extended, and seemed to show peculiar polarization. In the figure in Appendix A it looks like a bright spot on the N end of the THIN WISP, but seems disconnected from it on the other plates. The point we wish to stress is that there is activity in this region (generally between and to the west of S1 and S2) which is at the limit of detectability.

Other Motions

A few attempts were made during this study to measure motions of features other than the wisps. The dark "lane" in the NW edge of the nebula has long been known to move rapidly away from the center. It is almost certainly the same as the "partially cleared space" mentioned by Lampland (1921) as a changing feature, and was noted by Oort and Walraven (1956, Figure 11). This object would better be described as two bright elongated lanes separated by a dark lane. The displacement from S1 of the two maxima and the intermediate minimum in

intensity can be measured rather accurately on the Grant engine. The results for a sample of the 200-inch plates are shown in Figure II.4. Parallel linear motion is well defined by the points, with a velocity of 0".68/yr., or v = .015c. The dashed line has this average slope and goes through the points for the dark lane. This motion,[1] if unaccelerated, would put the dark lane at the center in 1840. It is hardly conceivable that this object has been accelerated since 1054 to the present velocity, but it must be admitted that these measurements are not sufficiently precise to detect such an acceleration were it still acting. Dips in intensity possibly identifiable with the lane can be seen on plates from 1909 and 1899. The positions have been included in Figure II.4, although these points should be given small weight. The earlier of these plates (Pub.Lick Obs., 8, 1908, Plate 9), taken on Christmas Eve of 1899, is rather poor in the reproduction available. The other plate, taken by Ritchey (1910, Plate VII; the original could not be located, but a good copy was found), is much better, and shows both the filaments and the continuum emission with quite high definition. After examining both of these early plates and the more

---

1. The same feature was also measured by Deutsch and Lavdovsky (1940). For an unknown reason they measured the motion to the NE (the principal motion is to the NW), obtaining "about 0".1 per annum.

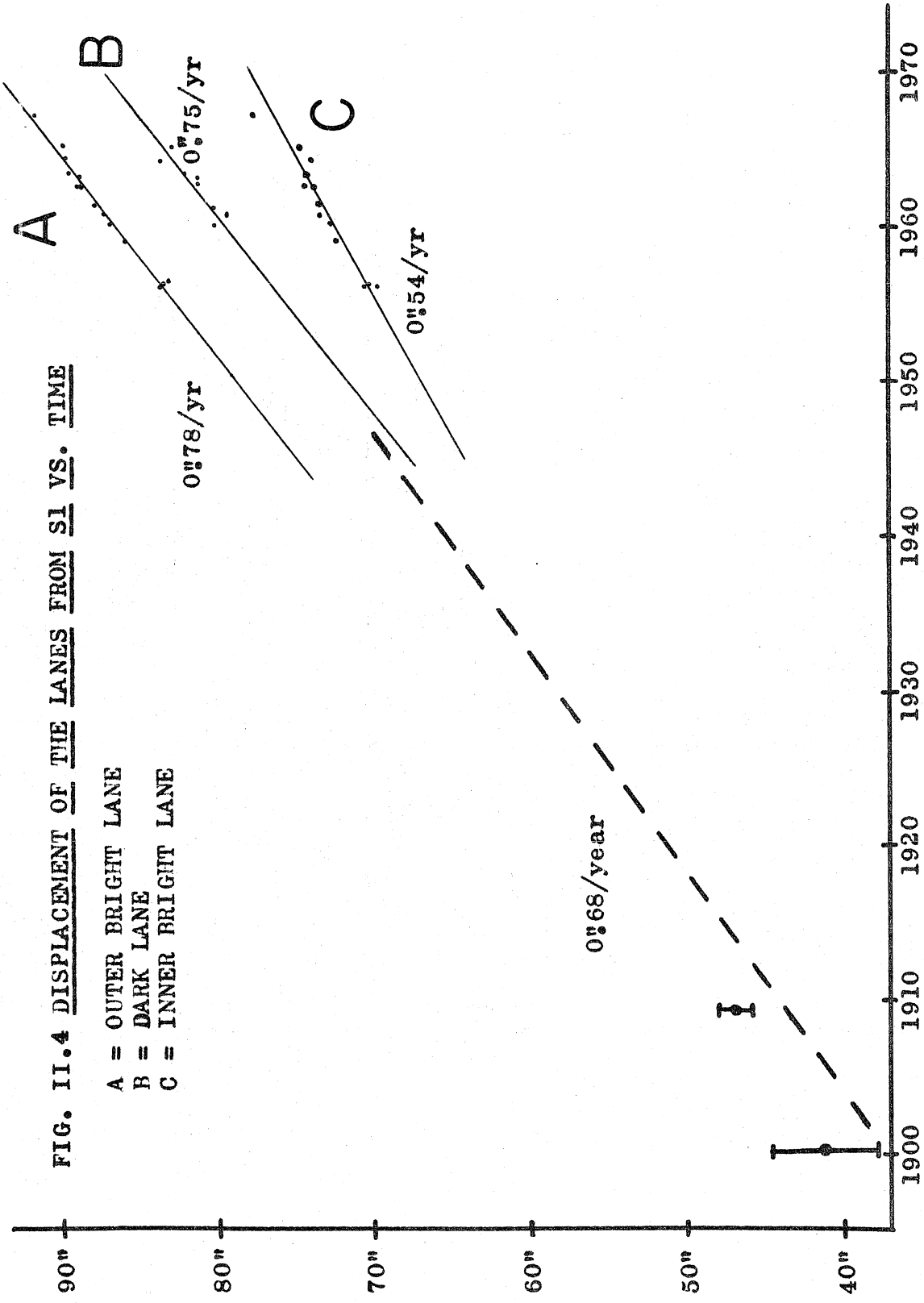

FIG. II.4 DISPLACEMENT OF THE LANES FROM S1 VS. TIME

A = OUTER BRIGHT LANE
B = DARK LANE
C = INNER BRIGHT LANE

recent ones, I have come to the conclusion that the two bright lanes now at the NW edge of the nebula are members of the wisp series which have propagated from the central region to their present positions. They are polarized similarly to the wisps. Their velocities are comparable to those of the wisps near the center (1" to 2" per year) and to the velocities we shall find in Chapter IV for motions in the intermediate region (1" to 6" per year). That their velocities are somewhat lower, near the edges of the nebula, may be evidence of a decrease of the field strength with increasing distance from the center; it may be also that the density of the thermal component increases outward. The lanes are in the NW quadrant, in approximately the region toward which the wisps seem to move. The difference and the lack of exact parallelism between the lanes and the wisps could easily be due to non-uniformity of the magnetic field. In fact, it is difficult to understand how the wisps could be preserved so well in the somewhat tangled field which the polarization suggests (Woltjer, 1957). Finally, it is evident from inspection of the plates that the wisp series extends quite far out into the NW quadrant, the members of the series gradually becoming increasingly diffuse and harder to distinguish because of the background. The region beyond the PLATEAU to the NW contains a number of diffuse elongated contours,

and the ones we have measured are merely the most obvious among them. This is perhaps most strikingly illustrated by the plate of 1909, on which there is a well-defined series of around a dozen wisps extending to the NW boundary of the nebula. We have already said that a particularly prominent dark space between these wisps can probably be identified with the dark lane now near the edge. If this identification is correct, the wisps beyond this dark space in 1909 must have by now left the visible extent of the nebula (or have perhaps reflected from the boundary).

Two other measurements were made. The polaroid plates which bring out objects elongated in the E-W direction show a sharply defined series of fibers near the northern end of the nebula. These are visible in the Frontispiece, which in fact is made from the two plates which were measured. Two fibers were found to move 1".53 and 1".47 in that period, indicating a velocity of 0".17/year, or $v = 4 \times 10^{-3} c = 1200$ km/sec. This motion is comparable to the general expansion of the filaments. A velocity of the same order of magnitude, but less well determined, was found for the inner edge of the BAY on the eastern edge of the nebula. Since this BAY seems to be connected with the general magnetic field in a fundamental way (Woltjer, as quoted by Mayall, 1962), it

would be expected to participate in the general expansion. There seems to be a trend for the faster motions to be concentrated in the NW quadrant, with some less conspicuous activity in the SE quadrant (see Chapter IV).

Despite the existence of these fast motions, it would be curious indeed if the continuum did not in some sense share in the general expansion of the nebula. We have just said that a few sharply defined features measured over our ten-year interval show this. In addition, three other measurements of the motion of the continuum features have yielded similar results (Deutsch and Lavdovsky, 1940; Johnson, 1963; Orlova, 1966). There are several problems which this kind of effort must overcome. The most difficult one is the lack of sharply defined features to measure (we picked the sharpest fibers and the edge of the BAY, but thereby sacrificed a representative sample). All three of the above studies employed microphotometer tracings, and measured peaks and level regions and sharp gradients in the density curves. (In Chapter IV we develop an extension of this technique.) This method is somewhat selective in choosing such features, but it is at least possible to make measurements all over the nebula. Another difficulty is that the early plates had spectral responses which admitted the filaments somewhat. Johnson attempted to check this contamination by measuring the features he had

selected on a plate that registered the filaments strongly, and found that there were no systematic differences between the measures on this plate and on the "standard" plates chosen to duplicate the early negatives as closely as possible. He concludes that the effect of the filaments is negligible, but the same results would be obtained if the features were dominantly filamentary. Another obvious check would be to inspect a direct plate and see how strong the filaments are in the location of the selected features; as nearly as can be discovered, none of the authors indicates whether or not this was done. It seems probable that some of the features measured in these studies are filamentary. It is unfortunate that it is not possible to evaluate more certainly to what extent these measurements refer to the continuum as opposed to the filaments, as this is a very important point in interpreting the results. For example, since Johnson seems to have been the most concerned with the influence of the filaments, and was the only one to obtain motions significantly different from the general filamentary expansion, it may be that there is a real difference of the sort which Johnson found (the results will be discussed below). Another problem is that in addition to the slow motions which would be measured by these three studies, using time intervals on the order of 60 years, there are faster

motions. To some extent the latter would be averaged out, but to some extent they will undoubtedly affect the measures, perhaps to the point of causing misidentification of features in some cases. This explains in part why the scatter in the velocities obtained is so great; some of the measured motions are <u>toward</u> the center.

It is difficult to decide how to consider the study by Duncan (1939). The plates used by him record primarily continuum radiation, but like the others admit the filaments also. The major difference is that Duncan made his measurements directly with a blink comparator, presumably of point-like features which can be located accurately by this device. We have seen that the continuum features are primarily elongated and fibrous, hardly suitable for the kind of measurement made by Duncan. Hence we shall not include his results in this discussion, on the basis that it is likely that the point-like filaments were measured for the most part. The measurements being carried out by Trimble (1968) will refer unambiguously to the filaments.

We shall now summarize the results of the three studies listed above. In all cases the scatter is too great for motions of individual features to have significance, so all data will be given in the form of averages. A convenient number is the date at which the

expansion converges to a point, assuming no acceleration. Deutsch and Lavdovsky (1940) obtain the date 1154 A.D. with an error of ±140 years. Including a correction for the three-dimensional distribution of the matter omitted by these authors, and using the same plates plus some modern ones, Orlova (1966) obtained 1100 A.D. ± 58 years. The weighted mean of these two figures, 1116 A.D., may be compared with Duncan's result of 1172 A.D. ± 20 years, and with Trimble's data 1140 ± 10 years (private communication). Johnson (1963) reports faster motions than any of the other studies. However, comparison cannot be made in a straightforward way, because Johnson finds an expansion velocity which is rather different in different directions. If we assume that the continuum features' fastest motions are responsible for this trend, we would expect that the most rapid "expansion" would be found along the major axis (to the NW). This relation is exactly opposite to what Johnson reports. On the other hand, the microphotometer traces made by Johnson along the major axis traverse regions of much stronger filamentary emission than do the ones roughly along the minor axis. It may be, therefore, that the effect of the slowly moving filaments along the major axis outweighs the effect of the faster motions of the continuum features there.

To summarize, we have found that there is motion

in the Crab Nebula, with a wide range of velocities. The fastest motion (up to 9".1/year) is exhibited by the main wisp, and the other wisps near the center. Other features in the continuum have intermediate velocities, ranging down to the rather slow velocity of the general expansion shown best by the filaments (e.g., the BAY and some of the well-defined fibers). The composite picture in the Frontispiece illustrates the intermediate motions rather well. If there were no changes in the nebula over the interval between the two plates (9.1 years), and if the cancellation of the positive and negative images were perfect, the picture would be uniformly grey. The slower velocities yield motion of one or two seconds of arc in this time (the scale is readily determined from the double star near the center with a separation of 4".9), which would be difficult to see. Note that the bays on both the east and west sides are almost invisible. The rapid motions of the wisps are too fast to be caught by this technique, but the intermediate motions on the order of 0".5/year show very well. The somewhat muddled wave-like appearance is suggestive of disturbances propagating outward from the center of the activity. As discussed in the Introduction, this activity is usually taken to be connected with the injection of energy into the nebula. The study of the

motions gives information about how the medium responds to the injection, but does not clarify the nature of the mechanism of injection beyond suggesting that relativistic motions are involved. In the next chapter we shall explore the added information provided by spectrophotometry of the continuum.

III. THE CONTINUOUS SPECTRUM

Consider the frequently suggested hypothesis that the process which generates the activity described in the previous chapter supplies[1] energy in the form of very high-energy ultrarelativistic electrons. One consequence of this proposition follows readily from the fact that for all relevant energy loss mechanisms (Kardashev, 1962) the loss rate increases with increasing energy: given certain reasonable assumptions about the energy distribution, if we follow a given bunch of electrons after their injection, their energy distribution must become steeper with time. The injection need not be in the form of discrete bunches, but may be a continuous process as long as there is some way to distinguish the old from the new electrons. An example would be continuous injection followed by a flow away from the point of injection. If there is no way to follow the electrons (e.g., if the injection takes place at a given location and the electrons are trapped there), then the time dependence of the energy distribution is governed by the injection. What is suggested in a general way by these considerations

1. This process, which will be called "injection" can be either in the form of addition of new high-energy electrons or by the acceleration of those electrons which are already present.

is that the energy distribution should become steeper farther from the injection region. Hence the spectrum of the synchrotron radiation would also become steeper, and this effect would be observable if it were large enough. We were thus inspired to carry out spectrophotometry of the continuum with high spatial resolution, especially in the active area, but also at representative points in the nebula and in the outermost regions.

None of the previous investigations are satisfactory for this purpose. Considering the widespread interest in the Crab, the number of observations of the continuum in the optical range is surprisingly small, probably because of the rather low surface brightness and the problem of contamination by the line emission from the filaments. Perhaps the earliest reference should be the lack of reports of a bright remnant in the years following 1054 (although to my knowledge an extensive search has not been made). The synchrotron radiation was originally invisible because the nebula was small and optically thick. It increased in total brightness as it expanded, and presumably could have attained naked-eye visibility before becoming optically thin and therefore decreasing in brightness. It would be valuable to check star maps based on observations in the years after 1054 for the appearance of a star in the position of the Crab.

Of some interest is Herschel's (Dreyer, 1888) description of NGC 1952 as "very bright". An attempt to calibrate his brightness notations by comparing them with modern photometry of planetary nebulae, even allowing for a dependence on the angular size of the nebula, failed. Still, the remark "very bright" compared to the present visual appearance of the nebula suggests that it was possibly much brighter then. Herschel's drawings (1912; see also Lassell, 1867) are too crude to allow any estimate of expansion, but the very general structure of the nebula has not changed since then.

Turning specifically to measurements of the continuous spectrum, the earliest photographic work seems to have been by Minkowski (1942) and Barbier (1945). The latter obtained a linear relation between log I and λ^{-1} (in microns), with slope -0.59 (the modern slope is around -0.40 in the same units). This is reasonable agreement considering the small wavelength range of Barbier's measurements (3300-4700Å). Walraven (1956) made photoelectric observations through wide-band filters, attempting to detect color variations across the nebula; contamination by the line emission prevented any definite conclusions. O'Dell (1962) used interference filters, some of which avoided line emission, to measure the continuum (as well as some line strengths) from the nebula as a whole and

from the central core. Most recently, Börngen and Chatschikjan (1967) have measured photographic UBV colors at many points in the nebula, with fairly high spatial resolution. As with Walraven, the filamentary contamination makes interpretation difficult. The authors promise a future paper correcting for the filaments.

The measurements reported here attempt to overcome some of the problems which plagued the earlier work, and to obtain improved spatial resolution. They were carried out with an interference-filter photometer at the 100-inch Newtonian focus.

The nocuous line emission from the filaments was suppressed by two methods. The first was the use of filters whose transmission bands fall in regions relatively free from lines. Of the eight filter used (data are given in Table III.1), only one transmits any strong lines: the doublet of [S II] at 6711Å and 6728Å falls in the band-pass of filter 6. This filter was therefore a useful indicator of the amount of contamination present. The filaments probably emit very faintly in a large number of lines other than those which have been reported (Mayall, 1937; Sanford, 1919; Woltjer, 1958; Münch, private communication). Lists of "planetary nebula lines" were searched, and the few such faint lines found are listed in

Table III.1. The substantial Doppler shifts must be kept in mind in evaluating the filters. To summarize, seven of the eight filters are free of all but very slight amounts of line emission.

The second method of suppressing the filaments was simply to measure areas of the nebula where they were weak (the beautiful Hα-interference filter plates by Münch show that there is no area of the nebula completely free of the small point-like filaments). The major strong filaments can be avoided rather easily, and quite some care was taken to select areas and diaphragm sizes which minimize the filamentary contribution and still cover representative parts of the nebula. Often strong filaments were located near the edges of the selected areas, so that accurate positioning of the diaphragms was necessary, and during nights of exceptionally bad seeing such configurations were avoided. The positioning was done by offsetting micrometrically from an easily visible star in the nebula (S8 in Figure II.1). Data on the diaphragms are given in Table III.2 and on the areas observed in Table III.3. The coordinates were measured off a large work print of an Hα plate, and are accurate to about 1". Once the telescope was set on a given area, the positioning was maintained during counts and reset after sky counts by means of a guide star. Hence the positioning was repeatable with an

TABLE III.1: FILTER DATA

No.	λ_c	$\Delta\lambda$*	λ_c^{-1}	log ν_c	E**	LINES
1	3478	400	2.876	14.936	3.4	H19-Balmer continuum,3HeI,5[OIII]
2	4190	150	2.390	14.855	4.1	HeI 4121,4144; HeII 4200; OII 4190
3	4706	162	2.124	14.805	4.9	HeII 4896; HeI 4731; misc. NIII,OII,CIII,[NeIV]
4	5484	116	1.823	14.738	3.8	[FeVI]; [ClIII]
5	6061	142	1.649	14.695	3.3	HeII 6005,6037,6074,6118
6	6786	183	1.474	14.646	2.2	[SII] 6717,6730
7	7453	193	1.342	14.605	.53	[ClIV] 7531
8	7950	370	1.258	14.577	.17	[ClIV] 8046

*These interference filters have nearly rectangular profiles, and little transmission occurs outside this bandpass (half-intensity width).

**This number is the approximate relative efficiency in arbitrary units, including bandwidth, transmission, and sensitivity of the S20 surface, but not atmospheric or telescope characteristics.

TABLE III.2: DIAPHRAM DATA

NAME	DIAMETER(mm.)	DIAMETER(")	AREA(sq.")	Δm*
A	0.74	11.8	109	0.00
B	0.95	15.2	181	0.54
C	1.50	24.0	452	1.53
D	2.35	37.6	1110	2.51
E	3.44	55.0	2380	3.34
F	5.15	82.4	5330	4.21
G	7.74	124.	12080	5.10
SPECIAL	.56x.19	9"x3"	27	-1.50

*Area expressed in magnitudes, relative to diaphram A.

TABLE III.3: OBSERVED REGIONS

No.	NAME	COORDINATES* x(EW)	y(NS)	DIAPHRAM(S)
1	Oke scan	7.57	2.83	C,D,E
2	south central	7.78	7.19	C,D
3		9.89	2.54	C
4	western ring	4.33	2.84	C
5		11.98	8.70	C
6	east bay	15.10	4.90	C
7	SW corner	4.72	6.93	C
8		5.35	0.68	C-A
9		3.25	-0.67	B
10	wisp	7.55	4.09	SPECIAL
11	wisp	7.47	3.92	A
12	arched filament	8.97	0.00	C
13	anticenter	8.69	5.22	B
14	on the east bay	12.65	5.30	C
15	SE end	16.75	6.64	C,D
16	NW end	1.44	-1.90	D
17	on the east bay	11.81	4.90	A
18	antiwisp	8.35	4.53	A
19	X-ray region	see notes		C

*The origin of coordinates is the star S8 in Fig. I.1, and the x-axis is parallel to the line joining S9 and S10. This line is 1^{o} 03' clockwise of true east-west. The coordinates are measured in milimeters at the Newtonian focus of the 100" telescope (1mm. = 16".2). X is taken as 10.00 at the origin and increases to the east; y is 0.00 at the origin and increases to the south.

NOTES TO TABLE III.3

1 This corresponds most nearly to the region scanned by Oke, and is the area of greatest general surface brightness (the "core" of the nebula). With diaphram D there is one minor filament, a few small points of filamentary emission, and a 16th magnitude star in the field. Accurate centering is rather critical, as there are strong filaments on the edges.

2 This is in the south central part of the nebula, a region fairly strong in the continuum. Centering is critical because of nearby stars and filaments, but within the region the filaments are quite weak.

3 Near region 1, and similar except that a smaller diaphram is used to discriminate against the filaments more strongly.

4 A region on the west end surrounded by a ring-like structure of filaments. The continuum is rather weak.

5 In the south east, with quite weak continuum.

6 This is located in the highly polarized "bay" on the east side. See also no. 17.

7 A region of faint continuum in the south west corner of the nebula, straddled by two bright stars.

8 A filament-free region in the western part of the nebula, with a fairly bright star in the center which can be subtracted by making measurements through A.

9 This is a small filament-free region in the NW.

10 The listed position is the usual location of the bright main wisp (and it was here in September, 1966). On the best nights the double star near the center could just be seen in the diaphram, and offsets were made to the wisp. Another method used on poorer nights was to set in the neighborhood of the wisp and make counts to maximize the counting rate (the wisp is a definite local maximum of surface brightness). The special diaphram is a very small elliptical pin hole in a piece of foil, and admits an area slightly larger than the size of the main wisp. The counting rates were on the order of tens per second.

NOTES TO TABLE III.3 (CONTINUED)

11 This is also the wisp area, but some measures were made with the larger diaphram A, in order to include other members of the wisp series.

12 This is the position of the very strong arched filament at the north end of the nebula, and was measured to check on the amount of filamentary contamination in the filters.

13 The Crab Nebula is rather symmetrical about the center, especially as seen in the polaroid plates at position angle 45^{o}. There is a region that is rather symmetrically related to the core (region 1), but not as bright. Unfortunately there are large, strong filaments running through it. This region is the clearest part of this feature. If C is used x=8.86 and y=5.39.

14 Located on the southern portion of the bay mentioned in note 6.

15 This is the very tip of the southeast extension of the nebula.

16 This is the very tip of the northwest extension of the nebula.

17 This region was selected for a measurement of the ultraviolet polarization which was never made. It lies in the bay, and is strongly polarized. Lying between two stars, it should be easy to locate and guide on.

18 As discussed in note 13, there is a great deal of symmetry in the nebula. There is no exact reflection of the wisp, but the "anvil" discussed in Chapter II is the next best thing.

19 When it was believed that the x-ray source was rather localized, it was decided to make a lattice of measures in the suspected region to check for a peculiarity in the optical spectrum. Since then it has been learned that the x-ray source is not strongly localized.

NOTES TO TABLE III.3 (CONCLUDED)

COORDINATES OF THE X-RAY LATTICE

No.	x	y
19.1	8.00	3.00
19.2	8.00	2.00
19.3	8.00	1.00
19.4	7.00	1.00
19.5	7.00	2.00
19.6	7.00	3.00
19.7	7.00	4.00
19.8	7.00	5.00
19.9	6.00	5.00
19.10	6.00	4.00
19.11	6.00	3.00
19.12	6.00	2.00
19.13	6.00	1.00

TABLE III.4: PHOTOMETRIC DATA

REGION/ DIAPHRAM	C_1	m_2	C_3	C_4	C_5	C_6	C_7	C_8	α	E(UV)	E(SII)	DATE
1/D	+.36	12.42	-.33	-.70	-.93	-1.24	-1.44	-1.54	2.25	+.07	+.03	1/16/67
1/D	+.35	12.48	-.37	-.69	-.97	-1.27	-1.42	-1.57	2.23	+.05	+.05	1/13/67
1/C	+.37	13.23	-.33	-.66	-.95	-1.24	-1.44	-1.59	2.27	+.07	+.02	1/13/67
1/D	+.35	12.48	-.35	-.69	-.96	-1.27	-1.45	-1.57	2.27	+.07	+.04	2/04/67
1/D	+.36	12.49	-.34	-.67	-.92	-1.28	-1.42	-1.59	2.24	+.07	+.08	2/04/67
2/D	+.37	12.90	-.40	-.76	-1.02	-1.47	-1.53	-1.68	2.38	+.05	+.17	1/13/67
2/C	+.39	13.76	-.35	-.75	-.99	-1.47	-1.56	-1.68	2.44	+.07	+.17	1/13/67
	±.01	±.01	±.01	±.01	±.01	±.01	±.02	±.04				
3/C	+.36	13.36	-.35	-.67	-.96	-1.26	-1.48	-1.62	2.31	+.08	+.03	1/13/67
	±.01	±.01	±.00	±.00	±.00	±.00	±.01	±.02				
4/C	+.35	14.37	-.38	-.62	-.98	-1.36	-1.56	-1.66	2.39	+.19	+.09	1/13/67
	±.01	±.01	±.01	±.01	±.01	±.01	±.02	±.04				
5/C	+.25	14.98	-.32	-.73	-.97	-1.75	-1.65	-1.56	2.46	+.24	+.45	1/16/67
5/C	+.41	14.87	-.34	-.71	-.92	-1.62	-1.42	-1.32	2.11	-.04	+.46	1/13/67
	±.02	±.02	±.01	±.02	±.01	±.01	±.03	±.09				

TABLE III.4 (CONTINUED)

REGION/ DIAPHRAM	C_1	m_2	C_3	C_4	C_5	C_6	C_7	C_8	a	E(UV)	E(SII)	DATE
6/C	+.18	15.84	-.27	-.73	-.96	-1.94	-1.52	-1.68	2.45	+.33	+.67	1/16/67
6/C	+.31	15.83	-.18	-.64	-.86	-1.89	-1.51	-1.38	2.31	+.21	+.73	1/13/67
	±.03	±.03	±.03	±.04	±.03	±.02	±.05	±.15				
7/C	+.30	14.68	-.42	-.87	-1.10	-1.54	-1.72	-1.88	2.68	+.19	+.08	1/16/67
7/C	+.23	14.68	-.42	-.75	-1.05	-1.45	-1.69	-1.86	2.59	+.26	+.06	1/13/67
	±.02	±.02	±.01	±.02	±.01	±.01	±.02	±.05				
10/	+.31	16.32	-.30	-.65	-.87	-1.24	-1.29	-1.35	2.01	+.05	+.14	1/16/67
SPECIAL	+.34	16.52	-.42	-.81	-.95	-1.27	-1.24	-1.42	1.96	-.08	+.11	3/07/67
	±.05	±.05	±.03	±.04	±.03	±.03	±.09	±.24				
11/A	+.35	14.91	-.33	-.70	-.93	-1.12	-1.50	-1.71	2.37	+.12	-.13	3/07/67
11/A	+.48	14.72	-.26	-.61	-.90	-1.18	-1.53	-1.56	2.37	+.04	-.02	3/07/67
	±.02	±.02	±.01	±.02	±.01	±.02	±.03	±.06				
12/C	+.15	14.63	-.45	-.68	-.98	-2.33	-1.85	-1.65	2.55	+.33	+.97	1/13/67
	±.01	±.02	±.01	±.02	±.01	±.01	±.02	±.06				

TABLE III.4 (CONTINUED)

REGION/ DIAPHRAM	C_1	m_2	C_3	C_4	C_5	C_6	C_7	C_8	α	E(UV)	E(SII)	DATE
13/B	+.33	14.78	-.34	-.64	-.92	-1.95	-1.54	-1.77	2.42	+.17	+.69	2/04/67
	±.02	±.01	±.01	±.01	±.01	±.01	±.02	±.04				
14/C	+.49	14.54	-.34	-.67	-1.05	-1.62	-1.63	-1.96	2.67	+.08	+.25	2/04/67
	±.03	±.02	±.01	±.02	±.02	±.01	±.03	±.05				
15/D	-.08	15.60	-.42	-.18	-.82		-1.74	-2.26	2.67	+.75		2/04/67
	±.06	±.08	±.05	±.14	±.06		±.09	±.14				
16/D	+.45	14.66	-.48	-.79	-1.18	-1.94	-1.89	-2.07	2.89	+.10	+.39	2/04/67
	±.05	±.04	±.02	±.04	±.02	±.01	±.04	±.07				
17/A	+.75	16.90	-.35	-.69	-1.16	-2.64	-1.90	-1.84	2.89	-.13	+1.16	3/07/67
	±.11	±.08	±.04	±.08	±.04	±.02	±.07	±.21				
18/B	+.37	14.86	-.40	-.74	-1.03	-1.46		-1.71	2.38	+.05	+.16	3/07/67
	±.02	±.02	±.01	±.02	±.01	±.01		±.07				

TABLE III.4 (CONCLUDED)

REGION/ DIAPHRAM	C_1	m_2	C_3	C_4	C_5	C_6	C_7	C_8	α	E(UV)	E(SII)	DATE
19.1/C	+.38	13.30	-.29	-.64	-.92	-1.24	-1.47	-1.67	2.36	+.11	+.02	2/04/67
19.2/C	+.34	13.48	-.33	-.65	-.95	-1.45	-1.52	-1.70	2.40	+.14	+.20	2/04/67
19.3/C	+.33	13.80	-.35	-.65	-.94	-1.70	-1.66	-1.79	2.53	+.20	+.39	2/04/67
19.4/C	+.31	13.76	-.37	-.71	-1.00	-1.83	-1.67	-1.78	2.56	+.21	+.48	2/04/67
19.5/C	+.36	13.46	-.33	-.67	-.96		-1.48		2.34	+.11		2/04/67
19.6/C	+.40	13.29	-.31	-.67	-.93	-1.25	-1.45		2.31	+.05	+.03	2/04/67
19.7/C	+.35	13.33	-.34	-.67	-.96		-1.47		2.32	+.10		2/04/67
19.8/C	+.34	13.61	-.37	-.65	-.95		-1.53		2.35	+.11		2/04/67
19.9/C	+.26	13.70	-.36	-.63	-.93		-1.61		2.42	+.23		2/04/67
19.10/C	+.34	13.55	-.34	-.68	-.97		-1.53		2.39	+.13		2/04/67
19.11/C	+.36	13.53	-.31	-.65	-.94		-1.48		2.33	+.11		2/04/67
19.12/C	+.31	13.64	-.34	-.69	-.96		-1.58	-1.68	2.44	+.17		2/04/67
19.13/C	+.42	13.76	-.34	-.69	-.98	-1.67	-1.67	-1.79	2.57	+.12	+.34	2/04/67
	±.01	±.01	±.01	±.01	±.01	±.01	±.02	±.03				

accuracy limited by the seeing. The procedure was to alternate eight counts on the nebula with eight sky counts, always ending with a set of nebular counts so that the systematic changes with hour angle (extinction and sky background) would cancel in the average. In the early runs it was found that the sky brightness varied quite smoothly with hour angle, and during one night (February 4/5, 1967) the sky was measured only infrequently, and then interpolated. Also, on one night (March 7/8, 1967) the sky was measured through a very large diaphragm in order to reduce the statistical errors. The added inconvenience of changing diaphragms frequently and determining the ratios of the areas of the diaphragms accurately were bothersome, but this procedure seemed to be a slightly more efficient use of the telescope time (especially since the largest errors are the statistical ones, due to low counting rates).

The observational results are listed in Table III.4. The first column identifies the region by its number in Table III.3 and the diaphragm size as given in Table III.2. The next eight columns give the intensities in terms of the magnitude measured through filter 2 (m_2) and the colors relative to this filter ($c_i = m_i - m_2$). The magnitude m_2 gives the intensity for the entire area admitted by the diaphragm, and can be reduced to an average surface brightness using the data given in Table III.2. The listed errors are those expected from statis-

tical fluctuations alone, and were calculated from the equations given by Baum (1962). Because of the low object/sky ratios for many of the areas, it is important to use these equations rather than the simpler form often employed. The statistical errors for Region 1 are all less than $0^m.01$, and have been omitted. The non-statistical errors for all the regions can be judged by comparing the five independent measurements of Region 1, and are seen to be typically $\pm 0^m.02$. The next column gives the spectral index, α, a measure of the slope of the continuum to be defined and discussed below. The next two columns give the excesses of the intensity measured through filters 1 and 6 over the amount expected from the other measurements, and will be discussed later in this chapter. The last column gives the date of the observation.

In connection with presenting the data graphically the question arises: which plane is more appropriate, the Log I-Log ν or the Log I-ν plane? The synchrotron theory predicts a linear relation in the former if the electrons emitting in the spectral range of interest are distributed in energy according to a power law. On the other hand, electrons near an upper cutoff combine to form an exponentially decreasing radiation spectrum, i.e. linear in the Log I-ν plane. In principle we could use this result to decide whether the optical electrons are near the upper

cutoff or not, a question which is important in connection with the nature of the X-rays. In practice the observational accuracy necessary to distinguish the two cases is rather too high. An elementary calculation shows that over the range covered by our filters the maximum difference between a power law and an exponential curve is on the order of $0^m.03$. Uncertainties in the shape of the reddening curve (the total amount of reddening enters in a less important way) plus observational and calibration errors would be comparable to or larger than this difference. If the measurements were extended to 10,000Å the difference between the two laws could be as large as $0^m.1$. Getting back to our measurements, the raw data are more linear in the Log I-Log ν plane (from the above discussion, this fact must be a reflection of the shape of the reddening curve, and hence provides no information about the intrinsic spectrum of the Crab), which is therefore used to display the data.

Region 1, the core of the nebula, was observed most often and with the best statistical accuracy.[1] Its colors from Table III.4 are plotted in Figure III.1, along with a scan with the 60-inch telescope of roughly the same

---

1. This is probably the only case for which the statistical error is not the largest source of uncertainty. The good agreement between data for different nights and different air masses indicates that the other errors are rather small.

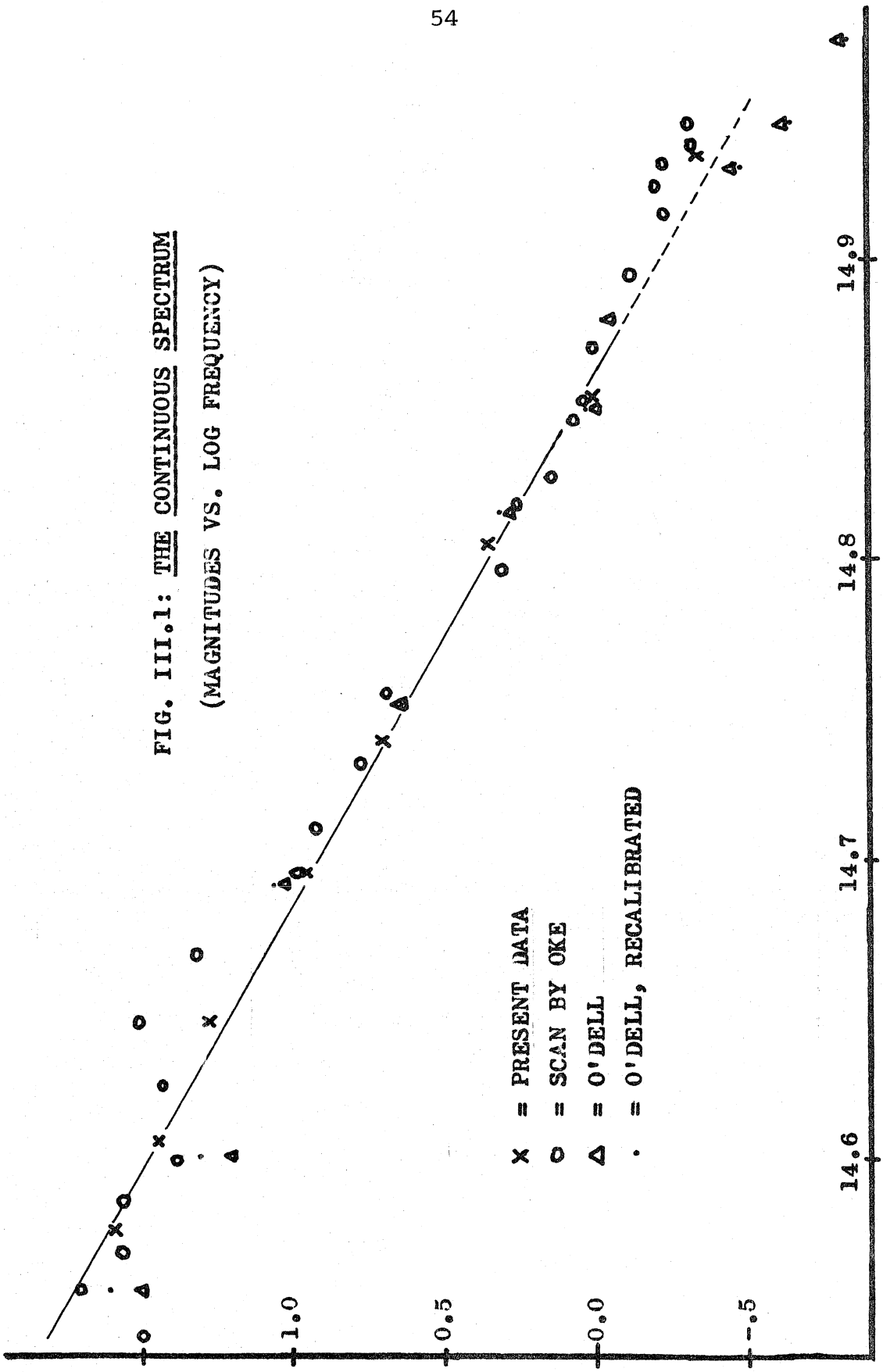

FIG. III.1: THE CONTINUOUS SPECTRUM

(MAGNITUDES VS. LOG FREQUENCY)

region, kindly communicated by J. B. Oke, and also O'Dell's (1962) measurements. The curves are shifted vertically to obtain approximate agreement at log ν = 14.855 (filter 2). The present data agree well with those of Oke, the only significant difference being in the region where the [SII], [NII], and Hα lines affect the continuum intensity in a way that is very sensitive to the positioning and size of the diaphragm. O'Dell's intensities are $0^m.1$ to $0^m.2$ fainter on the red and blue ends of the range covered. Part of this discrepancy is removed if recent improvements in the calibration of Vega (Oke, private communication) are included, as shown in the figure. The present data fit well to a straight line, except that the ultraviolet point is significantly too bright. Oke's scan shows the same effect even more clearly, the points in the ultraviolet gradually turning up from the linear relation. O'Dell's UV points show, if anything, the opposite trend.[1] The straight line drawn in Figure III.1 is a least-squares best fit to the points for filters 2-5, 7 and 8, weighted inversely by the statistical errors. Data for the other regions have

---

1. O'Dell's observations are older and made with smaller telescopes than the ones reported here. Also it should be mentioned that they refer to an unspecified area containing the whole nebula as well as a number of stars (25 stars averaging 15^m could influence the measured intensity of the nebula by roughly $0^m.1$). Nevertheless, it is not intended to reject his results. We simple take the concordant data of Oke and myself at face value in order to see what the implications are.

been treated similarly: the quantity α in Table III.4 is the slope of the least-squares line divided by 2.5 so that it corresponds to the usual "spectral index" of the radio astronomers. The excesses of the intensities in filters 1 and 6 above this line are listed in the same table. The latter can be directly interpreted as the emission in the [SII] doublet, and is a convenient index for the filamentary contamination. The ultraviolet excess is not so easy to interpret, and will be discussed below.

We first examine the distribution of the spectral index over the nebula. It will be assumed that the effects of differential reddening can be neglected, so that any differences observed are intrinsic. Figure III.2 shows a plot of the index for the various regions against their distance from the central star S1. Filled circles are regions lying in the NW half of the nebula, and the open circles are for the SE. This distinction was made because of the apparent asymmetry of the activity, which appears to be concentrated largely to the NW. It can be seen in the figure that there is a steepening of the spectrum with distance from the center. No particular significance is attributed to a linear relation, but it can be noted that the filled circles all fall very close to the line drawn in the figure. If all the regions are considered together, the trend is less obvious but still unmistakable.

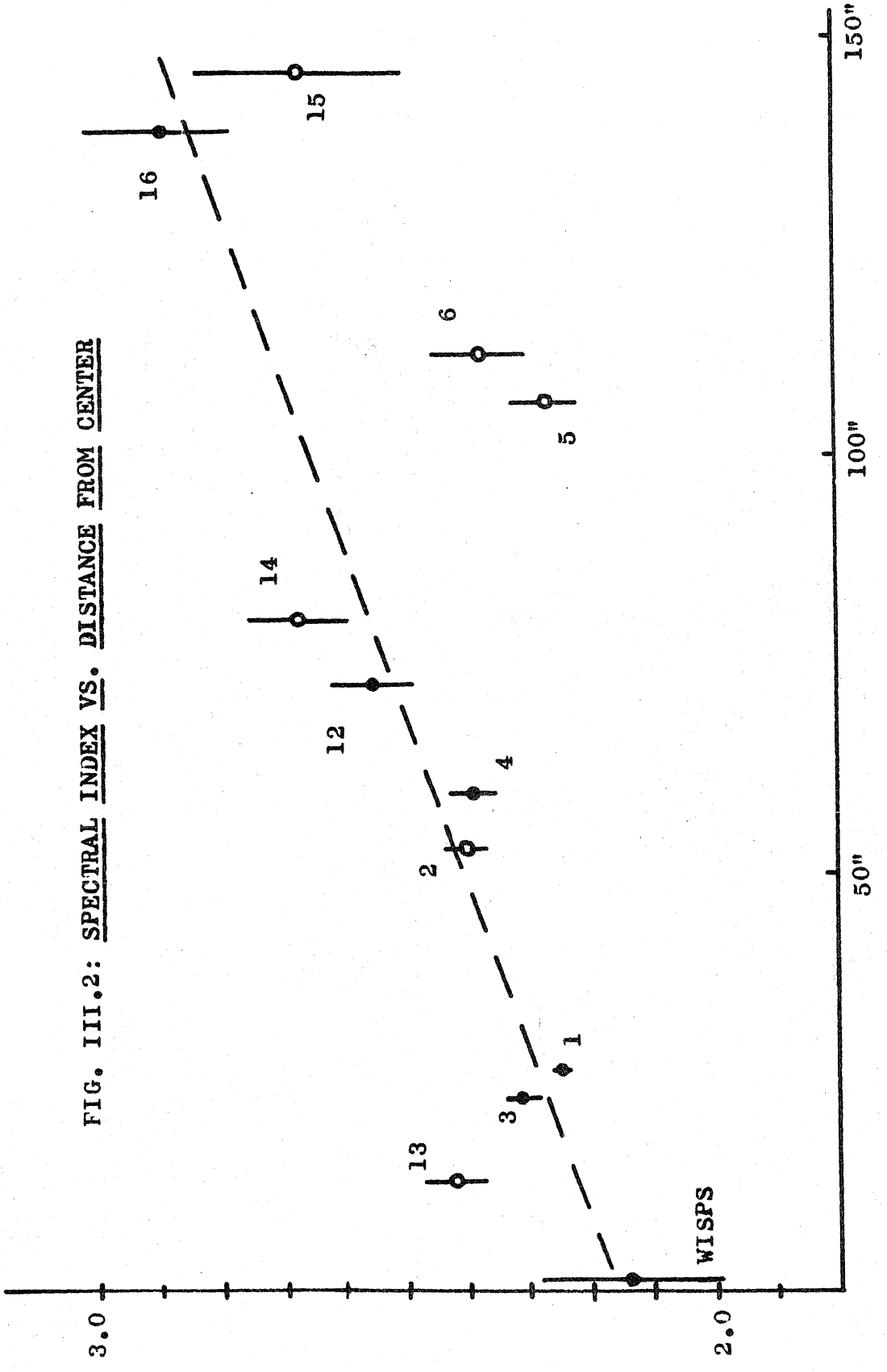

FIG. III.2: SPECTRAL INDEX VS. DISTANCE FROM CENTER

No region farther from the center than Region 1 has a small measured spectral index than does this region.

Unfortunately the most important observation, that of the main wisp, is the most difficult. Four measurements were made, two through a special diaphragm constructed to admit just the main wisp, and two through the standard circular diaphragm 12" in diameter. In both cases, location of the wisp was difficult because it cannot be seen visually. The methods used to set the diaphragm are described in the notes to Table III.3, #10. The success of these methods can be judged post facto by noting that the measured surface brightness for the wisp in the special diaphragm is very nearly the same as for the core of the nebula (Region 1). This is quite consistent with the known relative surface brightness from the direct plates, and assures that at least part of the wisp was in the diaphragm (for the surface brightness surrounding the wisp is low compared to the core). The spectral results for the four attempts are tabulated below. The wisp may have an index of $\lesssim 2.0$ if the higher value with diaphragm A is due to the contribution from the surrounding nebulosity (area of A/area of wisp ~ 7).

MEASUREMENTS OF THE MAIN WISP REGION

diaphragm	spectral index	average
special	2.01 ± .05	1.99
special	1.96 ± .10	
A	2.37 ± .10	2.37
A	2.37 ± .10	

Additional evidence for variation of the slope of the spectrum is obtained from the grid of measurements made in the NW quadrant (Region 19). The original inspiration was the possibility of detecting some peculiarity in the spectrum due to a small object in this region. In particular the X-ray source was thought to be localized in this general vicinity (Bowyer et al, 1964), but is now known to be rather large (Oda et al, 1967). These measurements were made under essentially identical conditions, on a very good photometric night (internal consistency of the standards was better than $0^m.01$ for all except m_8, which ranged over $0^m.03$). Transit occurred during the sequence of 13 measures, and sec z ranged from 1.026 to 1.059. Hence even gross errors in the extinction (which are certainly not present) would not affect the differences in the measured spectra. It is therefore established that the expected errors in the relative values of the spectral index are rigorously those due to statistics alone. On this basis the expected deviation of α is ±.01.

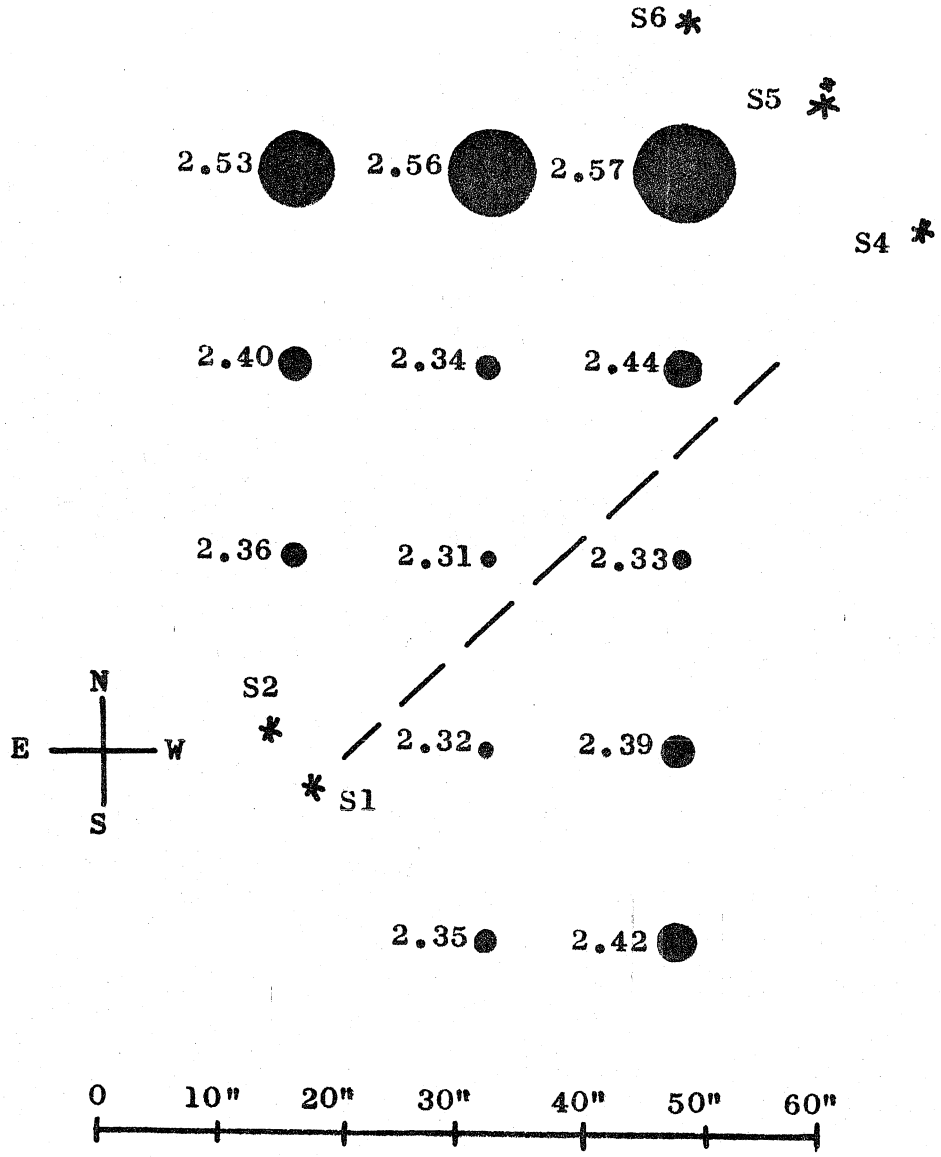

FIG. III.3: GRID OF SPECTRAL INDICES IN NW QUADRANT

Thus the smooth trends shown in Figure III.3 are real. The diameters of the circles shown are linearly related to the value of the spectral index, which is also written next to the circle. The centers of the circles are located at the points of the grid, the spacing being 16" and the diaphragm diameter 24" (moderate overlap). The slope in every case increases away from the line defined by the wisp series and their motions, and also increases outward along this line. These facts are taken as direct evidence of a connection between the activity and the slope of the spectrum. The sense and amount of the change are consistent with the trend indicated by the other more general measurements (Figure III.2).

Radio astronomy supplies interesting evidence on the matter of variations of the spectral index. There was much discussion of this point based on the earliest series of occultations (November 1955 through January 1956), but the reported large differences in the steepness of the spectrum are probably spurious. The more recent occultation observations (Andrew et al, 1964; Davies et al, 1966; Gotwols, Erickson, Fremouw, and Owren, 1966; Taylor, 1966; Krishnan, Zisk, and Cudaback, 1967) are much more reliable and consistent, primarily due to instrumental advancements. In particular we call attention to the results of Davies et al, at 404 Mc/s and 1420 Mc/s. Their effective resolution was about 10", and many of the

gross features visible in the optical region can be identified on their brightness strip distributions. The optically bright WISP/PLATEAU region is absent at radio frequencies, as might be expected from the flatness of the spectrum we have observed. Moreover, Davies et al, report the following: (1) by comparing the 1420 Mc/s data with the optical intensities of Woltjer (1957), the spectral index is 0.16 steeper at the edges (Woltjer's contour of intensity 5, compared to 300 at the center) than at the center; and (2) from the data at the two radio frequencies the index is 0.12 steeper at the half-intensity level than at the center. These results agree with our purely optical data, except that the amount of the change in α is somewhat larger than in the radio region. The meaning of the change in slope of the continuous spectrum across the face of the nebula will be considered in Chapter VI.

The other aspect of the spectrum which will be discussed is the so-called ultraviolet excess, defined above as the excess intensity as measured through the violet-most of the filters above a linear extrapolation of the measurements through the other filters. Is this excess real? The amount of the difference (E (UV) in Table 2.4) is rather small (generally $\lesssim 0^m.2$), but consistently positive except for a few cases in which the expected errors are large. The agreement on the

existence and approximate amount of the UV excess between the present data and the scan of Oke (observer, dispersing element, telescope, and date were all different) suggests that the absolute calibration is a possible source of error, as it was common to the reductions of both sets of data. (The extinction, of course, was determined completely independently even for different nights.) However, a calibration error of this size ($\gtrsim 0^m.06$) does not seem likely, and its effect would probably be obvious in the scans of other objects (e.g., stars whose atmospheres are believed to be well understood).

Next, consider the effect of interstellar reddening on the shape of the spectrum. The change in the slope of the reddening curve at around $\lambda^{-1} = 2.0$ is in the direction such that it would simulate the observed UV flux excess in a highly reddened object. For each magnitude of total absorption the differential increase in the UV-intensity (filter 1) over the blue (filter 2) is $^m.028$ (reddening data is taken from Whiteoak, 1966). Hence, to explain the excess of $0^m.065$ for Region 1 (the best determined case, and one of the freest from possible filamentary contamination) a reddening of $A_V \sim 2^m.3$ would be necessary. If this large value were correct, the dereddened intensity would vary as $\nu^{+0.41}$! This reversed slope cannot be absolutely ruled out, but it would require

an additional radiation mechanism or a peculiar energy distribution for the synchrotron electrons (cf. our remark on this point below). If we insist that the true spectrum be no flatter than the radio curve ($\alpha \sim 0.3$), the maximum reddening allowable is $A_V = 1.68$. So far we have not said anything about the actual value of the absorption to be expected. This is a very uncertain quantity. There have been two studies of reddening in stars in the direction of the Crab. The photoelectric data collected by O'Dell (1962) is more detailed and accurate, but only eight stars were included. Brodskaya (1963) presents photographic photometry and objective prism spectroscopy of 86 stars. Both authors graph A_V against distance. O'Dell's values for the total absorption are systematically larger than Brodskaya's (by $0^m.3$ to $0^m.8$). The best procedure would probably be to shift Brodskaya's mean curve to run through O'Dell's points, but even then high accuracy could not be expected. Since the exact distance to the nebula is not known, the reddening is even more uncertain. The limiting value of $A_V = 1^m.68$ proposed above comes at approximately 1700 pc. from both authors' data. A distance of 2000 pc. or more is certainly possible given this limit and the uncertainties involved, but would strongly imply a reddening of at least $1^m.6$ and $\alpha = 0.3$. Then, if the X-rays are a continuation of the synchrotron

spectrum, the "break" in the spectrum must come to the violet of the visible region. (It is interesting that if the radio and X-ray/gamma ray spectra are extrapolated with power laws, they meet at about 2000Å.)

Since reddening cannot explain all of the ultraviolet excess, we must also consider the possibility that it is a property of the radiation from the nebula. For example, the filaments are a source of ultraviolet radiation through lines and the Balmer continuum. If such contamination were the source of the excess, it would be strongly correlated with the [SII] excess, an effect which is not found. There is some correlation in the sense that when the [SII] index is very large, the UV excess is also larger than average (e.g. in Region 12, centered on the strong arched filament at the north end of the nebula, the [SII] excess is nearly a magnitude, and the UV excess is $0^m.33$. However, when the [SII] emission is only moderate or absent, there is a residual UV excess of between $0^m.06$ and $0^m.12$.

A second possibility is that the excess is due to thermal radiation adding to the synchrotron spectrum to produce the observed flattening in the ultraviolet. It has been suggested by a number of authors that the X-rays from the Crab are produced by a thermal gas with $T \sim 10^6$ to 10^8 °K and $n_e \sim 10^2$ cm^{-3}. The chief

objection to this has been (Shklovskii, 1966) that such a plasma in the known magnetic field would depolarize the radio emission via the Faraday rotation. Recently Sartori and Morrison (1967) have proposed a model which to some extent avoids this difficulty. The thermal gas is postulated to be located mostly in the north-west quadrant of the nebula, as suggested by the X-ray data (see especially Oda et al, 1967). The fact that the polarized radio emission is displaced toward the south-east relative to the total power centroid (Allen and Barrett, 1967, at 2 cm; Seielstad, private communication, at 21 cm.; but c.f. Davies et al, 1966) is taken as evidence of the depolarizing effect of the X-ray plasma. The bremsstrahlung spectrum in this model would have a long flat tail (perhaps more appropriately called the dog) extending into the optical range. Curiously enough, their model yields an intensity in the ultraviolet that would give an excess of about $0^{m}.06$ above the synchrotron spectrum[1]. In addition, however, the UV radiation would have to be strongest in the NW part of the nebula, and the present data do not indicate

---

1. The sum of the flat bremsstrahlung dog and the decreasing power-law synchrotron spectrum is roughly the observed flattened spectrum. However, when this point is considered more quantitatively it is found that the transition between the regions dominated by one of the two types of radiation is rather broad (roughly an order of magnitude in the frequency in this case).

any such skewness. Hence it does not seem very plausible that this is the explanation of the excess. Furthermore, the model of Sartori and Morrison would not be tenable if the X-ray emission were distributed rather like the optical radiation, a possibility that is entirely consistent with the X-ray measurements (Oda et al, 1967). In any case, the method of avoiding the Faraday rotation is artificial, and it has not been shown that it can explain the polarization data quantitatively.

Finally, it must be kept in mind that a synchrotron spectrum need not be linear, and under some conditions an initially linear spectrum will evolve into one with a flattened portion on the high-frequency end (Kardashev, 1962; De La Beaujardiere, 1966; Hirth, 1967; McCray, private communication). An accurate measurement of the ultraviolet polarization would clearly give an important clue about the nature of this excess.

To summarize the data, the observed continuous spectrum is described well by the $I \propto \nu^{-\alpha}$ law, with α increasing slowly with distance from the center of activity. This effect is most pronounced in the NW half of the nebula where a difference of $\Delta\alpha \sim 0.9$ is indicated between the wisp region ($\alpha \sim 2.0$) and the NW corner ($\alpha \sim 2.9$). For the whole nebula $\Delta\alpha \sim 0.4$. In addition, there is a flattening in the ultraviolet, some of which is due to the

curvature of the interstellar reddening law. If the extinction is $A_V = 1.6$ (which is likely if $d = 2000$ pc.) a residual UV excess of at least $0^m.02$ may be intrinsic to the nebula. Several possible sources of this ultraviolet radiation have been mentioned.

IV. ANALYSIS OF THE PLATES FOR WAVE PROPAGATION

In the following chapter we shall see how the wisps and their rapid motions should theoretically produce disturbances propagating outward into the nebula in the form of hydromagnetic waves. Indeed, as shown in Chapter II there are features beyond the main wisp which participate in the activity, and may be disturbances initiated by the motions of the main wisp itself. These wisps are seen out to distances on the order of 20" from the center. The motions even further out are perhaps slower and more regular than those near the center, but they are evidence that even near the edge of the nebula the hydromagnetic velocity is still a few percent the speed of light. The present chapter describes an attempt to detect motions in the intermediate regions of the nebula.

The first clue of a general field of motions appeared on a composite photograph made from two polarization plates taken about a year apart (see Zwicky, 1956, for a description of the technique). As expected, the composite demonstrated clearly the motion of the wisps. In addition the NW region of the nebula showed a mottled appearance, visually suggestive of a field of waves or ripples with fronts approximately parallel to the elongation of the wisps. There was no evidence for motions

in any direction other than toward the NW. Experimentation proved that the ripples show best with the polaroid orientation 45° (i.e., parallel to the wisps) and with the time interval roughly one year. The subtlety of the features precluded satisfactory photographic reproduction, but a similar composite is shown in the Frontispiece. This plate shows the more distinct and widespread changes which appear with longer time intervals.

A rigorous check of these photographic results is desirable, especially in the case of the changes detected for the smaller time intervals. Microphotometer tracings of the sandwiched negative and positive plates confirmed the visual appearance, in the sense that a series of wave-like features showed up on the tracings, and were larger than the noise due to granularity. But the real problem with the method of composite photography is the danger that spurious effects in the intermediate stages might cause incomplete cancellation of the stationary structure. In the present case most of the positives cancelled very well against their parent negative (the ones that didn't were rejected), but this does not insure that cancellation between different plates will be faithful. One can imagine a number of tests of this technique, such as repetition with different positives, correlation between different plates and different polaroid orientations, and cancellation of

an object which is known not to change.

The procedure that was actually adopted does away with the intermediate photographic processes altogether, and is based on photometry of the original plates. Because they exhibit activity most strongly, the plates with polaroid orientation 45° were used exclusively. Microphotometer scans were made along a path traversing the region of greatest activity as indicated by the composite plates. The path of the scan is shown by the line in Figure II.1. The slit was narrow (1".3) in the direction of motion, which was perpendicular to the apparent wave fronts. This gave resolution in the direction of scan comparable to that permitted by the seeing on most of the plates. A slit length of 5".5 gave a satisfactory integration over plate granularity and corresponded roughly to the length of the mottles as seen on the composite plates. A longer slit should reduce the noise, but it was felt that the signal from possible waves might be reduced too. The scans were stored digitally on magnetic tape in a form suitable for computer analysis. The sampling rate of the digitizer was such that even at the fastest speed of the microphotometer table the resolution was much greater than necessary. The resolution in intensity was also much greater than need be, given the inherent inaccuracies of the photo-

graphic process. Nearly all the information on the region of the plate scanned by the slit was stored on the tape. Information concerning variations along the slit is lost, but should be unimportant.

The conversion to intensity profiles was first effected by means of the wedges made for the plates by Münch. This calibration gave relative intensities which were consistent from plate to plate to an accuracy of about ±5 percent. The profiles could then be normalized to the same total intensity and used in the subtraction process to be described shortly. However, there is an easy way to greatly increase the consistency of the calibration. Ten short regions on the scan were used as standards of intensity. They were chosen to cover the relevant range of densities, and also were located in areas of the nebula not indicated to be active on the composite photographs. Since the intensity changes actually found are small, even if there are some variations in the ten regions the effect on the calibration is small. The intensities at these points were determined by averaging the values obtained with the calibration by the wedges. It will become clear that the method does not depend on these intensities being correct in an absolute sense. The calibration curve (intensity as a function of density) was constructed for each plate by fitting a 5th order

polynomial to the ten points in a least squares sense (giving higher weights to the densities relevant to the regions of the nebula scanned). The residuals from this calibration curve were always so small that the ten points were essentially forced to lie very nearly on the calibration curve, which should therefore represent very accurately the true relation between intensity and density. The order of the polynomial is low enough to avoid oscillations in the curve. Even if the intensity values for the ten standard points are slightly incorrect, this error will affect all plates in the same way.

Because of the rapid sampling rate, there were many more values of the intensity than needed, so the profiles were smoothed using a Gaussian filter, and the smoothed profiles were stored at intervals comparable to the width of the filter. This width was chosen to be roughly the resolution limit of the plate, so that no information be lost.

The final step in the procedure was to subtract the intensity profile for a given individual plate from the intensity profile averaged over a number of the plates. This method was found to be more satisfactory than subtracting one plate from another (less noise). The registration for this subtraction was conveniently provided by stars along the scan. The scale of the plates was

found to vary by less than one part in 10^3. The resulting intensity differences would be zero if there were no changes in the nebular intensity, and if there were no errors in the entire process of converting the true intensity to numbers. A sample of an intensity difference curve is shown in Figure IV.1, where the upper portion is the region to the NW of the center, and the lower to the SE. The intensity scale on the left of the figure refers to an arbitrary system of units in which the maximum intensity along the scan (where it crosses the core of the nebula) is 0.72 units.

These profiles show, as must be expected, a great deal of noise, part of which is due to the granularity of the plates. In a more general sense, some of the noise is due to the statistical nature of the entire photographic process. The density of a given area of the plate is a random variable, whose mean is related to the intensity focused onto that area of the plate. Consider, for simplicity, the image of an object that is perfectly uniform. A small area of the plate would have a density which might differ substantially from the "true" density corresponding to the actual surface brightness of the object. A larger area will on the average have a density closer to this ideal, because of the greater statistical sample. But no matter how large the area sampled, there will still be

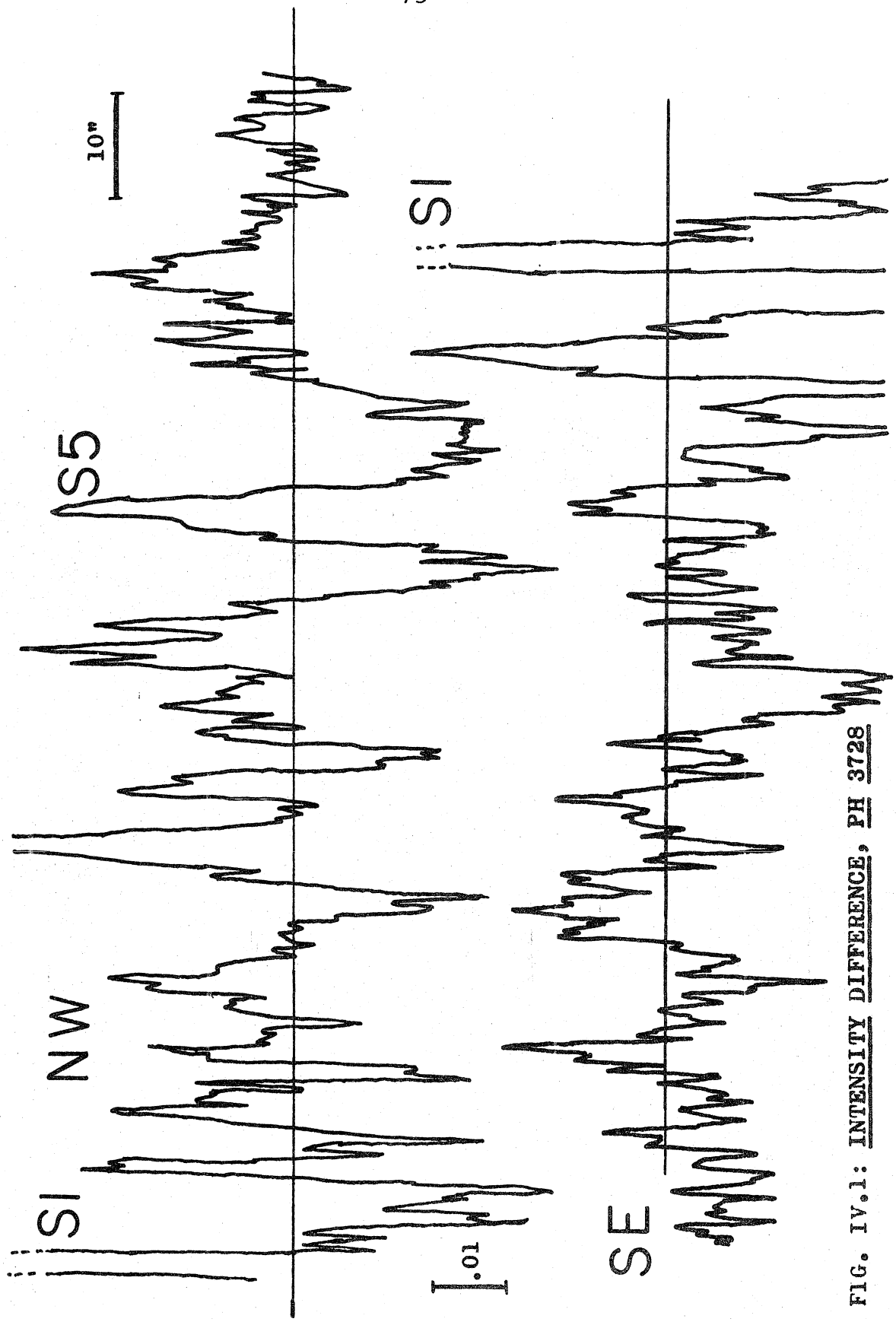

FIG. IV.1: INTENSITY DIFFERENCE, PH 3728

some randomness in the integrated density. Clearly this source of noise will be operative in a more complicated way when the intensity is not uniform, but rapidly varying as in the Crab Nebula. The scale[1.] of this particular kind of noise is not limited to the size characteristic of the plate grains. There will be some noise on all scales. This statistical process is not the only source of noise. Differences in the seeing on the plates obviously plays a role, and contributes noise on the scale of the size of the seeing disk. Also the calibration errors will introduce noise of a character which is hard to estimate. Registration errors will give noise that will depend on the size of the errors, and should primarily influence the phases of the Fourier components (see below). Clearly the total noise is a very complicated statistical process, and it would be difficult to predict its power spectrum a priori.

The problem is to extract a signal (any real intensity difference) from this noise. The graphs of many of the intensity difference profiles look to the eye as though there may be a signal consisting of "waves" of a rather ill-defined characteristic wavelength. Since

---

1. In speaking of the scale of the noise, we have in mind the description of noise in terms of its power spectrum - that is, in terms of spatial Fourier components of various wavelengths

there is bound to be some noise at this wavelength, a subjective judgement of this sort is hard to interpret. A better way to analyze the data is to perform a Fourier analysis and exhibit the component of the difference profile which varies at different frequencies. The advantage is that, for example, the high frequency components which cannot be significant are readily eliminated. This elimination was done to some extent in the smoothing process, which is essentially a filtering out of the high frequency components. For two sections of the scan (indicated by ticks on the line in Figure II.1) a finite Fourier series was calculated numerically. I.e., if x is distance on the plate and the length of the region scanned is L, we write the intensity difference profile as

$$I(x) = \sum_{n=0}^{\infty} A_n \cos\left(\frac{2\pi x}{L} n - \phi_n\right), 0<x<L.$$

A_n and ϕ_n are the amplitude and phase of the n-th Fourier component. The two regions were essentially radial paths from the center to the NW and to the SE. Neither included any of the main wisps, and both ended before the intensity dropped close to the sky background. It was suggested by the composite plates that the section to the NW would show real motions, while that to the SE seemed inactive and was meant to be a control region.

The amplitudes of the Fourier components as a function of spatial frequency (we shall call these curves power spectra, a term conventionally applied to the absolute square of the amplitude) are graphed for some of the plates in Figure IV.2. The abscissa is the harmonic number n: n=1 corresponds to a wave of length equal to the entire portion of the scan which was analyzed, namely 53".1. The intensity scale is as in Figure IV.1. The solid lines are the power spectra for the NW scan, the dotted for the SE. It can be seen that the power spectra for the NW region are generally larger than those for the SE for the longer wavelengths, $n \lesssim 20$. At the higher frequencies, the two regions' power spectra have comparable magnitudes. The indication is that the NW has more activity at these wavelengths. Plots of the phase of the Fourier components as a function of frequency show, for the most part, the expected random behavior. Often the low frequencies show some sign of non-random behavior, as would be expected if there is a real signal present at these frequencies. On a number of the plates the very highest harmonics had phases very nearly equal (i.e., nearly constant with frequency). The reason for this unreal behavior is not understood, but fortunately these components are not significant.

The result so far is interesting, but unsatis-

FIG. IV.2: POWER SPECTRA

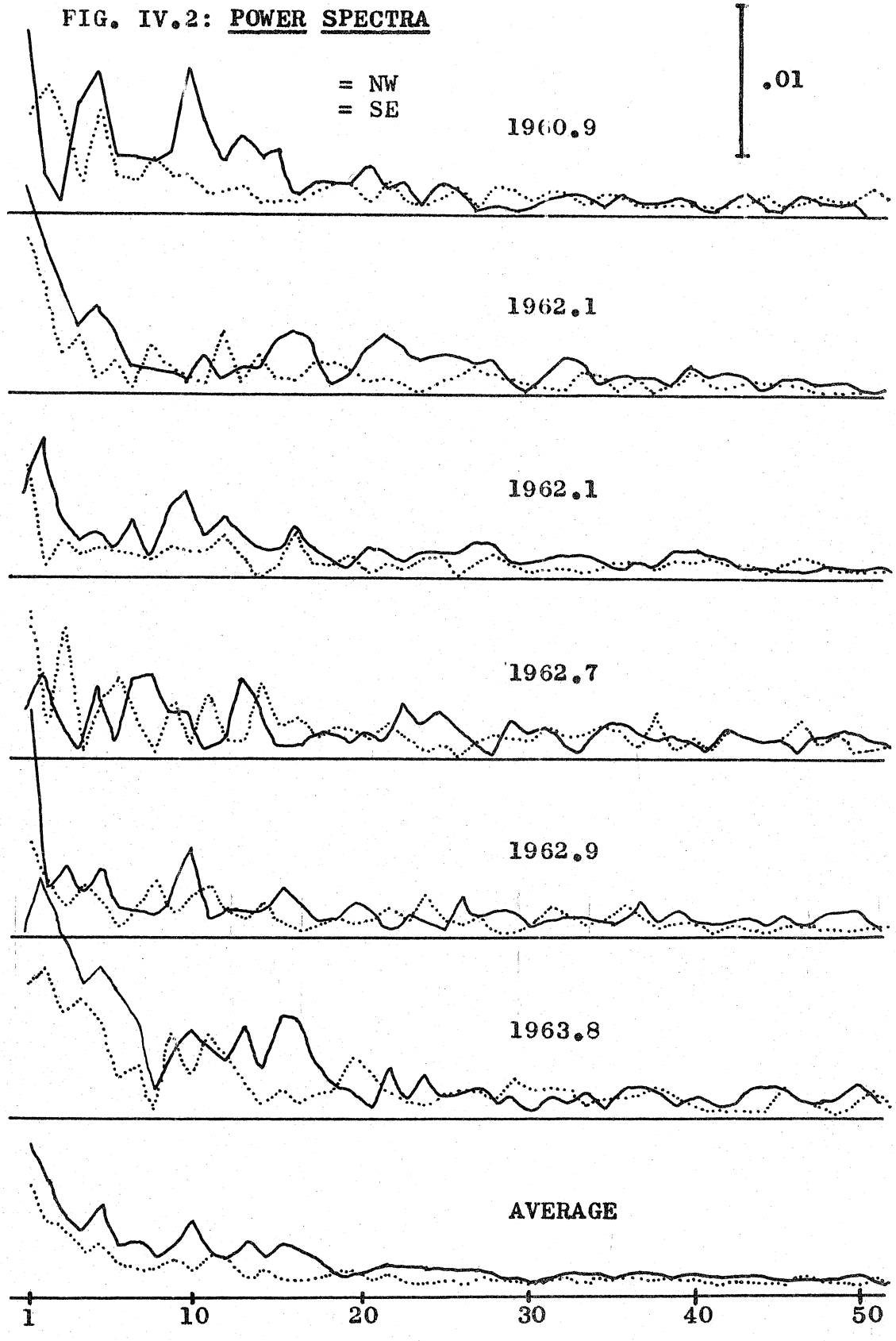

factory because of our lack of knowledge of the noise power spectrum. It is not clear whether the spectrum for the SE region is similar to the spectrum of pure noise, or whether there is some real activity in this part of the Crab also. Furthermore, it is not known how much of the difference between the power spectra of the two regions and the noise spectrum could be due to random fluctuations.

There is one further step in this analysis that may resolve these questions, and that is a more careful discussion of the phases of the Fourier components. The phase determines the displacement of the components from some fiducial point. Hence if the bumps in the power spectra are real in the sense that they represent actual disturbances in the nebula, then there should be a relationship between the phases for the various plates. The nature of the relation depends on the manner in which the disturbances are propagating. For example, if they are standing waves, the phase may depend on frequency (i.e., which Fourier component is being discussed), but should not vary with time. Or if a wave of a given frequency propagates at a constant phase velocity, the phase should be a linear function of time. Unfortunately, it is difficult to analyze the time dependence of the phase of a component of a given frequency.

Not only is there a great deal of scatter in the phases, but there also is an ambiguity of an integer multiple of 2π which usually makes it possible to fit the data with lines of several different slopes. The data were analyzed from this point of view, and the impression gained was that the slope of the phase-time relation is not very dependent on frequency. All attempts to find slopes proportional to frequency failed. It is clear that this method is highly subjective and the results just mentioned must be taken lightly.

Obviously we need to average the phases for a given plate over frequency in order to reduce the scatter. Unfortunately the nature of the average which must be taken depends on the manner of propagation. For example, if the disturbances are visualized as bumps containing a spread of spatial Fourier components, but the bump as a whole propagates at a constant velocity, the time-rate-of-change of the phase of any given component would be proportional to its frequency. This can be seen from the equation for the expansion written above: following a given part of a wave, dx/dt is proportional to $d(\phi_n/n)/dt$. Thus, the quotient phase/frequency should be averaged and examined for a linear dependence on time. The phase ambiguity is particularly troublesome in this average, and no conclusive result could be reached. For

the simpler direct average of the phase itself, the ambiguity was easily resolved and it was found that the vector averaged phase correlated very well with time. Figure IV.3 shows for the NW scan the time dependence of the average for harmonics n=3 through n=12 (λ = 17".7 to 4".4), which were judged to contain the most activity based on the power spectra. Since there is an ambiguity of $\pm 2k\pi$ (k any integer) in the phase, one is perfectly at liberty to add such a phase shift to bring the points as close as possible to the selected linear relation. That is to say, all the points are forced to lie somewhere in the region of the plane between the two dashed lines. There is a significant correlation to the extent that the actual points differ significantly from a random distribution within this region. Actually, it is more complicated than this, because the line is not just any line, but will be the one chosen to fit the points as well as possible. That is to say, even with a random distribution of points, the line can be chosen to minimize the scatter. The importance of this effect depends somewhat on the number of points (decreasing from the obvious singularity at two points to no effect with a large number of points). Neglecting this complication and taking a uniform distribution of points within the allowed region, the expected r.m.s. deviation of an individual point from

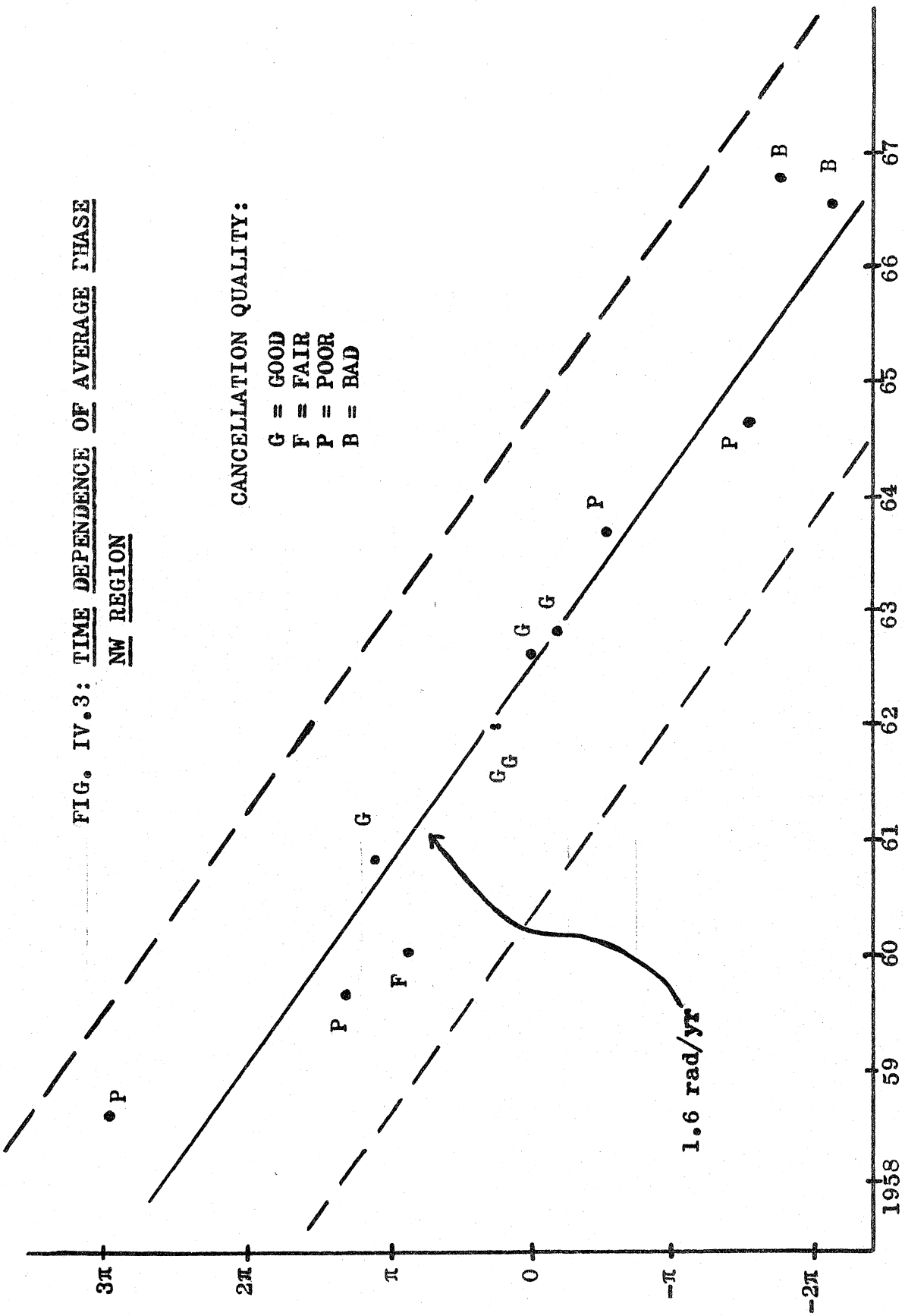

FIG. IV.3: TIME DEPENDENCE OF AVERAGE PHASE
NW REGION

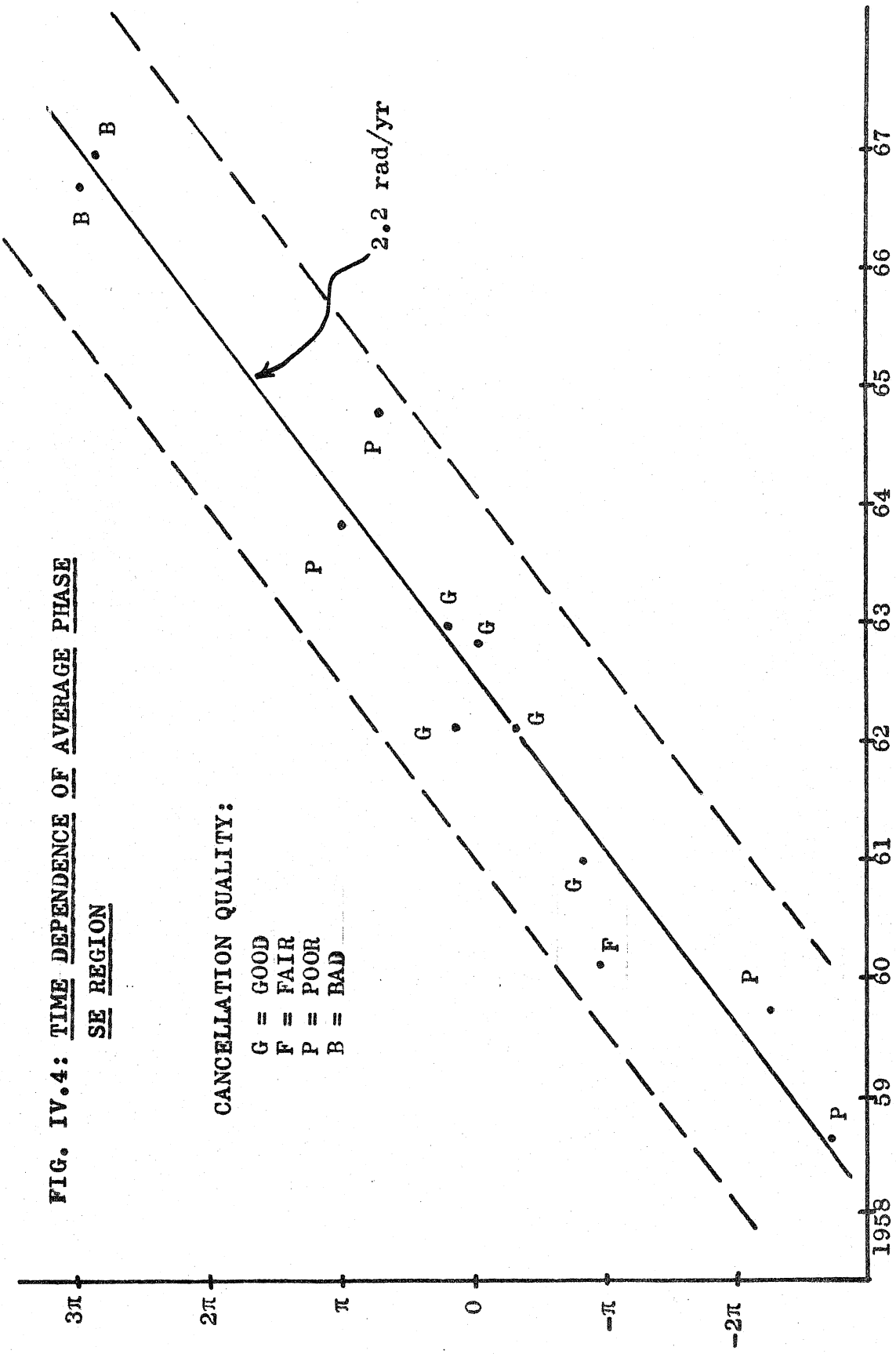

FIG. IV.4: TIME DEPENDENCE OF AVERAGE PHASE
SE REGION

the straight line is $\sqrt{\frac{2}{3}}\,\pi = 2.56$. The points in Figure IV.3 were weighted according to the quality of the cancellation, as judged from the smallness and smoothness of the intensity difference profile. The weighted r.m.s. deviation of the "good" points in Figure IV.3 from the straight line was 0.26 radians, for the "fair" points 0.78 radians, and 2.6 radians for the "poor" points. Hence the statistical evidence for the existence of a correlation between phase and time is very good. The averaged intensity profile with respect to which the subtraction was performed was obtained from the middle six plates in the time series. This no doubt explains why the cancellation seems better for these plates, and why the correlation with time is better. Possibly there are rather substantial changes over the complete time interval, perhaps enough to affect the calibration scheme. A less significant correlation is found for the region to the SE (see Figure IV.4). It has a slope of the opposite sign, which means that for both regions the motion is away from the center.

Thus from two different ways of looking at the data we obtain the indication that the rate at which the phase changes with time is roughly independent of frequency. This result is surprising but can be interpreted in a simple way as being due to perspective. Let the vector $\vec{a}$

lie along the line of the microphotometer scan and also perpendicular to the line of sight to the nebula, and let $\vec{k}$ be a vector in the direction of propagation of a wave of wavelength λ and velocity v. These quantities will also be the observed wavelength and velocity if the vectors $\vec{a}$ and $\vec{k}$ are parallel. But if $\vec{a}$ and $\vec{k}$ are at an angle θ, the apparent (projected) wavelength of the wave will decrease by the factor $\cos\theta$ and so will the apparent velocity. That is to say, the (spatial) frequency of the projection of the wave is larger, but the rate of change of the phase is observed to be the same. Our microphotometer scans along a given direction undoubtedly include disturbances propagating at a whole range of angles θ: some of the vectors $\vec{k}$ will have components toward or away from us (consider a spherical wavefront) and some will have position angles different from the scan direction. But if the actual phases of all the waves have the same time dependence, so will the observed projected waves. Thus our data would be explained if all the waves had <u>the same temporal frequency</u> ω.[1.]

---

1. If there were any intrinsic differences in wavelengths, the velocity of propagation would have to satisfy $2\pi v/\lambda$ = constant = ω. Any other distribution of the observed wavelengths would be due to projection. The analysis of the next chapter yields the theoretical result v = constant, so that the above relation could be satisfied only if all the waves had the same intrinsic wavelength. As only the projected wavelengths are observable, there is no observational check of this fact.

It is not necessary that the waves be strictly monochromatic, but only that they be generated, roughly speaking, at a characteristic frequency, which might be identified with the crude two-year periodicity in the motion of the main wisp noted in Chapter II. The period given by the slope of the line in Figure IV.3 is 3.5 years, so the numerical agreement is poor, but then so is the determination of the periods.

As described at the beginning of the chapter, this analysis was inspired by the suggestive but inconclusive results of composite photography. However, it should be noted that the technique can also be viewed as an extension of the method used by several authors (see Chapter II) to study motions in the Crab Nebula. Instead of measuring only selected features, we have in effect included the whole intensity profile. Also, because we were looking for faster changes on a shorter time scale and with small amplitudes, the analysis of the data had to be rather complex. The method has been only partially satisfactory, mostly because the effects appear to be near the threshold of detection set by the noise of the process. The difference profiles show significant changes with a time scale on the order of years, but the changes can only vaguely be described as propagating waves. Numerical Fourier analysis yields a description of the

changes in terms of sinusoidal components with a range in wavelength of about a factor of four, but with the propagation velocity of the individual components being roughly proportional to the wavelength. This curious behavior could be explained if the observed disturbances are waves of a single temporal frequency seen at various angles of projection. This frequency is on the order of 6×10^{-8} sec^{-1} ; the basic wavelength involved is somewhere in the upper part of the range 4"-18", corresponding to a propagation velocity $\lesssim$ 5"/year.

V. THE PROPAGATION OF DISTURBANCES IN A RELATIVISTIC GAS

The existence and motions of the wisps were the starting point of our development in Chapter II of some of the observational aspects of the activity in the center of the Crab. This chapter will begin from the same facts and probe into some of their theoretical implications. We shall presuppose that the wisps are localized enhancements of the general synchrotron emission. The direct plates (Chapter II) and the photoelectric data (Chapter III) prove that the wisps have a continuous spectrum, and the polarization plates show that they are strongly polarized. Thus the evidence for this assumption is the same as that for the synchrotron hypothesis in general. The theory of synchrotron radiation implies that such a feature must roughly speaking be an enhancement of the quantity

$$N\, B^{\frac{1}{2}(s+1)} \quad (s = \text{index in energy power law}), \qquad (1)$$

where N is the density of relativistic electrons (see the discussion in Chapter VI). Actually the quantity in (1) is approximate in several senses; the exact expression depends on certain assumptions, and is discussed in Appendix C. Let us ignore temporarily the observed motions and see

if the wisps can be interpreted as static features. In such an equilibrium situation it can be shown from the equations of motion given below that, as in the classical case, the magnetic and gas pressures must balance:

$$P + B^2/8\pi = \text{constant.} \qquad (2)$$

Thus in regions where the field happens to be stronger than average, the gas (particle) pressure is lower. The effects on the synchrotron emission tend to cancel, but the forms in (1) and (2) show that the cancellation is not exact, and visible inhomogeneities could be present. However, Parker (1967) and Lerche (in a series of papers referenced in Lerche, 1967) have shown that a gas-magnetic field system tends toward a uniform state in which the pressure is isotropic and the same everywhere. In addition to unstable waves which isotropize the pressure if it is initially anisotropic, there will be motions along the field lines which will eliminate pressure gradients. The latter will occur at roughly the speed of sound, which we will show is a few percent $\underline{c}$ in the Crab. These motions are therefore rapid enough to have established constant gas and magnetic pressure since the origin of the nebula, unless there have been disturbances subsequently. (The behavior of the main wisp discussed in Chapter II is possibly an example of this diffusion along the lines of B.)

Under these conditions the emissivity should also be constant. Thus the hypothesis that the plasma in the Crab is in static equilibrium is not consistent with the existence of the wisps and other obvious inhomogeneities. Indeed, it may be noted that the most striking departures from homogeneity (the wisps) exhibit the fastest motion, while the more slowly moving features (as discussed in Chapter II) are generally smoother.

This discussion has been rather academic, as the wisps and other features are observed to move. This motion is sufficient to disturb the plasma in the nebula, and one would expect propagation of the disturbances just as in a classical gas in a magnetic field. In this chapter we shall discuss the theory of such propagation, in order that a comparison between the observed and theoretical properties can be made. In this discussion it will always be assumed that there is both relativistic and thermal[1] gas making up the plasma, as the latter turns out to be important in determining the propagation velocities. Indeed, we will use this relationship to estimate the amount of thermal gas present. The subscripts "R" and "T" will distinguish quantities defined for the two

---

1. The thermal component consists of those particles which have a kinetic energy which is small compared to the rest mass energy.

components, and "B" will refer to the magnetic field.

The subject of relativistic magnetohydrodynamics has been developed by a number of authors (most recently: Tuab 1948, Harris 1957, Lerche and Parker 1966, Lerche 1967, Lichnerowicz 1967), and such quantities as propagation velocities for various modes are known. For the Crab, one can estimate the energies at which the usual magnetohydrodynamic approximations will break down. If we take the wisps ($\sim$2" wide) to be the smallest inhomogeneities, the condition that the gyration radius be less is $\gamma < 6\times10^{8}$. If the fastest time scale for changes is taken as 3×10^{6} sec (the braking of the main wisp), the condition that the gyroperiod be less is $\gamma < 1.5\times10^{8}$. (The fact that these two numbers are the same order of magnitude is not a coincidence.) Thus if the 500 kev. gamma radiation recently observed by Haymes et al (1967) is synchrotron, the electrons are beginning to violate the adiabatic invariants[1]; nevertheless, the majority of the plasma satisfies the usual MHD assumptions. That is to say, the magnetic field is strong enough that the relativistic version of the Chew, Goldberger, Low method (Scargle, 1968) is valid. In this note we showed that the energy-momentum tensor for a relativistic gas in a magnetic field is given

---

1. Whether or not this can really be so is an interesting question. If the orbits are not helical, the character of the synchrotron radiation is altered.

by[1].

$$T_{\alpha\beta} = \left[1 + \frac{P_\perp - P_\parallel}{2} \frac{8\pi}{B_0^2}\right] T^{(a)}_{\alpha\beta} + \frac{1}{2}(P_\perp + P_\parallel) g_{\alpha\beta} + (P_\parallel + \mathcal{E}) U_\alpha U_\beta, \quad (3)$$

where $P_\perp$ and $P_\parallel$ are the pressures perpendicular and parallel to the field lines, B_o is the magnetic field strength measured by an observer moving with the fluid (for whom we take $\underline{E}=0$; it is possible to include a component of $\underline{E}$ parallel to the field, which would be important for a calculation of the sort of collisionless damping studied by Barnes (1967), but is not important in the present context; the perpendicular component of $\underline{E}$ is zero because of the high conductivity of the fluid). $\mathcal{E}$ is the <u>total energy density</u>, including rest-mass energy, for the same observer, and $T^{(a)}_{\alpha\beta}$ is the electromagnetic tensor, which enters because of its contribution to the energy-momentum directly (the 1 in square brackets), and also because the magnetic field determines the direction about which the pressure is symmetric (the term proportional to $P_\perp - P_\parallel$). In a frame where there is no electric field, this tensor

---

1. We shall use c=1 except in cases where the meaning is clarified by writing $\underline{c}$ explicitly. The signature of $\underline{g}$ is +++- , so $g_{11} = g_{22} = g_{33} = -g_{44} = 1$, and all the other elements are zero.

can be written (Lichnerowicz, 1967):

$$T^{(2)}_{\alpha\beta} = \left(u_\alpha u_\beta + \tfrac{1}{2} g_{\alpha\beta}\right)\frac{B_0^2}{4\pi} - \frac{B_\alpha B_\beta}{4\pi}\,, \tag{4}$$

where $B^{REST}_\alpha = (B_1, B_2, B_3, 0)$. Substituting (4) into (3) yields

$$T_{\alpha\beta} = \left(p_\perp + \frac{B_0^2}{4\pi} + \varepsilon\right)u_\alpha u_\beta + \left(p_\perp + \frac{B_0^2}{8\pi}\right)g_{\alpha\beta} - \frac{B_\alpha B_\beta}{4\pi}\left[1 + \frac{p_\perp - p_\parallel}{2}\,\frac{8\pi}{B_0^2}\right]. \tag{5}$$

The equations of motion and conservation of energy are contained in the equations

$$\frac{\partial T_{\alpha\beta}}{\partial x_\alpha} = 0 \qquad (\beta = 1,2,3,4). \tag{6}$$

Now consider the case of one-dimensional motion perpendicular to a uniform homogenous magnetic field; that is

$$u_\alpha = (\gamma u, 0, 0, \gamma)\,, \tag{7}$$

where $\gamma = (1-u^2)^{-1/2}$, and

$$B_\alpha = (0,0,B_0,0)\,, \tag{8a}$$

$$E_\alpha = (0,0,0,0)\,. \tag{8b}$$

All quantities will be assumed to vary only along the direction of motion and with time. The four equations in

(6) reduce to the following two:

$$\frac{\partial}{\partial x_i}\left[\gamma^2 u^2\left(p_\perp + \frac{B_o^2}{4\pi} + \varepsilon\right) + \left(p_\perp + \frac{B_o^2}{8\pi}\right)\right] + \frac{\partial}{\partial t}\left[\gamma^2 u\left(p_\perp + \frac{B_o^2}{4\pi} + \varepsilon\right)\right] = 0 , \qquad (9a)$$

$$\frac{\partial}{\partial x_i}\left[\gamma^2 u\left(p_\perp + \frac{B_o^2}{4\pi} + \varepsilon\right)\right] + \frac{\partial}{\partial t}\left[\gamma^2\left(p_\perp + \frac{B_o^2}{4\pi} + \varepsilon\right) + \left(p_\perp + \frac{B_o^2}{8\pi}\right)\right] = 0, \qquad (9b)$$

the other two equations being trivial. The continuity equation,

$$\frac{\partial}{\partial x_\alpha}\left(\rho^o u_\alpha\right) = 0 , \qquad (10)$$

where ρ^o is the proper density of rest mass (see Synge 1957), becomes

$$\frac{\partial}{\partial t}\left(\rho^o \gamma\right) + \frac{\partial}{\partial x_i}\left(\rho^o \gamma u\right) = 0. \qquad (11)$$

Harris (1957, p. 1359; see also Taub 1948, p. 331) has shown that the energy conservation equation (eq. (9b)) can be replaced by an equation expressing the conservation of entropy along the streamlines, which - coupled with the equation of state - can in turn be replaced by an explicit relation between the pressure and the density ρ^o (<u>viz</u>. $P \propto (\rho^o)^{\Gamma}$). Hence, the motion is determined by equations (9a) and (11), plus the appropriate constitutive

relations. Equation (11) is exactly Taub's equation (5.13), and (9a) is equivalent to his equation (5.14) if his pressure, p, is replaced with $P_\perp + B_0^2/8\pi$ and his total energy density, $\rho_0 c^2 + \rho_0 \epsilon$, becomes our $\mathcal{E} + B_0^2/8\pi$.[1] Therefore, the results derived by Taub for the propagation of disturbances in a relativistic gas with no field can be carried over with no modifications (except for the substitutions mentioned) to the case of disturbances moving perpendicular to the field lines. Parallel propagation can be treated in a similar way if the substitution $P_\parallel \rightarrow P_\parallel - B_0^2/8\pi$ is added. Hence the characteristic velocities and Riemann invariants can be readily taken from Taub's paper. In particular the small amplitude limit for the propagation velocity can be determined by Taub's equation (5.15) with a bit of algebra:

$$v^2 = \frac{\Gamma P_\perp + B_0^2/4\pi}{P_\perp + \mathcal{E} + B_0^2/4\pi} \qquad \text{(remember c=1), (12)}$$

---

1. Harris (1957) has shown that the field contributes to the inertia of the plasma through its energy density, as well as a contribution equal to the pressure. Thus perpendicular to B the pressure is $B_0^2/8\pi$ and the inertia $B_0^2/8\pi$, while parallel to B the pressure is $-B_0^2/8\pi$ (a tension) and the inertia is zero.

where an equation of state of the form

$$\epsilon \equiv \mathcal{E} - \rho^0 = \frac{p_\perp}{(\Gamma - 1)\rho^0} \tag{13}$$

has been assumed, as well as the equation for the adiabatics mentioned above:

$$p_\perp \propto (\rho^0)^\Gamma \ . \tag{14}$$

For a gas in thermal equilibrium Γ is 5/3 at low temperatures and 4/3 at high temperatures (Jüttner 1911, Harris 1957), while for an ultrarelativistic gas Γ = 4/3 too (Lerche and Parker 1966). The value 4/3 will be adopted for the plasma in the Crab (see Chapter VI). Tidman (1966) has shown that in the first approximation the medium is dispersionless, so that equation V(12) gives both the group and phase velocities.

In a rather different way Lichnerowicz (1967) has treated the case where the pressure is isotropic, and derived the propagation velocity as a function of the angle θ between the field and the direction of propagation. The result is given in terms of the solutions of the equation

$$F(v^2) = 0 \ , \tag{15}$$

where

$$F(X) = \left(\mathcal{E} + P + \frac{B_0^2}{4\pi}\right)\frac{X^2}{v_s^2} - \left(\mathcal{E} + P + \frac{B_0^2}{4\pi}\frac{1}{v_s^2} + \frac{B_0^2}{4\pi}\cos^2\theta\right)X + \frac{B_0^2}{4\pi}\cos^2\theta \ ; \tag{16}$$

v_s is the speed of sound (set $B_o = 0$ in eq. (12)):

$$v_s^2 = \frac{\Gamma p_\perp}{p_\perp + \mathcal{E}} \tag{17a}$$

or

$$v_s^2 = \frac{\Gamma \frac{p_\perp}{\rho_o}}{1 + \left(\frac{\Gamma}{\Gamma - 1}\right)\frac{p_\perp}{\rho_o}} \quad . \tag{17b}$$

Equation (16) generally describes two modes (the "fast" and "slow" hydromagnetic modes), but for $\Theta = \pi/2$ one of them disappears and for the remaining one

$$v^2 = v_s^2 + \frac{B_o^2/4\pi}{p + \mathcal{E} + B_o^2/4\pi}\left(1 - v_s^2\right), \tag{18}$$

entirely equivalent to our equation (12) for $P = p_\perp$.

In order to evaluate these expressions for the propagation velocities we need estimates of the relevant physical parameters of the gas in the Crab Nebula. The strength of the magnetic field and the density of relativistic electrons are usually estimated by comparing the observed radiation intensity with the intensity calculated from the synchrotron theory, adding the assumption that the magnetic field and the particles have equal energy density. The rationale that this assumption approximately minimizes the total energy is of dubious validity except in establishing limits. On the other hand Ginzburg, Sazonov, and Syrovatski (1967) have shown that the relativistic[1].

1. The actual condition is $\frac{1}{4} N \langle E\, v_\perp{}^2/c^2 \rangle \ll B_o^2/8\pi$, from which it is clear that the thermal component can have no important effect.

energy density, U_R , cannot exceed approximately six times the magnetic energy density, U_B , without inducing instabilities and screening of the magnetic field due to the diamagnetism of the plasma. The point is that the gyration of the electrons produces a magnetic field which tends to cancel the external field. This implies, incidentally, that the effective magnetic field in producing the synchrotron radiation from a given region is smaller than the field imposed on that region, a point which is often overlooked. Conversely, if the pressure of the gas, which is mostly from the relativistic component, were much smaller than the magnetic pressure, the nebula would collapse at the Alfvén velocity (which would be nearly the speed of light)--on the condition that the magnetic field is generated within the plasma itself. It is possible that the field could be supported by currents within the filaments (which have sufficient inertia not to be collapsed by the field), but then it would be hard to understand why there is not more correlation between the filaments and the structure of the magnetic field. Since the nebula is not collapsing, but undergoing slightly accelerated expansion, we have

$$P_R \gtrsim P_B , \tag{19}$$

or in terms of energy densities ($P_R = \frac{1}{3} U_R$ in the ultra-relativistic limit, and $P_B = U_B$):

$$U_R \gtrsim 3U_B \quad . \tag{20}$$

This, together with the Ginzburg et al condition, gives

$$3U_B \lesssim U_R \lesssim 6U_B \quad . \tag{21}$$

Thus the effective magnetic field is probably somewhat weaker than the one corresponding to exact equipartition (10^{-3} Gauss; Oort and Walraven 1956), and we shall adopt

$$B_o \sim 5\times10^{-4} \text{ Gauss} \tag{22}$$

for the average field strength, recognizing that it could be rather smaller but not very much larger. The relativistic pressure which balances this magnetic pressure is, of course,

$$P_R \sim 1\times10^{-8} \text{ erg/cm}^3 \quad . \tag{23}$$

The density of relativistic electrons corresponding to this value depends somewhat on the form of the energy distribution function, but is on the order of

$$N_R \sim 5\times10^{-3} \text{ cm}^{-3} \quad . \tag{24}$$

Given these quantities, most of the important physical parameters are determined, and their approximate values

are given in Table V.1. The thermal gas density, N_T, is taken as an unknown parameter at this point.

TABLE V.1

QUANTITY	FORM	FORMULA	VALUE (erg/cm^3)
Energy density	Magnetic	$U_B = B_0^2/8\pi$	1×10^{-8}
	Relativistic (total)	$U_R = N_R m_0 c^2 \langle\gamma\rangle$	4×10^{-8}
	(rest)	$U_R = N_R m_0 c^2$	10^{-14}
	Thermal (internal)	$\epsilon_T = \frac{3}{2} N_T kT$	$8.28 \times 10^{-16} N_T T$
	(rest)	$U_T = N_T M_0 c^2$	$1.50 \times 10^{-3} N_T$
Pressure	Magnetic	$P_B = B_0^2/8\pi$	1×10^{-8}
	Relativistic	$P_R = \frac{1}{3} U_R$	1×10^{-8}
	Thermal	$P_T = 2 N_T kT$	$2.76 \times 10^{-16} N_T T$

The Sound Velocity

In the absence of a magnetic field, disturbances propagate longitudinally at velocity v_s given in equation (17) above. In a purely thermal gas the quantity P/ρ^0 is very small, and we have $v_s^2 = \Gamma P/\rho^0 << c^2$. In a purely relativistic gas the same quantity is large, and in the ultrarelativistic limit $v_s^2 = (\Gamma - 1)c^2 = \frac{1}{3} c^2$ (we adopt $\Gamma = 4/3$ in all the calculations). In a gas which is a mixture of thermal and relativistic particles the

sound speed is intermediate between these low and high values. In the Crab the pressure is dominated by the ultrarelativistic component and the proper rest mass density is mostly due to the thermal gas (see Table V.1). Thus in equation (17b) the quantity P/ρ^0 is given by P_R/ρ^0_T . The form given in (17a) is more convenient for the present calculations, and we rewrite it as

$$v_s^2 = \Gamma/Q \tag{25}$$

where

$$Q \equiv \frac{p_\perp + \mathcal{E}}{p_\perp} = 1 + (\mathcal{E}/p_\perp) \quad . \tag{26}$$

Note that both the relativistic and thermal components can contribute significantly to $\mathcal{E}$, through kinetic energy and rest-mass energy, respectively.

The Hydromagnetic Velocities

In terms of the parameter Q, equation (18) can be written

$$v^2 = \Gamma/Q + \frac{1 - \Gamma/Q}{1 + RQ} \tag{27}$$

where

$$R \equiv \frac{p_\perp}{(B_0^2/4\pi)} \tag{28}$$

has the value 1/2 for the parameters assumed here (indeed,

the arguments which led to these values insure $\mathcal{R} \sim 1$). If we assume that v has a known value of about 0.05 (see Chapters II and IV), equation (27) can be solved for Q and thence N_T :

$$Q = \frac{1+\Gamma\mathcal{R}-v^2}{\mathcal{R}v^2} \cong 1.33 \times 10^3 \qquad (29)$$

and the value of N_T is

$$N_T = 8.9 \times 10^{-2} \text{ cm}^{-3} \qquad (30)$$

(scaling roughly as v^{-2}). The corresponding value of the sound speed is

$$v_s = 0.031c \quad . \qquad (31)$$

The variation of v with the propagation angle θ can be studied easily from equation (15), which is a simple quadratic in v^2 . The result is that the fast mode we are considering here has only a slight angular dependence, being slightly faster (by roughly one part in Q, or one part in a thousand) in the perpendicular case. There is another mode described by equation (15), appropriately called the slow mode. It has a large angular dependence, and is fastest parallel to B. Typical speeds are 10^{-3} to $10^{-5}c$, so that the slow mode may be neglected for the present purposes.

We shall now discuss damping of hydromagnetic waves. Damping is important as a possible mechanism for transferring energy to the relativistic particles, and also because moderately strong damping would have observable effects on the activity. As discussed in Chapter II, there is no definite evidence that there is damping of the wisps. If, indeed, they propagate to the edge of the nebula almost unchanged, the medium must be essentially dispersionless and free of damping. We also saw in Chapter II that the ripples and wisps seem to be moving in one direction, namely perpendicular to the magnetic field. The composite photography discussed in Chapter IV showed also that the motion is basically confined to the perpendicular direction. Since the phase velocity (real part of ω/k) is nearly independent of direction, there are three possible reasons for this lack of motions at an angle to the lines of B. In the first place, such disturbances may be present, but not observable. In an Alfvén wave (low frequency transverse wave propagating along B) the change in the field, $\underline{b}$, is perpendicular to the ambient field, $\underline{B}_o$, so that the magnitude of the field changes by an amount of order b^2/B_o . In a magnetosonic wave (low frequency longitudinal wave propagating normal to B) the vector change is in the same direction as the ambient field, so the magnitude changes

by $\pm b$. The synchrotron intensity is very sensitive to the magnitude of B (see Appendix C), so Alfvén waves do not change the emission as much as do magnetosonic waves. Alfvén waves would probably be visible only through the bending of the field lines which they produce. For example, the situation shown on PH 5002 is a perfect example of "plucking the string" (the field lines through WISP 2) by WISP 1, and a kink in the field lines should propagate. A year later there should be two kinks in WISP 2 about 2" from the center of WISP 1 (taking the Alfvén velocity to be about 0.05c). These kinks are present on PH 5129 and 5130 (see Appendix A), although the bending is not as distinct as on the earlier plate. The bending of the wisp and the general irregularity of the disturbances may be associated with Alfvén type disturbances. In the second place, disturbances at angles to B may just not be excited. The main wisp seems to move characteristically perpendicular to the field, and as discussed in Chapter II, it may be the generator of the activity. But the motion of even the main wisp is not completely unidirectional. Also, irregularities in the field would be expected to deflect some of the motion. Third and last, there may be operative a damping mechanism which is dependent on direction and allows propagation normal to B (and perhaps also <u>along</u> B, in view of the motion described in Appendix B). The rest

of this section will be a discussion of possible damping mechanisms.

The usual sources of damping of waves are associated with collisions. In a relativistic gas of the densities we are considering, collisions are completely negligible because of the rapid decrease of the cross-sections with decreasing energy. Even collisions between the relativistic and thermal components are negligible. For self-collisions between the thermal electrons themselves, classical formulas (e.g. as developed by Spitzer, 1962) are applicable. Collisions are quite sufficient to thermalize the gas, unless the temperature is very high, in a time

$$t_{\text{thermalization}} \sim 10^{-2}(N_T)^{-1}\, T^{3/2} \text{ sec.} \qquad (32)$$

For collisional damping the relevant quantity is the time during which significant particle diffusion perpendicular to B can occur, and is given by Spitzer (1962, eq. (2-38)) as

$$t_{\text{diffusion}} \sim 2\text{x}10^{-13}\, T^{3/2}\, L^2 \text{ sec.}, \qquad (33)$$

where L is the length scale of inhomogeneities in the field. Even for L $\sim$ 0.1 wisp diameter (i.e., $\sim 10^{+16}$cm.) the diffusion time is immense, and we can neglect collision

effects on the propagation of magnetohydrodynamic disturbances.

There are basically two kinds[1] of <u>collisionless damping</u> which will be considered here, both of which are particle-wave resonance phenomena. The first is called <u>cyclotron damping</u> (Stix, 1962), and occurs if there are particles for which some harmonic of the cyclotron frequency

$$\Omega = \Omega_0/\gamma = \frac{eB}{m\gamma} \tag{34}$$

is equal to the frequency at which they experience the electric field of the wave, which is

$$\omega' = \omega\left(1 - \frac{v_{\parallel}}{v_{ph}}\cos\theta\right), \tag{35}$$

where ω is the wave frequency, $v_{\parallel}$ is the drift velocity of the particles parallel to B, v_{ph} is the phase velocity of the wave, and θ is the angle between the propagation vector of the wave and B. Because the waves we are interested in have frequencies very roughly of the order of 10^{-8} sec^{-1}, the non-relativistic cyclotron frequency

---

1. It should be pointed out that neither form of damping can be treated in the MHD approximation, for the averaging operation smoothes over such resonances.

$$\Omega_o = eB/m = 2.8\times10^6 \text{ B(Gauss) sec}^{-1} \qquad (36)$$

is much too large for resonance. For ultrarelativistic particles, the gyration frequency is decreased (eq. (34)) and the drift velocity can increase ω' (eq. (35)), so that resonance can occur at sufficiently high energies. The easiest resonance is at the fundamental gyration frequency, and the condition $\Omega = \omega$ can be written for ultrarelativistic particles as

$$\Omega_o/\gamma = \omega\left(1 - \frac{c}{v_{ph}}\cos\theta\cos\alpha\right), \qquad (37)$$

where α is the angle between the velocity vector of the particle and B (the pitch angle). Resonance can occur at the lowest energy if the particle is drifting mostly toward the wave ($\alpha \sim \pi$, $\theta \sim 0$). For these values, equation (37) becomes, neglecting unity compared to $c/v_{ph} \sim 10^2$,

$$\gamma_{RES} \sim \frac{\Omega_o}{\omega}\left(\frac{v_{ph}}{c}\right) \qquad . \qquad (38)$$

Taking $\omega \sim 10^{-6}$ sec^{-1} as the highest frequencies present (see the beginning of Chapter VI), and with $v_{ph}/c \sim 10^{-2}$, $\Omega_o \sim 10^2$, we have resonance for $\gamma \geq 10^6$.

Hence synchrotron electrons producing optical, X-ray and gamma-ray photons are supplied with energy by this mechanism. The values of γ_{RES} for protons are smaller by the rest-mass ratio, but there is nothing known with certainty about even the existence of ultrarelativistic protons and ions. For any kind of particle, the damping depends not only on the existence of particles able to resonate with the waves, but also on there being more particles just below the resonant energy than just above. It is this situation which produces a net flow of energy from the waves into the particles. Thus this is a self-consistent problem: the damping depends on the details of the particle distribution, and the distribution depends on the details of the energy input through damping. In addition, the spectrum of wave frequencies turns out to be an important but unknown factor. Therefore, we shall not make a detailed theoretical analysis,[1] but confine ourselves to a few general remarks.

First, in deciding whether electrons of energy

---

1. The treatment by Tidman (1966), which inspired the present discussion, can be applied directly to the damping of waves propagating parallel or perpendicular to B by a possible ultrarelativistic proton component of the gas in the Crab. The modifications necessary to treat the electron component are simple and obvious. The case of propagation at arbitrary angles is difficult, and apparently has not been treated in any detail.

$mc^2\gamma_{RES}$ exist, one cannot use their short synchrotron lifetimes as counterindicative evidence. For it is just these electrons which would constantly be supplied with energy by the waves. We should look at it the other way: if waves with a spectrum of frequencies (say from $\omega \sim 10^{-5}$ sec^{-1}, which resonate with the "optical" electrons, to $\omega \sim 10^{-8}$ sec^{-1}, which we have just seen resonate with gamma-ray producing electrons) are generated at the center of the Crab, then electrons of the corresponding energies should exist. Their distribution in energy, and hence the spectrum of the synchrotron radiation, would depend on the spectrum of wave frequencies.

Next, we can deduce from Tidman (1966) the relative importance of damping for parallel and perpendicular propagation. If L is the characteristic damping length (over which the amplitude decreases by a factor of, say, e), we obtain from Tidman's equations (42) and (43) the expression

$$\frac{L_{\parallel}}{L_{\perp}} = \frac{(s+1)(s+2)}{2\pi}\left(\frac{v_{ph}}{c}\right)^2 , \qquad (39)$$

where s is the usual index in the power-law for the distribution of energies for the particles which do the damping. For the electrons in the Crab ($s \sim 1.5$ to 2.5, $v_{ph}/c \sim 0.05$),

$$L_{\parallel}/L_{\perp} \sim 10^{-2} \text{ to } 10^{-3}, \tag{40}$$

which is to say that waves may propagate relatively freely perpendicular to B (as observed). The physical reason, as pointed out by Tidman, is that the parallel waves resonate with the less energetic particles, which gain energy more rapidly and are more numerous ($s > 0$).

Finally, in connection with the interpretation of the spectrophotometry, it will be important to know what effect this damping would have on the energy distribution of the electrons. The effect depends sensitively on the frequency spectrum of the waves, which is known only roughly (as outlined in the summary in the following chapter), so that a detailed calculation is not justified. We shall briefly consider the case of waves propagating perpendicular to the field, as the wisps seem to be examples of this "magnetosonic" disturbance. Tidman's expression for the imaginary part of the frequency can be written in terms of the energy distribution function $n(\gamma)$ as follows:

$$\omega_i = \frac{\pi}{2} \frac{1}{N} \left(\frac{V_A}{c}\right)^3 \left(\frac{\omega_e}{\Omega_0}\right)^2 \Omega_0 \gamma^{11} \frac{d}{d\gamma}\left[\gamma^{-2} n(\gamma)\right], \tag{41}$$

where $N = N_R + N_T$ is the total particle density, V_A

is the Alfvén velocity, ω_e is the non-relativistic plasma frequency, and Ω_o is the non-relativistic gyration frequency. By evaluating the rate at which energy is transferred to the particles by a disturbance which contains energy density $u(\omega)d\omega$ (erg/cm^3) in the frequency range $(\omega, \omega + d\omega)$, we can calculate the rate of increase of energy for particles of a given energy:

$$\frac{d}{dt}(m_o \gamma c^2) = \frac{\omega_i \omega u(\Omega_o/\gamma)}{\gamma n(\gamma)} , \tag{42}$$

where we have made use of the condition for resonance $\omega = \Omega_o/\gamma$. Hence

$$n(\gamma)\frac{d\gamma}{dt}\Big|_{DAMPING} = \frac{\pi}{2m_o c^2}\frac{1}{N}\left(\frac{V_A}{c}\right)^3 \omega_e^2 u\left(\frac{\Omega_o}{\gamma}\right)\gamma^2 \frac{d}{d\gamma}\left[\gamma^{-2} n(\gamma)\right]. \tag{43}$$

The effect on the energy distribution can be obtained by solving the well-known continuity equation

$$\frac{\partial n(\gamma,t)}{\partial t} + \frac{\partial}{\partial \gamma}\left[n(\gamma,t)\frac{d\gamma}{dt}\Big|_{DAMPING} - a\gamma^2 n(\gamma,t)\right] = 0, \tag{44}$$

where the synchrotron loss rate has been written $-a\gamma^2$. If we substitute a power-law for $n(\gamma)$ in the expression (43), we can obtain a solution valid for small departures from a power-law energy spectrum. In this approximation

the continuity equation becomes formally equivalent to that for synchrotron losses plus injection of electrons with a power law spectrum, and can readily be solved (Kardashev, 1962):

$$n(\gamma,t) \cong K\gamma^{-s}\left[1+C\,t\,\gamma^{r-2}\right], \tag{45}$$

$$C = \frac{\pi}{2}\frac{N}{m_o c^2}\beta_A^3\,\omega_e^2\,(s+1-r)(s+2)u_o, \tag{46}$$

where the initial spectrum is taken to be $K\gamma^{-s}$, and the spectrum of the waves in the region of interest is assumed to be representable by a power law:

$$u(\Omega_o/\gamma) = u_o\gamma^r \propto \omega^{-r} . \tag{47}$$

Hence for $r > 2$ the electron energy spectrum at least initially becomes <u>flatter</u> due to cyclotron damping, and for $r < 2$ the spectrum becomes <u>steeper</u>. The constant C determines the time τ in which there is a significant change in the spectrum:

$$\tau = \frac{\gamma^{2-r}}{C} = \frac{m_o c^2\gamma^2}{\frac{\pi}{2}N\beta_A^3\omega_e^2(s+1-r)(s+2)u(\omega)}, \tag{48}$$

$$\cong 2\times 10^{8}\,\mathrm{sec}\left(\frac{\gamma}{10^{6}}\right)^{2}\left(\frac{\beta_A}{0.01}\right)^{3}\left(\frac{\Delta B}{10^{-6}}\right)^{-2}, \qquad (49)$$

where we have written the numerical coefficient in terms of the approximate values $\gamma \sim 10^{6}$ (optical electrons), $V_A \sim 10^{-2}c$, and ΔB (the perturbation of the field strength in the wave) $\sim 10^{-6}$ Gauss. Because of the high sensitivity to the roughly known parameters β_A and ΔB, the time scale is quite uncertain, and because of the lack of knowledge of the form of the wave spectrum, even the sign of the effect on the electron energy spectrum is uncertain.

The other form of collisionless damping of hydromagnetic disturbances we shall discuss has been developed by A. Barnes (1966, 1967) for a classical gas. It arises from resonance between the component of the wave electric field along the magnetic field (as opposed to the perpendicular component in cyclotron damping) and the random particle motion. It is related to Landau damping and "transit time damping". I have not been able to extend either of Barnes' two methods of performing these calculations to the relativistic case, but it seems hopeful that the procedure used by Tidman (1966) can be applied with merely an increase in the complexity of the

algebra (all the integrals are easily evaluated). A few considerations suggest the role that this form of damping might play in the Crab. The amount of damping per wavelength becomes small for waves propagating nearly parallel to B (within 20°) or nearly perpendicular to B (within 5°). This is reminiscent of the motion of the main wisp described by Baade in Appendix B. The general mechanism is operative if $P_{gas} \gtrsim (1/2)P_{magnetic}$, a relation which holds for the relativistic gas pressure in the Crab. Finally, we can judge in a crude way how effectively waves in a relativistic gas will be damped by Barnes' mechanism. The particles all have essentially the same speed, c, and the average speed along the field lines will be some fraction of c. Hence one would expect damping for waves whose phase velocities are relativistic. It seems reasonable that there will be many particles capable of damping the moderately relativistic waves we have observed, although quantitative estimates cannot be made without performing the calculations for the relativistic gas.

We have reviewed some of the physics of a relativistic gas which seems relevant to our study of activity in the Crab Nebula. Except for the estimation of the values of the physical parameters in the nebula, we have not made a specific application of this theory to the observations. This task will be the main burden of the concluding chapter.

VI. CONCLUSION

It is important to see to what extent the observational results in Chapters II, III, and IV can be understood in terms of the theoretical discussion in Chapter V. We consider in turn the nature of the wisps and other disturbances, their motions, and their energy content. A few general remarks can be made about the results concerning the spectrum. Let us begin with a summary of the observations.

We saw in Chapters II and IV that, superimposed on the slowly expanding general structure, there is a variety of changes which occur in the Crab Nebula. For the most part these changes can be described as motions in the sense that intensity patterns appear to change location. The distinction between changes and motions is largely semantical on the observational level, but there is a real difference on the level of physical description which will be discussed shortly. The velocities of the various patterns range over two orders of magnitude, from $\mu \sim 0''.1/\text{yr}$ (some sharply defined continuum features near the edges) to $\mu \sim 10''/\text{yr}$ (the fastest observed motion of the wisp). The actual velocity projected on the plane of the sky is given by

$$\frac{v}{c} = 2.38 \times 10^{-2} \mu\ (''/\text{yr}) \left(\frac{d}{1500\ \text{pc.}}\right).$$

If the time dependence of the position of the main wisp is Fourier analyzed, the highest frequencies present are on the order of 10^{-6} sec^{-1} (the abrupt halt of the main wisp in 1955 took place in 0.1 year or less), with some indication of a preferred characteristic frequency of about 10^{-8} sec^{-1} (two year period) and some components at smaller frequencies. The motions are generally perpendicular to the ambient magnetic field (magnetosonic disturbances), but there are probably also Alfvén disturbances (wiggles in the field lines). The activity is much stronger in the NW quadrant, or at least its effects are more readily perceived there.

The most significant result of the spectrophotometry is that the continuous spectrum shows a slight but definite variation across the nebula, and is flatter near the center and steeper toward the edges. In addition, the region of greatest activity (the area of the wisp series) has a generally flatter spectrum. There is a small ultraviolet excess, partially caused by the shape of the interstellar reddening curve.

Let us begin our analysis of these observations by discussing the basic nature of the wisps. As argued in Chapter II we can regard the wisps as regions in which the synchrotron emissivity is greater than in the surrounding medium (self-absorption can be neglected).

Increased emissivity may be due to one or more of the following (α = pitch angle; φ = observation angle, both measured from the magnetic field):

(1) stronger magnetic field

(2) greater density of electrons

(a) of appropriate energies ($\nu_c \sim \nu_{obs}$)

(b) of appropriate pitch angles ($\alpha \sim \varphi$).

A quantitative statement of these factors can be made (see Appendix C) if the forms of the distribution functions for energy and pitch angle are assumed, but this restriction is not necessary for the present discussion. Effect (2b) can be important when the pitch angle distribution is strongly peaked in some direction, rather than approximately isotropic. The arguments for isotropy given in Chapter V are not relevant here because of the short time scale of the activity. For example the "injection" process might give the electrons momenta preferentially normal to the magnetic field (this is the case for energy injection via pure cyclotron damping). Anisotropy is also produced by transverse compression of the plasma, for as can be seen from eq. (4) of Appendix C, the pitch angles of all the electrons increase with the field strength. To see what the effects of these "flat" distributions (i.e., a preponderance of nearly circular orbits) might be, we consider the simple configuration shown in Figure VI.1.

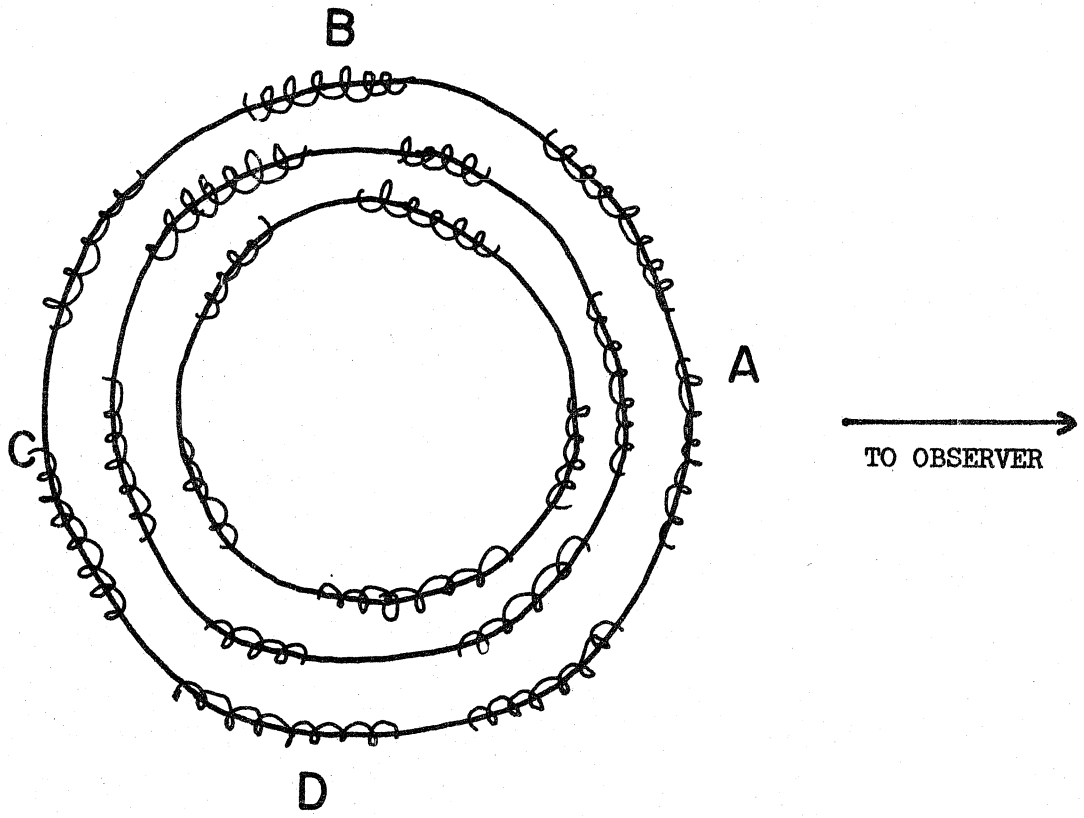

FIG. VI.1: TORROIDAL MAGNETIC FIELD CONFIGURATION

A plasma of ultrarelativistic electrons with pitch angles mostly near $\pi/2$ is embedded in a torus of closed circular field lines. Then because of the "searchlight" effect (condition (2b) above) the observer will receive radiation most strongly from the points nearest and farthest from him (A and C), and only weakly from the regions B and D. For a moderately peaked distribution of pitch angles the effect is strong, because it is augmented by the natural tendency for synchrotron radiation to be strongest perpendicular to the field. Even for an isotropic distribution the radiation varies strongly with the angle φ (as $(\sin\varphi)^{1.5}$ for the Crab; see Westfold, 1959), and would show a concentration at points A and C. We have in mind the identification of the bright spot at A with the main wisp, and that at C with the wisp-like feature in the ANVIL. The curvature of the wisp is somewhat variable, but it generally has a radius of curvature larger than half the distance from the ANVIL to the main wisp, which we take as due to the fact that the torus is not seen face-on. In fact, the effects which localize the radiation to points A and C depend on the torus being viewed approximately edge-on. Because of the variation of the curvature it is difficult to make a quantative estimate of the angles. But if we are viewing the torus rather obliquely it follows that there

would be a rather large radial component of the motion of the wisp. This fact could provide an explanation of the apparent asymmetry of the activity in general, and specifically of the faintness of the ANVIL relative to the wisp series. The effect which we adduce is the fact that the observed intensity of an object is altered if it has a relativistic radial velocity (see e.g., Kristian and Sachs, 1966). There are several factors which contribute: the time it takes for the radiation emitted during a given interval to sweep by the observer, the Doppler shift, and the relativistic alteration of the solid angle. For observations in a fixed band pass, the effect depends on the spectrum of the source. For a flat spectrum the ratio observed intensity/emitted intensity can be written

$$(1 \pm \beta \cos^2 \phi)^3,$$

where β is the magnitude of the velocity in units of c. For a decreasing spectrum of the sort we are dealing with, the factor is larger. Hence an approaching wisp would be brighter than a receding one by a factor even larger than the above expression. Given the observed velocities of the wisps on the plane of the sky, it does not require a very extreme angle ϕ to make the intensity ratio between the wisps equal to the observed value

of approximately 3. The main objection to this explanation is that the motion of the wisps inward should reverse the intensity changes, so that the ANVIL should sometimes be brighter than the wisp series. It should also be mentioned that the electrons must actually participate in the motion of the wisp for the intensity effect to be operative, a point which will be returned to below. This model has been discussed to demonstrate that the asymmetry shown by the wisps may be due to aspect effects. We do not propose it as a specific model for the wisp region.

Other causes of variation in intensity must be present, in particular to explain the sharp variations exhibited by the wisp series in the direction perpendicular to the field. The remaining causes are that there are more electrons whose critical frequencies ($\nu_c = \frac{3}{2} \frac{eB \sin\varphi}{m_0 c} \gamma^2$) lie near the observed range (condition 2a) and that the magnetic field is stronger (condition 1). These are related because the critical frequency depends on B and because, to the extent that the particles are frozen to the field, changes in B are accompanied by changes in the density. As noted in Chapter V, only the extremely energetic electrons can penetrate the field lines to a significant extent. (One could therefore picture the stellar remnant injecting these electrons into the field, where

they too become trapped and lose energy rapidly.) The majority of the electrons, and certainly those which emit at optical frequencies, must be solidly frozen to the field. This argument (stated in a different way by Shklovskii, 1957) eliminates the possibility that the wisps actually move relative to the field lines. Hence, the wisps and other inhomogeneities are regions where the plasma is more compressed relative to the surrounding medium, and both the field and electron density are increased. The increase in intensity is due to all of the several effects listed above, and a simple quantitative analysis is given in Appendix C.

This key result brings us to the motions of the wisps, which can be of two sorts: (1) the compressed region can maintain its identity and move, carrying the field along (bulk motion), or (2) the compression can propagate as in a sound wave, so that the peak in intensity appears to move relative to the field lines (no bulk motion). We now attempt to decide which of these is the true description of the wisps' apparent motions. Because of the unchanging general structure of the nebula, we can assume that the magnetic field is quasi-stationary, and for the most part participates in the slow expansion only. Thus, if the main wisp actually continues to move outward, it must be an example of the

second kind of motion, or else it would drag the field with it. However, we have seen that the photographic evidence points toward the main wisp being a single feature which moves back and forth. Hence, if it is a propagating compressional wave, the wisp must somehow be reflected at the two extremes of its motion. It would seem difficult to explain these reflections without postulating barriers or discontinuities for which there is no direct evidence. The alternative is that the main wisp is a permanent blob of plasma which moves about but always returns because it is anchored to the field. An analysis of the mechanics of such motion provides useful information. Since the bulk velocities are not highly relativistic, a simple quasi-Newtonian treatment is sufficient. We assume that the blob is given an initial velocity βc in a direction perpendicular to the field. The observed behavior is a braking and complete reversal of this motion, which suggests a resilient restoring force. The magnetic field seems ideal for this purpose. However, with the values for the physical parameters adopted in the previous chapter, the inertia provided by the thermal component overwhelms the field. The wisp would penetrate much farther than observed if the only braking force were that provided by the magnetic field. An

obvious solution is to postulate that the thermal gas (which is conveniently unobservable) is much rarer in the wisp region. One can visualize the sluggish thermal gas being squeezed out of the wisps along the field lines by whatever forces generate the motion. In this way it would be possible for the inertia of the wisp to be small enough for the observed motion to result. The interpretation of the main wisp as a compressional wave also requires different conditions, because the magnetosonic propagation velocity would have to be larger in the wisp region than in the nebula generally. In fact, both interpretations require that the thermal density in the wisp be roughly a hundred times less than in the main body of the nebula. As a result of this discussion, we see that the question of whether or not mass motion occurs in the main wisp is not easily answered. It does seem less artificial to suppose that mass motion <u>is</u> involved, because the reversal of the motion is provided in a natural way by the magnetic field. The wisps beyond WISP 1 are not observed to oscillate, although the evidence is meager. It seems reasonable that these outer wisps are compressional disturbances propagating outward.

The velocities of such disturbances were derived in Chapter V. The value $\Gamma = 4/3$ was adopted

there for convenience, although by definition the thermal gas is not hot enough for this value. From the way Γ enters, however, it is clear that the error introduced is not large. The logical sequence which seems most appropriate is to regard the magnetic and gas pressures as approximately determined by the kind of arguments outlined in the previous chapter, and then the observed velocities allow determination of the otherwise unknown remaining parameter, the thermal gas density. We saw that $N_T = 10^{-1}$ gave a velocity of about 0.05c, appropriate for the intermediate motions. If the other parameters are constant throughout the nebula, the suggestion is that the thermal density is smaller (10^{-3}), near the center where the motions are perhaps an order of magnitude faster, and larger (10^{+1}) near the edges. These numbers should not be taken too seriously, since differences in the field strength and gas pressure may also affect the propagation velocities (but recall the arguments for uniformity in these quantities alluded to at the beginning of Chapter V). However, it is quite certain that the fastest motions take place in regions where the thermal gas is substantially rarer than in the interstellar medium.

There is a large range in the intensities of the waves, ranging from the main and secondary wisps

which dominate the PLATEAU area to subtle ripples at the level of a few percent of the average surface brightness. Shklovskii (1957) claimed that the ratio of the volume emissivity in the wisp to that in the "hole" is on the order of 1000. The actual value is certainly much smaller. As a by-product of the work described in Chapter IV, we obtain measurements of the surface brightness in the wisps. As the slit size was roughly comparable to the main wisp, the values obtained refer to an average intensity over the wisp. This average surface brightness (with the background subtracted out) is typically a factor of two less than the surface brightness in the brighter parts of the nebula. Of course the very central parts of the wisps, especially when there is a sharp core present, have a higher surface brightness. The visual appearance of the plates is very misleading in this connection, because the eye is quite sensitive to the differences in density and tends to ignore the background surrounding the wisps. For example, the "hole" looks quite dark, but is in reality about 80 percent as bright as the brightest parts of the nebula, excluding the wisps. The actual volume emissivity depends on the line-of-sight depth of the wisp, which Shklovskii assumed is comparable to the smaller dimension in the plane of the sky. This is a reasonable assumption, but it is also possible that we are

viewing a sheet nearly edge-on. Such a sheet could have an emissivity not much greater than average, and would be inconspicuous seen face-on. Thus there is considerable uncertainty, but even if the wisp is sausage-shaped, its emissivity is probably only a factor of 10 greater than the faintest part of the surroundings. Since the point-like cores may not be resolved, it is impossible to estimate their surface brightness. Because the intensity depends so strongly on the compression factor (roughly as the third power; see eq. (21) of Appendix C), the necessary perturbation in the field is not large, as we see in the following table, based on the results of Appendix C with $s = 1/2$:

TABLE VI.1

j'/j	B'/B	ΔB (for $B \sim 10^{-4}$ Gauss)
1.1 (waves)	1.03	3×10^{-6}
10 (wisps)	2.2	120×10^{-6}
100 (wisp cores?)	4.6	360×10^{-6}

Let us take 10^{-5} Gauss as a representative magnetic perturbation, and use this value to estimate the energy content of the field of waves. Barnes (1967) has given the following expression for the energy density

in waves propagating perpendicular to the ambient field:

$$U_{waves} = \frac{(\Delta B)^2}{4\pi}\left(1 + \frac{P_{gas}}{P_B}\right) .$$

Taking $P_{gas} \sim P_B$ (cf. eq. (19) of the previous chapter), and the nebular volume as 3×10^{56} cm^3 (5' diameter at 1500 pc.), we have

$$U_{waves} = 2 \times 10^{-11} (\text{ergs/cm}^3)(\Delta B/10^{-5})^2 ,$$

and for the total energy in the nebula,

$$E_{waves} = 5 \times 10^{+45} (\text{ergs})(\Delta B/10^{-5})^2 .$$

We can only speculate about the damping rates. If waves lose 1 percent of their energy per wavelength (the value found by Barnes for the least damped modes in typical directions), the effects on the disturbances would be essentially unobservable, except perhaps as a slight dispersion of the forms of the features after several wavelengths (Tidman showed that if the damping is small, so is the dispersion). Assuming the waves pervade the whole nebula, this damping would supply energy directly

to the particles at the rate 10^{36} erg/sec. This is of the same order as the synchrotron losses of 4 x 10^{36} erg/sec (Kardashev, 1962). Hence, damping of the disturbances observed in the Crab Nebula is a plausible mechanism for supplying energy to regenerate the radiation losses.

At this point we shall attempt to draw a picture of the center of the activity. Our picture is phenomenological to the extent that it merely represents the observed structural features (of the wisps and the magnetic field). It is speculative also, in that it suggests relations between the observed phenomena that are not directly implied by empirical evidence. We do not propose a model for the process of generation of the relativistic electrons; we assume that there is a condensed remnant (probably the small radio source) which somehow throws out high-energy particles. This is an assumption which is not trivial because at best all we know is that <u>energy</u> is supplied. Those electrons which have small enough energies to be trapped by the magnetic field will tend to drag outward the field lines which do not actually penetrate the remnant, forming the field configuration pictured in Figure VI.2 (the observer is, roughly speaking off to the right-hand side of the diagram). The particles which are ejected along the lines threading the remnant would form a narrow tube of emission which we identify

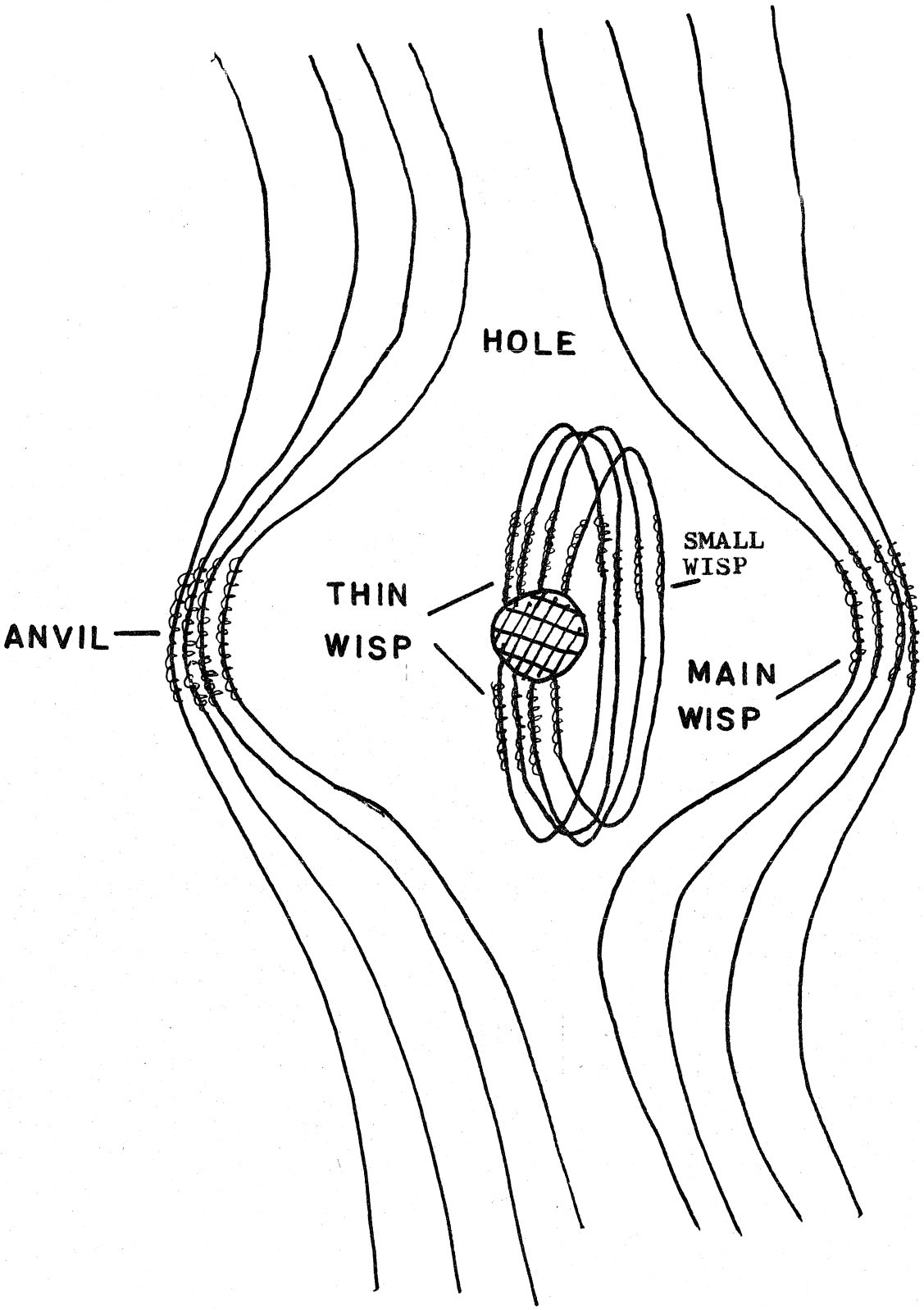

FIG. VI.2: PROPOSED PICTURE OF THE ACTIVE REGION

with the THIN WISP. The remnant itself is invisible. The region just outside has been swept clean of magnetic field and plasma, and therefore would be a dark volume which we associate with the "hole". The electrons which are currently ejected by the remnant travel freely to the region where the field lines are compressed together, at the points labeled "main wisp" and "ANVIL". The lower-energy electrons are stopped abruptly, and the most energetic ones do not get much farther. There would generally be a balance between the outward particle forces and the inward magnetic pressure forces, with the wisp remaining near a characteristic position. Fluctuations in the particle flux from the remnant would disturb the equilibrium and rapid inward and outward motions would result. We suppose the thermal gas to be long ago squeezed out along the field lines and not replenished as is the relativistic gas. The hydromagnetic velocity would therefore be that of a pure ultrarelativistic gas in a magnetic field, namely a large fraction of the speed of light (see eq. V(12)), as observed. Thus the main features of the observations are explained by this model. The major problem is that the three-dimensional picture is not clear. If the ejection is axi-symmetric, we can use the limb-brightening effect to explain the wisps, but then the "torus" explanation for the differing inten-

sities of the two sides does not apply. It could be that the magnetic configurations are simply different on the two sides. In order for the torus to apply strictly, the ejection would have to be in a plane through the magnetic axis, a highly artificial supposition. Another difficulty lies in understanding how the main wisp can be seen within the hole most of the time, rather than right at the edge.

Let us turn to the problem of interpreting the spectrophotometry. We will not be concerned with the nature of the spectrum, say at the center of the nebula, because that probably depends on the energy distribution produced by the acceleration process, about which we know very little. We discuss only what changes might occur across the nebula. Changes in the energy distribution can be brought about by three general causes:

(1) energy and/or particle gain,

(2) energy and/or particle loss,

(3) change in the magnetic field.

If the details of the energy supply mechanism were known, effect (1) could be evaluated. It was made reasonable in Chapter V that cyclotron damping has some importance in this connection, but we found that even qualitative remarks could not be made without knowing more about the disturbances. On the other hand, the losses are rather

well understood (Kardashev, 1962), and in particular synchrotron losses dominate. If there is a migration of electrons from the center of the nebula outward (along the field lines), the distribution near the edges will be older and hence steeper. Also, if there is leakage of the higher energy particles from the edges, a similar steepening would occur. These two effects are reasonably likely to exist, and are unambiguous. Unfortunately, there are other effects which confuse the matter. For example, if the field were weaker at the edges, the synchrotron losses would be slower there, and under some conditions the evolutionary effect could be reversed. Conversely, a larger field near the edges would amplify the evolutionary differences between the center and edge. Even this matter is not so simple, because it is possible for field changes to produce changes in the form of the energy distribution. We proved in Appendix C that a power law spectrum is not altered by a change in the field (except that the cut-offs are shifted), but this conclusion is altered for any other distribution. To be definite, let us suppose that the distribution function becomes steeper with increasing energy (as indicated by the radio, optical, and X-ray data). As the field increases[1.], all electrons increase in energy by the same relative amount

1. Changes in the field can refer to spatial variations coupled with migration (convective derivative), or to changes with time (partial time derivative).

(see Eq. (5) of Appendix C), thus shifting the distribution toward higher energy. This brings the flatter part into play, and the observed spectrum would be flatter. A decrease in field strength would similarly produce a steepening of the spectrum. The spectrum observations in the NW quadrant can be explained in this way, since the field is stronger in the wisps and weaker in the surrounding plasma. Unless the field increases with distance from the center, the general steepening of the spectrum at the edges can be explained as a combination of the physical effects just discussed.

There are several areas in which further work is needed. On the observational side, it has already been noted that important ambiguities could be cleared up with a series of direct plates with very fine time resolution. The variation of the spectral index over the nebula should be confirmed and investigated further, both optically and in the radio region. The ultraviolet excess should be checked with careful, accurately calibrated observations. Far infrared and ultraviolet spectral observations will undoubtedly clarify the nature of the continuous spectrum. An important theoretical need is for a detailed discussion

of damping of MHD waves in a relativistic plasma. Non-linear problems such as large amplitude disturbances and the formation of shock waves may be important, and have not been considered here.

APPENDIX

A. DESCRIPTION OF THE 200-INCH CONTINUUM PLATES

This appendix contains a qualitative description of the central region of the Crab Nebula as it appeared at each of 25 "epochs". The epochs correspond to runs on the telescope, and in every case the plates grouped into an epoch are separated by no more than four days. Except where noted, the plates are 103a-D emulsion with a Corning 3484 (yellow) filter, defining the spectral region 5200-6500 Å. The filter transmits 2.5% at 5185 Å and rises sharply, reaching 27% at 5285 Å; the D emulsion is about 15% efficient (relative to its efficiency at 6000 Å) at 6500 Å. The weak lines 5875 Å of HeI, 6300 Å of [OI] (Minkowski, 1942), and H-alpha on the tail of the band pass are the major contributors to the small amount of filamentary contamination. In this listing the plate number is followed by the initial of the observer (B = Baade, M = Münch, A = Arp, Z = Zwicky). If two images are on one plate, the suffixes a and b distinguish them. The date, exposure time, seeing, and position angle (if the plate is with a polaroid filter) follow. The angle given is the position angle of the minimum transmission of the electric vector by the polaroid HN 38 filter. This corresponds to the direction of the magnetic field in the nebula for synchrotron emission, which has the electric vector directed perpendicular to the ambient magnetic field (Westfold, 1959). Any remarks about polarization in this appendix are rough estimates based on visual inspection. Because of the strong polarization and the marked elongation of many of the features discussed, it is possible to estimate the strength of the polarization and whether or not it is aligned with the direction of the extension of the feature. The usual sense of polarization is such that this direction of elongation is parallel to the magnetic field, as discussed in the text.

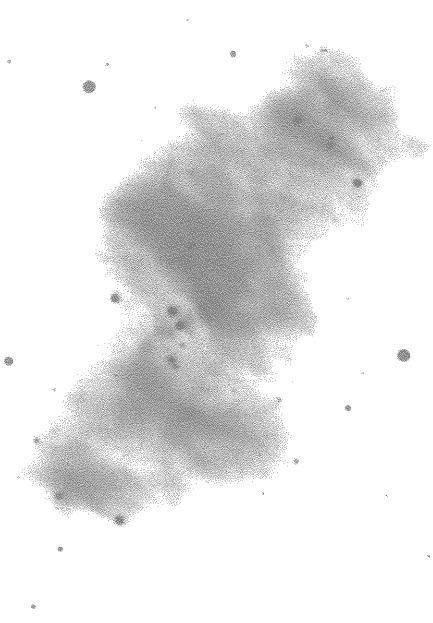

(a) PH 1347 1955.931

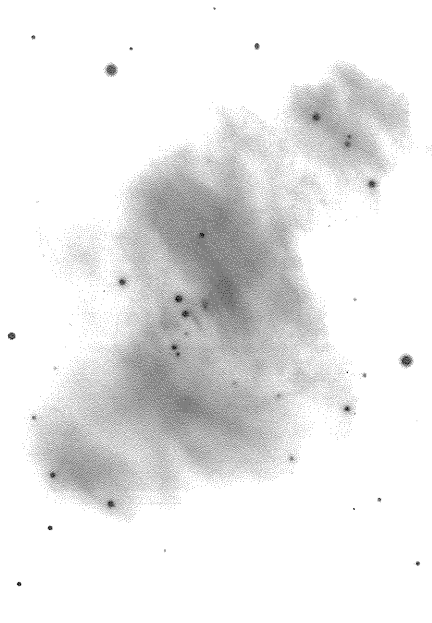

(b) PH 3055 1958.638

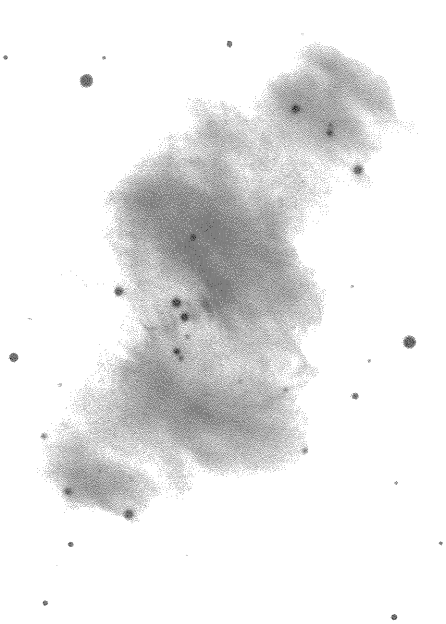

(c) PH 3728 1960.947

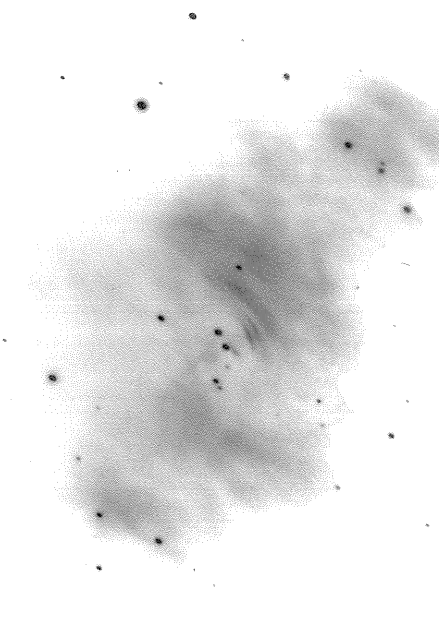

(d) PH 3896 1962.088

FIGURE A.1

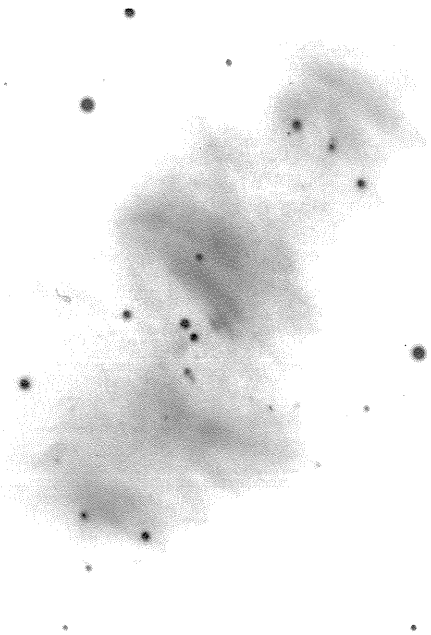

(a) PH 4020 1962.734

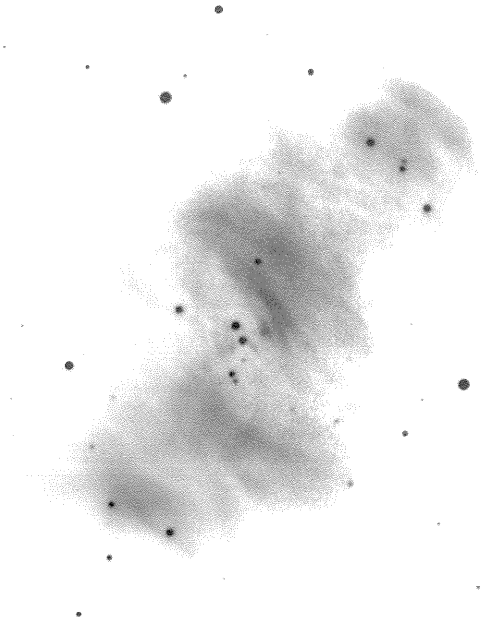

(b) PH 4104 1962.912

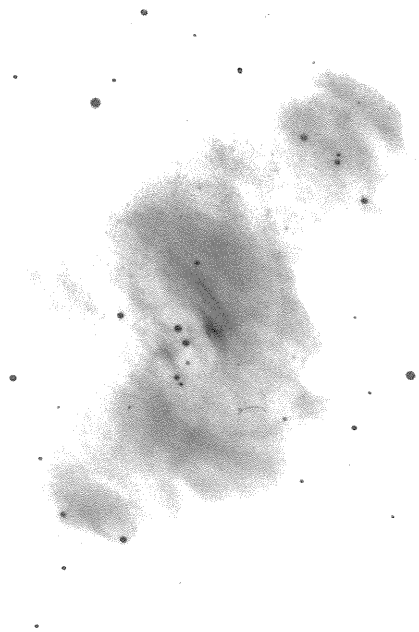

(c) PH 4321 1963.802

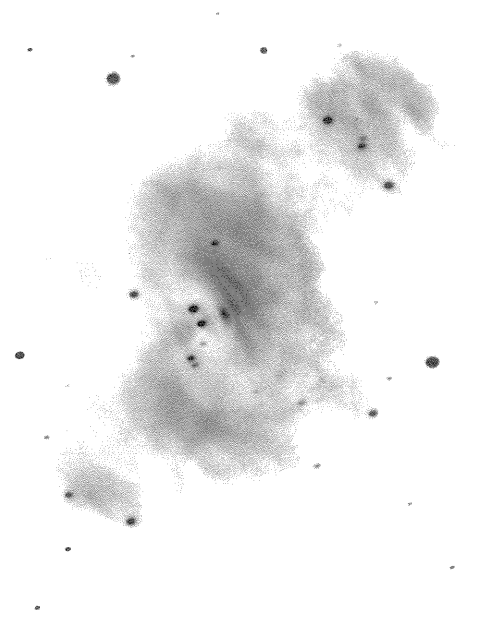

(d) PH 4986 1966.698

FIGURE A.2

The general structure of the central region, and the changes disclosed by the present series of plates, are discussed in the text, in Chapter II. To clarify the terminology used here, we shall merely restate that the wisps define a characteristic direction, roughly parallel to the line between the two stars near the center of the nebula. This line will frequently be referred to in this appendix. For example, a wisp being "opposite" S1 means that it falls on an imaginary perpendicular to this line errected at S1. The region to the SW of a point opposite S1 is sometimes called "past S1". For the meanings of the descriptive terms "THIN WISP", "PLATEAU", etc., see Chapter II. Epochs for which there is a plate in Figure A are indicated by an asterisk.*

/1/ September 19-22, 1955

PH 1281-B	Sept. 19, 1955.715	30^m	3	
PH 1291-B	20, 1955.717	10	3-4	
PH 1292-B	20, 1955.717	5	4	
PH 1299-Ba	21, 1955.720	20^m	2-3	0°
PH 1299-Ba	21, 1955.720	20	2	45°
PH 1300-B	21, 1955.720	20	2-3	90°
PH 1305-B	22, 1955.723	20	3-4	135°

The large number of plates with different exposure times and seeing makes it possible to form a very good picture of the nebula at this epoch. Fig. II.1 is from this epoch.

THE THIN WISP extends from approximately tangent to the seeing disk of S2 at its NE end, to about 4" past S1 at its SW end. Midway between S1 and S2 it is 1".7 NW of the line between the two stars, and about 2" past S1 it is 1".5 from the same line. It is perfectly straight as well as can be judged visually. It is definitely brighter and sharper at its SW end, and becomes diffuse at the NE end. Unfortunately, seeing differences in the set of polaroid plates affect the images considerably, and it is difficult to estimate the polarizations of the sharply defined features.

THE SMALL WISP. Between S1 and S2 there is a faint wisp 3".6 from the line between the two stars, and is also parallel to them. It is somewhat confused with the diffuse end of the THIN WISP, but is definitely separated from it on the profiles displayed by

the Grant measuring engine, and is consistent in position and appearance on all the plates. It is extremely vague on the polaroid plates.

WISP 1 is just on the edge of the PLATEAU. It is about 5" long, but fades out gradually at the ends so the total extent is somewhat longer. It is about 1" wide and appears to be resolved in this dimension (the seeing is quite good on some of the plates). There is no definite indication of curvature of this wisp on any of the plates. Also, the wisp seems symmetrical both along its extension and perpendicular thereto.

WISP 2 may really consist of two wisps superimposed. The main feature is about the same width as WISP 1, but about twice as long (10"). It also fades out gradually at its ends, and may traverse the entire PLATEAU. Starting opposite the midpoint of S1 and S2 it bifurcates, one branch continuing straight and the other extending towards the south. Each of these wisps is polarized according to the rule "electric vector perpendicular to the direction of the extension of the wisp".

WISP 3 can be seen beyond WISP 2, and is very similar in size, shape, and orientation. Both are somewhat curved toward S1 and S2. WISP 3 may be fainter than WISP 2, but this is not certain because of the changing background.

WISP 4. There is a hint of a wisp beyond WISP 3, best seen on the shortest exposure (5^m direct) and the 45° polaroid. It is shorter than the other outer wisps, possibly due to its faintness. It is much like a faint version of WISP 1, and is located more or less opposite it.

THE ANVIL is very uniform (other than a streak parallel to the other wisps on PH 1291, presumably a flaw, there is no wisp-like structure evident), except for two curious point-like objects on the edge of the ANVIL nearest S1. They appear to be strongly polarized in the direction perpendicular to the wisps. (Since these features have no obvious direction of elongation, they do not necessarily violate the usual rule.) These features are marginally visible, but can be seen on at least three plates. The ANVIL itself is not strongly polarized.

REMARK: While the spacing between the wisps in the series varies from epoch to epoch, there is a characteristic value well-represented in these plates. The average separation of the centers of the wisps is about 3" or 4".

/2/ October 13, 1955

PH 1314-B	Oct. 13, 1955.780	10^m	3-4	
PH 1315-Ba	Oct. 13, 1955.780	20^m	3-4	$67^\circ.5$
PH 1315-Bb	13, 1955.780	20^m	3-4	$157^\circ.5$

THE THIN WISP extends from midway between S1 and S2 on the NE to about 4" past S1 on the SW. The difference in the extent of the THIN WISP to the NE between this epoch and the previous one may or may not be real.

THE SMALL WISP reported at the previous epoch is not apparent to visual inspection, although a small feature on the Grant profile was measured at the same location to within 0".1, so it is undoubtedly real.

WISP 1 appears somewhat asymmetrical in that to the NE it trails off gradually into a thin streamer, whereas the SW end is abrupt. This fact makes it difficult to judge the position of the wisp in this direction. Its brightest part is 5" long. This wisp can be easily measured in the perpendicular direction, and it is 0".2 further from S1 than at the previous epoch, confirming Baade's remarks in Appendix B.

WISP 2 is possibly the remnant of the bifurcation seen at epoch /1/. It is very faint and at an angle to the usual direction.

WISP 3 is well-defined and runs down the middle of the PLATEAU for 10" or more. It may have a kink in it about midway between S1 and S2.

THE ANVIL shows the two spots mentioned at the previous epoch, again polarized roughly perpendicular to the wisps. At the SE end of the ANVIL there is a larger, more diffuse patch with roughly the same direction of polarization as the two spots. This feature may be elongated parallel to the wisps, but that is not certain. Note that if the two spots were blended by the seeing, they would simulate a wisp-like feature parallel to the main series of wisps.

REMARK: The plate with the polaroid at $157^\circ.5$ shows WISPS 2 and 3 extended much more to the south than on any of the other plates. They curve around so that their southern ends are more nearly parallel to the polaroid filter, which undoubtedly explains this fact.

/3/ November 14-17, 1955

PH 1344-B	Nov. 14, 1955.868	20^{m}	1	90°
Z329	17, 1955.876	30	2	90°
Z330	17, 1955.876	30	2	0°

Baade's plate is nearly useless because of the poor seeing. Zwicky's plates were 103a-D emulsion, with a GG11 and a plastic polaroid filter.

THE THIN WISP is quite broad, mostly to the SW of S1 but with a diffuse extension between S1 and S2.

WISP 1 is about 5" long, definitely curved toward S1 (i.e., S1 is on the same side as the center of curvature), and somewhat past the edge of the PLATEAU.

WISP 2 is well defined, with a core about 5" long and a total length of between 15 and 20".

*/4/ December 7-8, 1955

PH 1353-B	Dec. 8, 1955.934	10^{m}	5	
PH 1346-B	7, 1955.931	20^{m}	2-3	22°.5
PH 1347-Ba	7, 1955.931	20	2-3	67°.5
PH 1347-Bb	7, 1955.931	20	2-3	112°.5
PH 1348-B	7, 1955.931	20	2-3	157°.5

The direct plate was taken "through thickening haze! (sky covered afterwards)," and is essentially useless because of underexposure (naturally the seeing was exquisite). The seeing for the polarization plates was poor, but the positions of the wisps could be measured very accurately.

THE THIN WISP is too diffused by the seeing to show much of interest. It seems to be in its usual position.

THE SMALL WISP may be present in the same position as before, although it is difficult to distinguish it from the end of the THIN WISP. It is strongest on the polaroid which should emphasize features elongated at 22°.5.

WISP 1 is present, but ill-defined. It is about 5" long, possible with a core near the SW end (located a bit SW of the point opposite S1).

WISP 2 is nearly washed out by seeing, but looks much as it did at earlier epochs.

THE ANVIL shows some structure near the position of the two bright spots seen before, but in the form of a wisp-like feature curved toward S1, with indefinite polarization.

/5/ March 9, 1956

PH 1360-B March 9, 1956.183 10^m 3+

THE THIN WISP and THE SMALL WISP. This plate is very difficult to interpret. There is no trace of the THIN WISP to the SW of S1 where it is normally strongest. The seeing is good, and can't be responsible for this disappearance. Between S1 and S2 there appear to be two very faint, thin wisps--roughly in the usual position of the THIN WISP and the SMALL WISP, respectively. Moreover, to the SW of S1 are two features parallel to the ones just mentioned, somewhat further from the S1-S2 line. All four of these features are quite sharp, and could be plate flaws.

WISP 1 is well-defined, and has its center displaced from its usual position opposite S1 toward the SW (see Appendix B), by roughly 2". It is about 5" in length.

WISP 2. There is possibly a very faint, short section of a wisp between WISPS 1 and 3, centered between S1 and S2.

WISP 3 is very strong and long (total intensity probably 5 times that of WISP 1), extending for 10" or more. It is slightly curved toward S1, and may extend a bit more toward the SW than usual.

THE ANVIL. The edge of the ANVIL toward S1 is a wisp-like feature, possibly curved toward S1.

REMARK: There is no wisp structure visible beyond WISP 3.

/6/ October 10, 1956

PH 1570-B Oct. 10, 1956.772 7^m 2

THE THIN WISP. There is a plate flaw in this region, extending from S1 at position angle 280°. The true THIN WISP shows up only as a very diffuse region to the SW of S1.

WISP 1 is not well-defined, but its center of gravity is nearly opposite S1 again. The brightest part of the wisp is 5" long.

WISP 2 has its usual appearance in such seeing.

THE ANVIL has a wisp-like structure toward S1, but this is nearly blended into the ANVIL itself.

REMARK: There are a number of flaws on this plate, the largest one obscuring the SW extension of WISP 2.

/7/ November 30, 1956

PH 1597-B Nov. 30, 1956.912 7^m 4

THE THIN WISP is here very narrow and curved toward WISP 1. It is brightest to the SW of S1 where it extends about 2". In the other direction it extends about 4" and curves so that its end is about 2".5 west of S2.

THE SMALL WISP. Between the THIN WISP and WISP 1 there are some features--not a single small wisp, but perhaps 3 or 4 fragments that are jumbled together.

WISP 1 is quite curved toward S1. It is brightest at its NE end, which comes to a narrow point. Thus while the wisp as a whole is somewhat SW of S1, its center of gravity is slightly to the NE. The wisp is about 4" in length.

WISP 2. It is not clear what to call "WISP 2". There is a small fragment due north of WISP 1. In that position it would normally fall on top of WISP 1, which however curves from its usual position toward S2 so that this does not happen. Since this feature follows the curvature of WISP 1 if extended to the NW, and is displaced away from S1 by roughly the same amount that WISP 2 normally is, we shall call this very faint object "WISP 2."

WISP 3 is very long and about 2" wide, in its usual position.

WISP 4. There is some indication of a feature about 4" beyond WISP 3, curved away from S1.

THE ANVIL is generally uniform, with a hint of a diffuse wisp toward S2.

/8/ December 28, 1956

PH 1624-E Dec. 28, 1956.988 7^m 3+

THE THIN WISP is almost absent, appearing only as a faint streak very close to S1 on the SW side and perhaps visible on the NE side also.

WISP 1 is rather sharply defined. It is widest opposite S1 and narrows toward the NE; toward the SW it narrows to a thin streamer. The brightest part is 3" long, but with the streamer it extends a total of about 6". WISP 1 has tipped over to a smaller position angle, as noted by Baade (Appendix B).

WISP 2 is more prominent and longer on this plate than on any other. From the point opposite S1 it extends 10" to the SW and 35" to the NE. If extended about 10" more to the NE this wisp would run directly into the bright filament which leads to the very strong filamentary arch at the north end of the nebula. Just opposite S1 WISP 2 broadens with a suggestion of a shorter wisp breaking off, although this region is somewhat confused by what seems to be a small plate flaw.

WISPS 3 and 4. There are two smudges beyond WISP 2 opposite WISP 1 at about the right distances to be members of the wisp series.

THE ANVIL has a faint wisp-like feature on the side toward S1, extending from opposite S1 to a few " beyond S2.

REMARK: The wisps, especially WISP 2, are very bright relative to the PLATEAU, and at this epoch most of the intensity from the core of the nebula must come from the wisp series.

/9/ September 21, 1957

PH 1740-B Sept. 21, 1957.720 7^m 3-4

THE THIN WISP is well-defined from S2 to almost 5" beyond S1. Its SE edge is very sharp, but to the NW it fades away gradually.

WISP 1 has a curious appearance, as though it is composed of two wisps, one tipped at an angle (about 20°) to the other. The two are not well separated, so the whole feature looks like a fan opening toward the NE, and quite pointed at the other end. The length is a bit hard to judge, but is about 4 or 5".

WISP 2 is rather faint and complicated in structure. It may really consist of a long wisp with a branching toward the SW.

THE ANVIL is not well defined, and shows little remarkable structure. It does, however, appear to be more extended in the NS direction than previously.

/10/ November 19, 1957

PH 1772-B Nov. 19, 1957.882 7^m 3

THE THIN WISP is sharply bounded on the SE, but fades very gradually in the other direction. This may be partly due to blending with a SMALL WISP. The THIN WISP reaches from about 4" past S1 to S2.

WISP 1 has a nucleus somewhat SW of the point opposite S1, and extends rather far in the other direction (a few " or more past S2). The nucleus is about 4" long, but the total extent of the wisp is about twice this value.

WISP 2 is almost absent. What is there may not be a single wisp, but fragments of a wisp which twists around in a peculiar way.

THE ANVIL has a wisp sticking out from the middle of its northern boundary, extending about 5" to the NNE.

/11/ December 20, 1957

PH 1792-B Dec. 20, 1957.966 8^m 4

THE THIN WISP is rather diffuse, considering the seeing, and is definitely curved away from S1. It extends 3-4" to the SW of S1, and in the other direction extends about the same amount, but not directly toward S2 as is usual (it curves off to the right).

THE SMALL WISP. There is a small, faint wisp between the curved THIN WISP and WISP 1.

WISP 1 begins opposite S1, extends about 3" to the NE, where it abruptly drops in intensity and continues on for 5" or more.

WISP 2 is a very weak smudge, shorter than WISP 1, and to the SW of its customary position.

THE ANVIL is very diffuse, and seems to extend to the north into regions from which it is usually separated by a dark lane.

/12/ February 13-16, 1958

PH 1806-B	Feb. 13, 1958.118	8^m	1-2
PH 1816-B	16, 1958.126	8	3-4

THE THIN WISP is brightest between S1 and S2, is quite diffuse, and may be curved toward WISP 1.

WISP 1 shows a curious doubling. Its core, opposite S1, is single, but the extensions in both directions seem to consist of two parallel spikes. The core is 3" or less in length, and the spikes bring the total length to about 6".

WISP 2. There is no definite WISP 2, just a general brightening of the whole central PLATEAU region.

THE ANVIL shows some structure south of its usual position, in the form of a wisp which is broad opposite S1 and extends to the south, reaching a faint star in that region and coming to a point.

*/13/ August 22, 1958

PH 3054-Ma	Aug. 22, 1958.638	15^m	1	90°
PH 3054-Mb		15	1	180°
PH 3055-Ma		17	2	135°
PH 3055-Mb		17	2	225°

THE THIN WISP is sharply defined from S1 to the SW , but is quite weak between S1 and S2. Even though the seeing is different on the plates, it is clear that the THIN WISP is strongly polarized in the usual direction. There is a knot showing peculiar polarization on the end of this wisp near S1, as this end is hooked toward S1 on two of the plates (the one oriented perpendicular to the wisps and one of the two at 45° to the wisps). The strange feature at the SW end of the wisp is due to a bubble in the Corning filter, and appears on a number of the plates.

THE SMALL WISP. On the two plates in better seeing, there is a slight hint of a feature between S1 and S2, to the NW of the THIN WISP.

WISP 1 has a nearly stellar core, which is strongly polarized. It is directly opposite S1. The total extension of the wisp is less than 3".

WISP 2 is a faint streak about 5" long, approximately centered opposite WISP 1. It is not visible on PH 3054, probably because of the bad seeing, but is definite and strongly polarized on PH 3055.

WISPS 3 and 4 are evident on PH 3055. WISP 3 is straight and similar to WISP 2, but WISP 4 curves toward WISP 3 and they meet at their SW ends. They are 5" apart to the NE.

THE ANVIL has some vague wisp-like structure parallel to the other wisps. It is polarized, but not in a way that can be described simply.

/14/ October 9, 1959

PH 3439-M	Oct. 9, 1959.769	20^m	3	0°
PH 3440-M		20	3	90°
PH 3441-M		20	3	45°
PH 3442-M		20	3	135°

These polaroid plates were taken on the finer-grained IIa-D emulsion, which has a very similar characteristic curve to the 103a-D.

THE THIN WISP is essentially absent. There is only an extremely diffuse brightening spread out between S1 and WISP 1.

WISP 1 is 4-5" long in its brightest part, and is centered opposite S1. There is a faint extension to the NE, about 3-4" long.

WISPS 2, 3, and 4. There is a faint indication of three more wisps beyond WISP 1, but they are not very bright or sharp.

THE ANVIL is composed of two distinct wisps farther from S1 than usual (one is 5", the other 7" from that star). They are strongly polarized along their extension (parallel to the wisps on the other side). At this epoch the ANVIL was strikingly like the wisp series.

/15/ February 21, 1960

PH 3490-Ma	Feb. 21, 1960.140	20^m	0°
PH 3490-Mb		20	90°
PH 3491-Ma		20	45°
PH 3491-Mb		20	135°

The seeing is rather poor (about 2).

THE THIN WISP again is totally absent, but this may be partly due to the seeing in this case.

WISP 1 is only slightly more extended (3") than the rather large star images. It is centered 1" or less SW of its usual position opposite S1.

WISP 2. There is a rather bright, broad wisp beyond WISP 1, extending about 15" from opposite the SW end of WISP 1 to the NE.

THE ANVIL shows no definite detail.

*/16/ December 13, 1960

PH 3727-Ma	Dec. 13, 1960.947	15^m	2-3	0°
PH 3727-Mb		15	2-3	90°
PH 3728-Ma		15	2-3	45°
PH 3728-Mb		15	2-3	135°

THE THIN WISP. There is a sharp, strongly polarized wisp about 5" long, a bit SW of being opposite S1. It is rather further (about 2") from S1-S2 than usual.

WISP 1 is thickest at a point 1" or so NE of the point opposite S1, ends rather abruptly to the NE, but thins and trails off gradually to the SW. The total length is roughly 6".

WISP 2 is rather straight along most of its length, but at its SW end bifurcates into two pieces.

WISP 3. There is possibly a broad feature beyond WISP 2, but it is not clearly defined.

THE ANVIL is composed of two wisp-like features parallel to the other wisps. They curve toward each other at the SW end of the ANVIL, and both have fainter straight extensions to the NE. The sharp E-W feature in Figure A.1(c) to the E is a flaw.

*/17/ February 2-3, 1962

PH 3895-Ma	Feb. 2, 1962.088	17^m	3	90°
PH 3895-Mb		17	3	0°
PH 3896-Ma		15	3	45°
PH 3896-Mb		15	3	135°
PH 3897-Ma	Feb. 3, 1962.090	20	2-3	0°
PH 3897-Mb		20	2-3	90°
PH 3898-Ma		20	2-3	45°
PH 3898-Mb		20	2-3	135°

THE THIN WISP has a very narrow, faint part which runs closely to S1 in the region to the NW of the star. This straight section joins a much brighter section to the SW which is curved toward WISP 1 and is rotated about 30° counterclockwise from its usual orientation.

WISP 1 is quite narrow and well defined. Microphotometer traces show that a great deal of the apparent width of the wisps is due to the seeing (by comparison with traces of faint star images), but that the profiles are definitely wider than given by the seeing alone. The brightest region of WISP 1 is about 4" long, but it extends several " in both directions.

WISP 2 is very similar and close to WISP 1. The main difference is that it is curved toward WISP 1 and its center is displaced 1 or 2" to the NE from the center of WISP 1.

WISP 3 is rather broader than the previous wisps, and is about 15 to 20" long. The separation between this and WISP 2 is slightly greater than that between WISPS 1 and 2.

WISP 4 is parallel to WISP 3, and about the same distance from it as WISP 2 is from WISP 1. It is slightly fainter than WISP 3. Both outer wisps are slightly curved toward S1.

THE ANVIL is weak on these plates, and shows no obvious structure.

*/18/ September 26, 1962

PH 4019-Ma	Sept. 26, 1962.734	17^m	2-3	0°
PH 4019-Mb		17	2-3	90°
PH 4020-Ma		17	2-3	45°
PH 4020-Mb		17	2-3	135°

THE THIN WISP. There is absolutely no trace of this wisp, even as a diffuse object. The plates are rather weak.

WISP 1 may be double. It is quite small and nearly as wide as long (about 1"x2"). It is opposite S1 and not very bright.

WISP 2 is twice as long as WISP 1, somewhat fainter, and in its usual position.

WISP 3 is similar to WISP 2, but fainter. It extends diffusely quite a distance to the NE.

THE ANVIL is very weak on these plates, with no distinctive structure.

*/19/ November 30-December 1, 1962

PH 4104-Ma	Nov. 30, 1962.912	20^m	2-3	45^o
PH 4104-Mb		20	2-3	135^o
PH 4106-Ma	Dec. 1, 1962.914	25		0^o
PH 4106-Mb		25		90^o

THE THIN WISP is a broad, rather faint patch, detached from S1 by 1" or more. Its position angle is about 320^o, so it is rotated significantly clockwise from its usual position.

WISP 1 is very unusual. The brightest part is definitely thicker than it is long. There is no indication of doubling, although this might be hidden by the seeing. There is also an extension of this nearly rectangular core (3"x2") to the NE by a few ".

WISP 2 is in its usual position, and is quite long and fairly bright. It is slightly thinner than the thickest section of WISP 1.

WISP 3 fuses with WISP 2 to the NE, and branches away from it (starting opposite S2) to the SW.

THE ANVIL contains two short wisps which are at the SW end, opposite S1. Their polarization is directed more nearly NS than than that of the other wisps, but they may be directed that way too (orientations are hard to judge because the wisps are so short).

*/20/ October 21, 1963

PH 4320-Ma	Oct. 21, 1963.802	20^m	3	0^o
PH 4320-Mb		20	3	90^o
PH 4321-Ma		20	3	45^o
PH 4321-Mb		20	3	135^o
PH 4322-M		36	2-3	0^o

The last plate listed is a 103a-U, with RG 10 and polaroid filters.

THE THIN WISP. On the polaroid in position angle 45^o there is a diffuse suggestion of the THIN WISP, mostly between S1 and S2. About 3" west and 1/2 " south of S2, possibly on the end of the THIN WISP, is a remarkable feature. It is slightly more extended than stellar images, but it is quite condensed and point-like. Its polarization is such that it changes position and shape with the polarization angle. If it is a knot on the end of the THIN WISP, it is peculiar because it has some polarization perpendicular to the usual direction. It is even apparent on the weak plate PH 4322.

WISPS 1 and 2. The "first" wisp is actually composed of two wisps which intersect opposite the point midway between S1 and S2. The more distant of the two is brighter, quite thin, nearly 10" long, and basically straight. The inner wisp curves around and becomes parallel to the outer one, and they both extend rather far to the SW. The joined wisps extend only 2-3" beyond S2 to the NE.

WISPS 3 and 4 may intersect also, but near their SW ends. They are well defined for quite a distance (10 or 15"), but only rather far to the NE of their usual position.

THE ANVIL contains a very bright and narrow wisp 6".35 from S1. This wisp is rather strongly polarized in the usual sense. There is some other fainter and more diffuse structure in the ANVIL which is polarized in other directions, and is particularly striking on PH 4320a.

/21/ October 9-11, 1964

PH 4642-Ma	Oct. 9, 1964.769	20^m	2	90°
PH 4642-Mb		20	2	0°
PH 4643-Ma		20		135°
PH 4643-Mb		20		45°
PH 4651-M	Oct. 11, 1964.775	80	3	270°

PH 4651 is the same plate-filter combination as PH 4322.

THE THIN WISP appears as a trace on the 45° polaroid only. It is close to and approximately even with S1.

WISP 1 shows some signs of being composite, but is basically thin, sharply pointed on the NE end, blunt to the SW, and with a faint diffuse fragment extending to the south. The core is about 3" long.

WISP 2. There is only one other wisp, rather long and consisting of two straight segments intersecting nearly opposite S2.

THE ANVIL shows some indistinct knotty structure, mostly concentrated at the south end.

*/22/ September 13, 1966

PH 4986-A	Sept. 13, 1966.698	20^m	good	45°

THE THIN WISP is only a diffuse spot between S1 and S2.

WISP 1 is elliptical, about 2"x4", in its usual position opposite S1.

WISP 2 is well defined for 20 or 30". It curves around WISP 1 as though the latter were pushing against it. This is the only clear case of an interaction between the wisps.

WISP 3 is similar to WISP 2, and is parallel to it, following the curve around WISP 1. Although a bit fainter to the SW, it can be traced as far as can WISP 2 in that direction.

THE ANVIL may consist of two wisps parallel to the wisps on the other side.

/23/ October 15, 1966

PH 5002-A	Oct. 15, 1966.786	20^m	2	45°

The seeing is very bad. There are no detectable differences from the previous epoch.

/24/ PH 5011-A Dec. 7, 1966.931 20^m 1 45°

Terrible seeing. No detail visible.

/25/ November 10, 1967

PH 5129-Ma	Nov. 10, 1967.860	20^m	3	90°
PH 5129-Mb		20	3	0°
PH 5130-Ma		20	3	45°
PH 5130-Mb		20	3	135°

THE THIN WISP is nearly as bright as WISP 1, and is curved markedly toward it. It is about 1"x5", approximately centered opposite S1.

WISP 1 is about 6" long, and tapers to points at both ends. It is slightly curved toward S1.

WISP 2 is 10" or more in length, and is slightly thinner than WISP 1. It curves around WISP 1 slightly, exhibiting rather angular bends. There are no obvious features beyond WISP 2.

THE ANVIL is almost featureless, and is shaped much as it was on the earliest plates in the series. But in addition, there is a diffuse jet extending to the north.

APPENDIX

B. MOVING LENS ON 200-INCH PLATES
1955 SEPTEMBER TO 1957 DECEMBER
(NOTES BY DR. WALTER BAADE)

PH 1291B → PH 1314B 1955 Sept. 20 → 1955 Oct. 13	motion away from central star
PH 1314B → PH 1360B 1955 Oct. 13 → 1956 March 9	motion of lens now in PA. $30^{\circ}+180^{\circ}$ (towards SSW - direction of its own extension)
PH 1360B → PH 1570B 1956 March 9 → 1956 Oct. 10	motion of lens has reversed itself and is coming back (motion reverse to that observed for preceding interval)
PH 1570B → PH 1597B 1956 Oct. 10 → 1956 Nov. 30	lens moves <u>toward</u> central star! ridge begins to move away from it
PH 1597 → PH 1624B 1956 Nov. 30 → 1956 Dec. 28	lens essentially stationary, but it tips over to smaller P.A.
PH 1624B → PH 1740B 1956 Dec. 28 → 1957 Sept. 21	both lens and ridge moving <u>away</u> from star fast (ridge getting faint and narrow)
PH 1740B → PH 1772B 1957 Sept. 21 → 1957 Nov. 19	lens still moving away from star but getting faint; ditto faint remnants of ridge
PH 1772B → PH 1792B 1957 Nov. 19 → 1957 Dec. 20	lens (faint) has again reversed motion and is now again moving <u>toward</u> star

1958 January 3
Walter Baade

APPENDIX

C. SYNCHROTRON RADIATION FROM A HYDROMAGNETIC DISTURBANCE

Consider a gas composed of relativistic electrons in a magnetic field. We shall calculate the spectrum and spatial distribution of the radiation when a disturbance passes through the gas, altering the field and particle densities. We assume that the disturbance propagates slowly enough that the changes are adiabatic, and fast enough that radiation losses can be neglected.

The synchrotron radiation is completely determined by the magnetic field and the distribution of the particles in momentum space. For the present calculation the field can be arbitrary, and we shall represent it as $\underline{B}$ in the undisturbed medium, changing to $\underline{B}'$ as the disturbance passes ($\underline{B}'$ is an arbitrary function of space and time). We assume that the distribution of momenta is initially azimuthally symmetric about the field, constant in space, and a power law in the electron energy:

$$N(\gamma,\alpha;\underline{x},t)d\gamma d\alpha d^3xdt = \begin{cases} K_o\,\gamma^{-s} & \gamma_1 < \gamma < \gamma_2 \\ 0 & \text{otherwise} \end{cases} f_o(\alpha)d\gamma d\alpha d^3xdt \qquad (1)$$

where γ is the dimensionless energy ($\gamma = E/m_oc^2 = (1-v^2/c^2)^{\frac{1}{2}}$), and α is the pitch angle (angle between the velocity of the particle and the magnetic field).

If the change is slow enough, the following relations for the relativistic momentum follow from the perpendicular and parallel adiabatic invariants:

$$P_\perp' = \sqrt{(B'/B)}\;\; P_\perp \qquad (2)$$

$$P'_{\parallel} = P_{\parallel} \tag{3}$$

(unprimed quantities are the initial values, primed ones are the disturbed values). These equations give the changes in the pitch angle and energy:

$$\tan \alpha' = \tan \alpha \sqrt{(B'/B)} \quad , \tag{4}$$

$$\gamma' = \gamma \sqrt{1 + [(B'-B)/B]\sin^2\alpha} \quad . \tag{5}$$

We can now calculate the change in the distribution by equating the number of particles originally in a given area of γ-α space to the number in the transformed area:

$$N'(\gamma',\alpha')d\gamma' d\alpha' = N(\gamma,\alpha)d\gamma d\alpha \quad , \tag{6}$$

where we have implicitly assumed that the disturbance is symmetric about the original magnetic field. In the usual way, the relation between N and N' is given in terms of the Jacobian:

$$N'(\gamma',\alpha') = N[\gamma(\gamma',\alpha'),\alpha(\gamma',\alpha')]\, \partial(\gamma,\alpha)/\partial(\gamma',\alpha') \quad , \tag{7}$$

where

$$\partial(\gamma,\alpha)/\partial(\gamma',\alpha') = \begin{vmatrix} \partial\gamma/\partial\gamma' & \partial\gamma/\partial\alpha' \\ \partial\alpha/\partial\gamma' & \partial\alpha/\partial\alpha' \end{vmatrix} \tag{8}$$

$$= (\partial\gamma/\partial\gamma')(\partial\alpha/\partial\alpha') \tag{9}$$

$$= \sqrt{[(B/B')(1+\tan^2\alpha')/(1+(B/B')\tan^2\alpha')\ ]} \tag{10}$$

where the derivatives in (8) have been evaluated using equations (4) and (5). Thus

$$N'(\gamma',\alpha') = K_0 \begin{cases} \left(\gamma' \sqrt{\frac{1+(B/B')\tan^2\alpha'}{1+\tan^2\alpha'}}\right)^{-5} & \gamma_1' < \gamma' < \gamma_2' \\ 0 & \text{OTHERWISE} \end{cases} f_0 \sqrt{\frac{B}{B'}} \left(\frac{1+\tan^2\alpha'}{1+\frac{B}{B'}\tan^2\alpha'}\right)^{1/2} \tag{11}$$

where f_o stands for

$$f_o\left(\tan^{-1}\left[\sqrt{\frac{B}{B'}}\tan\alpha'\right]\right). \tag{12}$$

If we assume that $\gamma_1 \ll \gamma \ll \gamma_2$ for the electrons which produce the radiation of interest, then for reasonable disturbances the same relation holds for the primed quantities (which are given in terms of the unprimed quantities by eq.(5)). Hence

$$N'(\gamma',\alpha') = K_o(\gamma')^{-s}\left(\frac{1+\tan^2\alpha'}{1+\frac{B}{B'}\tan^2\alpha'}\right)^{\frac{s+1}{2}}\sqrt{\frac{B}{B'}}\, f_o\left(\tan^{-1}\left[\sqrt{\frac{B}{B'}}\tan\alpha'\right]\right). \tag{13}$$

One way to interpret this is to say that the distribution (1) goes over into one of the same form with the same K_o and exponent s, but the angular distribution changes thus:

$$f_o(\alpha) \rightarrow \sqrt{\frac{B}{B'}}\left(\frac{1+\tan^2\alpha'}{1+\frac{B}{B'}\tan^2\alpha'}\right)^{\frac{s+1}{2}} f_o\left(\tan^{-1}\left[\sqrt{\frac{B}{B'}}\tan\alpha'\right]\right). \tag{14}$$

It should be kept in mind that this formula gives the change in the distribution function refering to a volume which is frozen to the matter. In general there will be another factor for the change in the total density (proportional to K_o).

In terms of the distribution function, we can now evaluate the synchrotron emissivity. At angle φ between the direction of observation and the field, and for a distribution of the form (1) (dropping the subscript "o"), the synchrotron volume emissivity is (Westfold, 1959; Field, 1964)

$$j_\nu(\varphi) = \frac{1}{2\sqrt{3}}\frac{e^2K}{c}\left[\frac{f(\varphi)}{\frac{1}{2}\sin\varphi}\right]\left(\frac{2}{3}\nu_\perp\right)^{\frac{s+1}{2}}\nu^{-\left(\frac{s-1}{2}\right)}\left[G_s\left(\frac{\nu}{\nu_{c2}}\right)-G_s\left(\frac{\nu}{\nu_{c1}}\right)\right] \tag{15}$$

where

$$\nu_\perp = \nu_{Bo}\sin\varphi\,, \tag{16}$$

$$\nu_{B0} = \frac{eB}{m_0 c}, \tag{17}$$

$$\nu_{ci} = \frac{3}{2}\nu_\perp \gamma_i^2 . \tag{18}$$

The function $G_s(x)$ is defined in terms of Bessel functions, and is a different function for different polarizations. Again assuming $\nu_{c1} \ll \nu \ll \nu_{c2}$, the factor in square brackets in (15) is constant, and we have the often quoted formula

$$j_\nu \propto K\left[\frac{f(\varphi)}{\frac{1}{2}\sin\varphi}\right]\left(\frac{3}{2}\nu_\perp\right)^{\frac{s+1}{2}} \nu^{-\left(\frac{s-1}{2}\right)} . \tag{19}$$

From this equation and the results above, it is a simple matter to derive the dependence of the emissivity on B. For example, if B changes because of a disturbance which causes compression and expansion only perpendicular to B (e.g., longitudinal waves propagating perpendicular to B), then because the matter and field are frozen together, the total electron density is proportional to B'. Hence both K and $\nu_\perp$ are proportional to B' in equation (19), and the total dependence on the magnetic field is

$$j_\nu \propto \left(\frac{B'}{B}\right)^{\frac{s+2}{2}} \left(\frac{1+\tan^2\alpha'}{1+\frac{B}{B'}\tan^2\alpha'}\right)^{\frac{s+1}{2}} f_0\left(\tan^{-1}\left[\sqrt{\frac{B}{B'}}\tan\alpha'\right]\right). \tag{20}$$

The dependences on α' and f_o are not very important in most applications. The maximum energy change of the relevant electrons occurs when $\alpha' \to \pi/2$, and this corresponds, of course, to $\varphi = \pi/2$ (observing perpendicular to B). In this case the last factor in equation (20) approaches $f_o(\pi/2)$, and we have simply

$$j_\nu \propto \left(\frac{B'}{B}\right)^{s+3/2} . \tag{21}$$

A similar calculation was performed by Shklovskii (1957), who arrived at an exponent of s+1 in equation (21), in place of our $s + 3/2$. It appears as though all the assumptions are the same as those adopted here, but Shklovskii does not exhibit enough of the intermediate work to be sure of this.

BIBLIOGRAPHY

Allen, R.J., and Barrett, A.H. 1967,A.J.,72,288. "Intensity and Linear Polarization Observations of Cassiopeia A, Cygnus A, and Taurus A at 1.97 cm."

Andrew, B.H., Branson, N., and Wills, D. 1964, Nature,203,171. "Radio Observations of the Crab Nebula During a Lunar Occultation"

Baade, W. 1942 Ap.J.,96,188. "The Crab Nebula"

Baade, W. 1956 B.A.N.,12,#462,312. "The Polarization of the Crab Nebula on Plates Taken with the 200-inch Telescope"

Barbier, D. 1945,Ann.Astroph.,8,35. "Recherches Sur Les Nebuleuses II. Le Spectre Continu de la Crab Nebula dans la Region des Courtes Longueurs d'onde"

Barnes, A. 1966,Phys.Fluids,9,1483. "Collisionless Damping of Hydromagnetic Waves"

Barnes, A. 1967, preprint: "Stochastic Electron Heating and Hydromagnetic Wave Damping"Phys. Fluids, 10, (1967) 2427

Baum, W. 1962 in Astronomical Techniques, ed. by W. Hiltner, U. of Chicago Press

Beaujardiere, O. De La 1966, Ann.Ap.,29,345. "L'Evolution du Spectre De Rayonnement Synchrotron"

Bell, S. and Hewish, A. 1967,Nature,213,1214. "Angular Size and Flux Density of the Small Source in the Crab Nebula at 81.5 Mc/s"

Börngen, F. von and Chatschikjan, E. 1967,Astr.Nach.,289,253. "Polarimetrische und kolorimetrische Untersuchungen am Crab-Nebel. II."

Bowyer, S. et.al. 1964,Science,146,912. "Lunar Occultation of X-ray Emission from the Crab Nebula"

Branson, N. 1965,Observatory,85,250. "The Emission Spectrum of the Crab Nebula"

Brodskaya, E.S. 1963, Contributions from the Crimean Astrophysical Observatory, 30, 126. (in Russian) "Interstellar Absorption in the Direction of the Crab Nebula"

Brosche, P. 1966, Z. für Ap., 64, 1. "Zur Bewegung des Krabsnebels"

Colgate, S. and White, R.H. 1966, Ap. J., 143, 626. "The Hydrodynamic Behavior of Supernovae Explosions"

Davies, R.D., Gardner, F.F., Hazard, C. and Mackey, M.B. 1966, Aust. J. Phys., 19, 409. "The Lunar Occultation of the Crab Nebula Observed at Parkes on June 21, 1963"

Deutsch, A.N. and Lavdovsky, V.V. 1940, Pulkova Circular No. 30, p.21. "The Expansion of the Crab-Nebula (NGC 1952) and the Proper Motions of Stars in its Neighborhood"

Dreyer, J.L.E. 1888, Mem. R. Astro. Soc., 49 "A New General Catalogue of Nebulae and Clusters of Stars"

Duncan, J.C. 1939, Ap. J., 89, 482. "Second Report on the Expansion of the Crab Nebula"

Field, G.B. 1964, Lectures at the California Institute of Technology

Ginzburg, V.L., and Ozernoy, L.M. 1966, Ap. J., 144, 599. "On the Significance of Coherent Plasma Radio-Wave Emission for Quasi-Stellar Radio Objects and Supernovae Remnants"

Ginzburg, V.L., Sazonov, V.N., and Syrovatski, S.I. 1967 Preprint No. 83, Lebedev Physics Institute (in Russian) "On the Synchrotron Emission and its Reabsorption"

Gotwols, B.L., Erickson, W.C., Fremouw, E. and Owren, L. 1966, P. A. S. P., 78, 199. "Two Lunar Occultations of the Crab Nebula"

Gower, J.F.R. 1967, Nature, 213, 1213. "Position of the Low Frequency Radio Source in the Crab Nebula"

Harris, E.G. 1957, Phys. Rev., 108, 1357. "Relativistic Magneto-Hydrodynamics"

Haymes, R.C. et.al. 1967, preprint submitted to Ap.J. "Observations of Gamma Radiation from the Crab Nebula" Ap.J. 151 (1968) L9

Herschel, W. 1912, The Scientific Papers of Sir William Herschel, Royal Astronomical Society, London

Hewish, A. and Okoye, S.E. 1965, Nature, 207, 59. "Evidence for an Unusual Source of High Radio Brightness Temperature in the Crab Nebula"

Hirth, W. 1967, Z. für Ap., 65, 48. "Synchrotronstrahlung und Variation von Elektronenenergiespektrum"

Johnson, H.M. 1963, Pub. N.R.A.O., 1, 261. "The Expansion of the Amorphous Part of the Crab Nebula"

Jüttner, F. 1911, Ann. Physik, 34, 856.

Kardashev, N.S. 1962, Astr. Zhur., 39, 393 (Sov. A.J., 6, 317) "Nonstationariness of Spectra of Young Sources of Nonthermal Radio Emission"

Krishnan, T., Zisk, S.H., and Cudaback, D.D. 1967, Ap.J., 150, 67. "The Crab Nebula at 1420 MHz."

Kristian, J. and Sachs, R.K. 1966, Ap.J., 143, 379. "Observations in Cosmology"

Kronberg, P.P. 1966, Nature, 212, 1557. "Small Diameter Components in the Crab Nebula at 1422 MC/S."

Lampland, C.O. 1921, P.A.S.P., 33, 79. "Observed Changes in the Structure of the 'Crab' Nebula (N.G.C. 1952)"

Lassell, W. 1867, Mem. Royal. Astr. Soc., 36, 1. "Observations of Planets and Nebulae at Malta"

Lerche, I. 1967, Ap.J., 150, 651. "Non-Relativistic Equations of Bulk Motion of a Relativistic Gas. II. Electromagnetic Effects and Suprathermal Waves"

Lerche, I. and Parker, E.N. 1966, Ap.J., 145, 106. "Non-Relativistic Equations of Bulk Motion of a Relativistic Gas"

Lichnerowicz, A. 1967, Relativistic Hydrodynamics and Magneto-hydrodynamics, Benjamin, New York

Mayall, N.U. 1937,P.A.S.P.,49,101. "The Spectrum of the Crab Nebula in Taurus"

Mayall, N.U. 1962,Science,137,91. "The Study of the Crab Nebula"

McCray, R. 1966,Science,154,1320. "Possibility of Maser Action in Cosmic Radio Sources"

Melrose, D.B., and Cameron, A.G. 1967, preprint: "Neutron Stars and Cosmic Ray Production"

Minkowski, R. 1942,Ap.J.,96,199. "The Crab Nebula"

Oda, M. et.al. 1967,Ap.J.,148,L5. "The size and position of the X-ray Source in the Crab Nebula"

O'Dell, C.R. 1962,Ap.J.,136,809. "Photoelectric Observations of the Crab Nebula"

Oort, J.H., and Walraven, Th. 1956,B.A.N.,12,#462,285. "Polarization and Composition of the Crab Nebula"

Orlova, O.N. 1966,Pub.Astr.Obs.Pulkova,24,115. (in Russian) "An Investigation of the Expansion of the Crab Nebula and Proper Motions of Surrounding Stars"

Parker, E.N. 1967, Lectures at the California Institute of Technology

Piddington, J.H. 1955,Nature,176,875. "The Four Possible Waves in Ionized Gas in a Magnetic Field"

Ritchey, G.W. 1910,Ap.J.,32,26. "On some Methods and Results in Direct Photography with the 60-inch Reflecting Telescope of the Mount Wilson Solar Observatory"

Sanford, R.F. 1919,P.A.S.P.,31,108. "Spectrum of the Crab Nebula"

Sartori, L. and Morrison, P. 1967,Ap.J.,150,385. "Thermal X-rays from Non-thermal Radio Sources"

Scargle, J.D. 1968,Ap.J., in press, "On Relativistic Magneto-hydrodynamics" Ap.J. 151 (1968) 791

Scheuer, P.A.G. 1966, Lecture at the California Institute of Technology, March 23

Shklovskii, I.S. 1957, Astr. Zhur., 34, 706 (Sov. A.J., 1, 690). "On the Nature of the Optical Emission from the Crab Nebula"

Shklovskii, I.S. 1964, P.K. Shternberg State Astronomical Institute, July 30. "The Supernova of 1054--a Double Star?"

Shklovskii, I.S. 1966, Astr. Zhur., 43, 10 (Sov. A.J., 10, 6). "Remarks on the Synchrotron-Radiation Spectrum of the Crab Nebula"

Simon, M., and Axford, W.I. 1967, Ap.J., 150, 105. "Thermal Instability Resulting from Synchrotron Radiation"

Spitzer, L. Jr. 1962, Physics of Fully Ionized Gases, Interscience, New York

Stix, T.H. 1962, The Theory of Plasma Waves, McGraw-Hill, New York

Synge, J.L. 1957, The Relativistic Gas, Interscience, New York

Taub, A.H. 1948, Phys. Rev., 74, 328. "Relativistic Rankine-Hugoniot Equations"

Taylor, J.H.Jr. 1966, Ap.J., 146, 646. "Lunar Occultations of Five Radio Sources"

Tidman, D.A. 1966, Ap.J., 144, 615. "Damping of Interstellar Plasma Waves by the Cosmic Ray Gas"

Trimble, V. 1968, thesis, California Institute of Technology, in preparation

Walraven, T. 1956, B.A.N., 13, #478, 293. "Photo-electric Observations of the Polarization and Surface Brightness of the Crab Nebula Made at the Observatoire de Haute Provence"

Westfold, K.C. 1959, Ap.J., 130, 241. "The Polarization of Synchrotron Radiation"

Whiteoak, J.B. 1966,Ap.J.,144,305. "The Wavelength Dependence of Interstellar Extinction"

Woltjer, L. 1957,B.A.N.,13,#478,302. "The Polarization and Intensity Distribution in the Crab Nebula Derived from Plates Taken with the 200-inch Telescope by Dr. W. Baade"

Woltjer, L. 1958,B.A.N.,14,#483,39. "The Crab Nebula"

Zheleznyakov, V.V. 1966,Astr.Zhur.,44,42(Sov.A.J.,11,33). "A Coherent Synchrotron Mechanism for Radio Emission from Cosmic Sources"

Zwicky, F. 1956,P.A.S.P.,68,121. "Composite Analytical Photography of Polarized Objects"